

Review

# Inkjet Printing with (Semi)conductive Conjugated Polymers: A Review

Daniil A. Lukyanov \*  and Oleg V. Levin 

Institute of Chemistry, Saint Petersburg University, 7/9 Universitetskaya nab., St. Petersburg 199034, Russia;  
o.levin@spbu.ru

\* Correspondence: lida93@yandex.ru

**Abstract:** Functional inkjet printing is an emerging manufacturing technology for the production of various planar elements and electronic devices. This technology offers affordable freeform and highly customizable production of thin film micron-scale elements on various substrates. Functional inkjet printing employs various inks based on organic and inorganic materials with diverse functional properties, and among them, conjugated polymers are of particular interest due to their electrical, photophysical, and electrochemical properties. This paper provides an overview of inkjet printing with conjugated (semi)conductive polymers, including the fundamentals of the technology and its scope, limitations, and main challenges. Specific attention is drawn to the synthesis and chemistry of these polymers in connection with the patterning and functional properties of the inks composed thereof. Practical aspects of this technology are also highlighted, namely the manufacturing capabilities of the technology and particular applications for the fabrication of various electronic elements and devices.

**Keywords:** inkjet; printing; conductive polymers; micromachining; organic electronics; synthetic metals



**Citation:** Lukyanov, D.A.; Levin, O.V. Inkjet Printing with (Semi)conductive Conjugated Polymers: A Review. *ChemEngineering* **2024**, *8*, 53. <https://doi.org/10.3390/chemengineering8030053>

Academic Editor: Erol Sancaktar

Received: 8 April 2024

Revised: 29 April 2024

Accepted: 6 May 2024

Published: 8 May 2024



**Copyright:** © 2024 by the authors. Licensee MDPI, Basel, Switzerland. This article is an open access article distributed under the terms and conditions of the Creative Commons Attribution (CC BY) license (<https://creativecommons.org/licenses/by/4.0/>).

## 1. Introduction

Inkjet technology, developed in the early 1950s and used in commercial printers since the 1980s, is now experiencing its renaissance as a tool for the precise and controllable patterning of freeform functional structures. Inkjet printing (IJP) allows the deposition of solutions or dispersions of functional materials in specific locations on a substrate by dispensing the (sub)picoliter droplets from the digitally positioned nozzle. Inkjet printing combines the benefits of both printing and additive manufacturing technologies, thus becoming a unique tool occupying a certain place in the palette of micromanufacturing techniques. IJP technology is used for sensors [1], biomedical probes [2], energy storage [3] and self-powered [4] devices, miniaturized and embedded electric circuits [5], as well as Internet of Things devices [6].

Modern lab-scale and industrial micromanufacturing employs different patterning techniques, including inkjet, intaglio, screen, and spray printing, with their particular advantages and limitations (Figure 1). Among them, IJP enables freeform micrometer-scale patterning over the short and simple manufacturing process, making it the most flexible and adopted manufacturing tool. The minimal pattern accessible via IJP is ~10 μm in length and <100 nm in height and shows high size and position reproducibility. IJP is a low-cost process, compatible with a large variety of the substrates and materials, which makes it the perfect tool for prototyping, custom, and on-demand digital manufacturing. IJP is an attractive technology due to the affordable equipment compared to other functional printing techniques, but at the same time, it is less scalable than the intaglio or screen printing techniques. As a result, IJP is more cost efficient compared to screen or intaglio printing at moderate production volumes, but inferior to them in mass production due to the higher time costs.

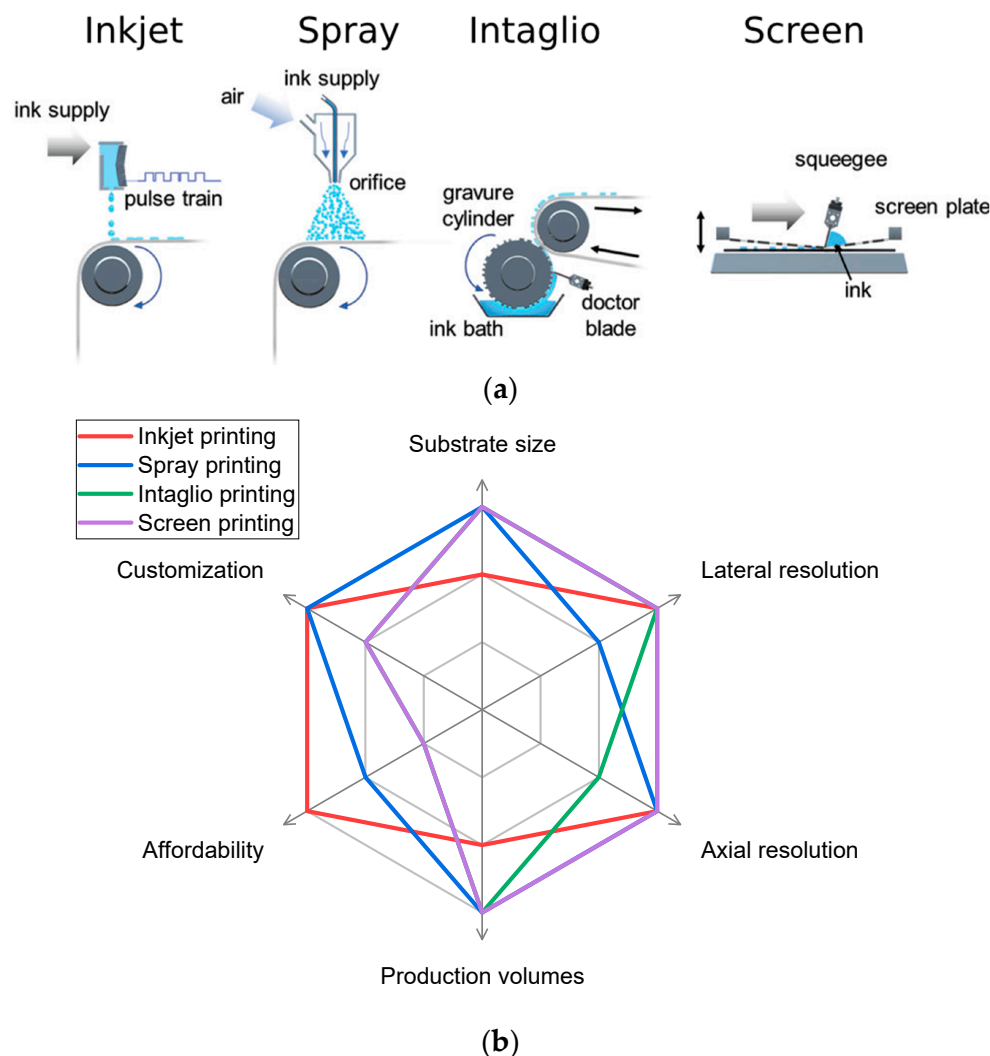


**Figure 1.** (a) Schematic illustration of various functional printing techniques; figure adopted from [7]; (b) performance comparison radar plot for these techniques.

Due to the emerging role of organic electronics, the demand for electrically conducting organic and polymeric materials is growing, and conjugated polymers (CPs) perfectly fulfil these needs. The ease of the structural modification of the CPs' structure allows the fine-tuning of their electrical, electrochemical, and photophysical properties, providing a family of materials for different purposes in organic electronics. CPs exhibit high chemical and dissolution stability, tensile strength and elasticity, a wide range of electrical conductivities, work functions, and band gaps, as well as good adhesion and film formation properties [8]. The deposition of CPs can be carried out using each of the abovementioned techniques using solution or dispersion inks.

A sole review dedicated to printing with conjugated polymers using different printing techniques was published in 2010 [9]. However, to date, an extensive effort has been made towards printing, and in particular inkjet printing, with conductive polymers. At the same time, a number of review papers have recently been published devoted to the implementation of IJP technology for the production of various kinds of microelectronic devices for analytical [1,10], biomedical, and diagnostic [2,11] purposes, semiconducting elements [7,12], and photovoltaic [13,14] and energy storage [15] systems. However, these reviews are not focused on CPs as functional materials and do not provide a sufficient overview of this topic.

The present paper contains an overview of the fundamentals and requirements of IJP, the types and properties of CPs, the ink formulations and suitable substrates for the

printing with conductive polymers, as well as the applications of the IJP patterning of CPs. Considering this, the review represents the first comprehensive and focused overview of the fundamentals and applications of the inkjet printing method applied to conjugated (semi)conductive polymers.

## 2. Fundamentals of Inkjet Printing

### 2.1. Principles

Inkjet printing (IJP) is a process of digital patterning by the deposition of liquid droplets from a nozzle. Depending on the mechanism of droplet generation, the inkjet operation can be in continuous mode (CIJ) or drop-on-demand mode (DOD). In CIJ mode, the liquid is dispensed continuously under a constant pressure, forming a jet [16]. Under the dispensing conditions, the continuous jet breaks into a series of droplets with a highly reproducible volume. The deposition of the droplets is controlled by an electrostatic deflector. Uncharged drops are collected and recycled. Due to the high printing speed and low resolution, CIJ printers are used for high-throughput applications such as barcode printing and product marking [17].

In DOD mode, each droplet is dispensed on demand using the nozzle with an actuated fluid chamber. Dispensing of the individual droplets is governed by the pressure pulses generated by the thermal or piezoelectric pulse actuators for thermal and piezoelectric DOD inkjet printing, respectively. The thermal IJP fluid chamber contains the heating element, which generates the pressure pulse by boiling the solvent and, thus, is limited by low-boiling-point solvents and thermally stable materials [18]. The fluid chamber for piezoelectric IJP is equipped with a piezoelectric actuator, which generates the pressure pulse, which ensures the compatibility of this technology with a large variety of solvents and inks. Although both technologies are widely present on the graphic printing market, the IJ patterning of functional materials is mostly based on piezoelectric technology due to the compatibility with complex ink formulations [19]. Acoustic inkjet printing, when the droplet formation is driven by an acoustic wave in liquid, is known, although it is rarely used for the printing of CP-based ink [20].

### 2.2. Requirements for Inks

The physical properties of the inks for IJP must meet specific requirements. First of all, to be properly jetted, the dynamic viscosity of the ink should be relatively low, starting from 1 to 30 cP [21]. Since the inkjet nozzles are normally designed for Newtonian liquids, the possible non-Newtonian behavior of the polymer- and particle-based inks should also be considered [22]. The jet breakup and droplet formation are also affected by the dynamic surface tension of the ink: the surface the optimum value of the dynamic surface tension should exceed 20–40 mN m<sup>-1</sup>, although inks with higher surface tension are also suitable [23]. The wettability of the substrate, in turn, increases with decreasing static surface tension. This demands the fine-tuning of the surface tension properties of the inks [23].

Due to the small diameter of the nozzle, additional restrictions are applied on the particle or polymeric inks to prevent nozzle clogging. The riskiest are the particle inks with highly anisotropic particles such as fibers and nanotubes, since only a few particles can create an obstacle capable of blocking the whole flow. The typical size of the particle or macromolecule/globule should not exceed 100–200 nm. To comply with this requirement, the inks should be centrifuged and filtered through a fine (usually 0.22 μm) membrane filter prior to use. To decrease the material losses, inks may be treated with ultrasonic irradiation, aiming to break the larger particles into smaller ones.

A more complex criterion of the printability of inkjet inks could be described by the Ohnesorge (Oh) or inverse Fromm (Z) numbers (Equation (1)):

$$Z = \text{Oh}^{-1} = \frac{\sqrt{\rho\gamma d}}{\eta}, \quad (1)$$

where the optimal ink rheology corresponds to the  $1 < Z < 10$  range [24]. A more detailed description of the fluid dynamics of inkjet printing may be found elsewhere [25,26]. To adjust the viscoelastic properties of the inks, additives modify the surface tension and viscosity.

Solution inks based on linear polymers usually suffer from an excessive viscosity, which increases with the increasing  $\tilde{M}_w$  of the solute. The depression of the viscosity may be achieved by choosing a less viscous solvent or co-solvent, reducing the concentration of the polymer or increasing the temperature. The viscosity of the dispersion inks with nearly spherical particles is usually near the viscosity of the pure solvent, although they tend to exhibit non-Newtonian behavior. The particles suspended in the inks insignificantly change the surface tension of the solvent, while most linear polymers, especially amphiphilic ones, reduce this value. To lower the surface tension of the solutions or dispersion, surfactants such as sodium dodecylbenzenesulfonate or Triton are used. The ink formulation is the crucial step of the printing process, and therefore, the rheology of the functional ink should be evaluated and adjusted prior to printing.

The stability of ink formulations is a critical issue for the inkjet printing process, since the IJP equipment is extremely sensitive to the presence of the solid particles in the inks, which leads to nozzle clogging and serious damage to the printheads. In the case of polymer-based solution inks, particle formation may occur owing to the cross-linking of the polymer chains induced by the oxidation by the atmospheric oxygen in photochemical processes induced by ambient light. Cross-linking may be prevented by the addition of stabilizers and radical inhibitors; nevertheless, the inks should be filtered prior to use. Particle inks may suffer from precipitation and agglomeration, which are prevented by different methods. The precipitation stability of particle inks increases with decreasing particle size, decreasing the density difference between the particle and the medium, and increasing the solvent's viscosity. In most cases, dispersions of CPs filtered through a 0.22  $\mu\text{m}$  membrane are stable against precipitation on a long-time scale, although the precipitation can be reversed by agitating or shaking the inks. The aggregation behavior of particle inks is more complex and depends mostly on the structure of the particle surface. In most cases, aggregation is prevented by the addition of the appropriate surfactants.

### 2.3. Patterning Parameters

The typical diameter of a nozzle for IJP is 10–50  $\mu\text{m}$  and produces droplets ca. 25–200  $\mu\text{m}$  in diameter and 1–250 pl in volume, which determines the patterning resolution. The diameter of the dot on a solid surface like glass or plastics increases with the increasing wettability of the substrate by the ink, which can be quantified as the contact angle, but absorptive substrates such as paper or fabric exhibit more complex behavior due to the absorptive drying of the droplet [27]. The typical printed dot size starts from ca. 3  $\mu\text{m}$ , which corresponds to a resolution of ca. 8000 dpi. The accuracy of the droplet deposition, however, can be improved using feedback tools such as droplet imaging [28]. The assessment of the printing lateral resolution could be performed by visual analysis and direct size measurements on the images from optical, electron, or atom-force microscopy. The latter can also provide axial resolution.

Since the inkjet inks should not be viscous, the solid content of the inks usually does not exceed 1–2%, so the typical thickness of the printed pattern lies below a micrometer. Patterning on the solid surfaces suffers from the coffee ring effect, which leads to the migration of the ink material to the rim of the dot [29]. This effect is usually undesired due to the non-uniformity of the resulting dot/line, and substantial efforts are made to suppress it, although sometimes, this effect can be utilized to achieve advanced microstructuring [30]. Suppression of the coffee ring effect during IJP can be achieved by the addition of rheology modifiers to the ink, by governing the heat-, co-solvent-, or surfactant-induced Marangoni flow opposite the coffee ring effect flow, or by altering the wetting of the surface by pre-treatment or by physical stimuli [30]. The stability of inks is usually assessed by monitoring the stability of the dispersion parameters over time. The most useful are the monitoring of the optical properties (transmission and scattering) or dynamic viscosity. More direct

observation of the particle size distribution changes can be provided by a refractometric particle size analyzer.

Multi-layer printing by IJP is possible, which, in principle, enables additive manufacturing by 3D inkjet printing [10]. Although the thickness of one printed layer is usually too low to consider 3D printing in the common sense, this method is very suitable to create thin-film multilayered structures and all-inkjet-printed devices [31].

Depending on the interaction of the ink material with the substrate and post-treatment of the printed pattern, several results may be obtained [32]. The deposition of non-reactive inks can give absorbates, coatings, or composites. Printing solution inks containing small molecules such as organic dyes or dissolved polymers on absorbing substrates afford absorbates. Composites are formed during the filtration of particle-based inks such as graphene or insoluble conductive polymer formulations through the layer of the porous or fibrous substrate like paper. Coating of the substrate is possible in the case of low substrate wetting and good film-forming ability. Polymeric materials in solution and, to a lesser extent, in dispersion tend to form elastic films after drying.

Several approaches employing chemical reactions in the printing process or afterwards have been developed. Using a reactive ink, which can interact with the surface, chemical modifications such as grafting are possible [33]. Some materials can be formed by printing with precursor inks with subsequent physical or chemical treatment of the patterns. Sintering and annealing, thermal, chemical, UV or radiation curing, or gas phase or liquid phase treatment with reducing or oxidizing agents are all methods used for the post-treatment of the printed patterns [33]. For the patterning of conductive polymers, the gas phase polymerization approach can be employed [34,35]. First, the pattern of the oxidant is printed on the substrate, which is then subjected to the vapors of the monomer. The monomer vapors polymerize on the oxidant traces, forming a conductive polymer. The approach when the material is formed during or after the printing by means of chemical reaction is called reactive printing.

Inkjet printing combines high resolution with the freeform patterning of solutions and dispersions at a low price, becoming a unique tool for laboratory, industrial, and in-home micromanufacturing. As a templateless technique, IJP is inferior to screen and intaglio printing in the mass production of electronics, but surpasses them in customizability. Currently, only rare examples of the implications of IJP in the electronics industry are known, but the implications of this technology in the digital manufacturing sphere are continuously growing. Although inkjet technology was originally intended for 2D patterning due to the low layer thickness, it is also suitable for the fabrication of 3D structures with a micrometer-scale Z-axis dimension.

#### 2.4. Printing Equipment

CP inks can be patterned by both home and specially designed (professional) inkjet printers [36,37]. Among the home printers used for functional inkjet printing, Epson instruments are equipped with piezoelectric IJ nozzle chambers, while Canon and Hewlett-Packard bear thermal IJ chambers. The most significant difference for printing with functional inks arises from the action mechanisms of these nozzle chambers: thermal IJP requires a low-boiling-point (100 or below) solvent in the ink formulation, while piezoelectric head printers can operate with high-boiling-point formulations. Piezoelectric printheads are preferable for printing with particle inks or inks containing reactive substances, because the heating of such inks may induce the coagulation of the dispersion or decomposition/polymerization of the substance followed by the formation of insoluble products. Home printers usually bear up to six nozzles, while professional printers may be configured for more nozzles. The obvious advantage of the home IJP instruments is their affordable price, starting from ca. USD 200 for a paper-fed printer. Advanced models with functions like print-on-DVD, which enables printing on planar substrates, or ink feeding from external tanks, will cost below USD 500, which is ca. 2 orders of magnitude less expensive compared to professional printers.

Professional material printers such as the Dimatix Material Printer or Microdrop Autodrop provide ample opportunities for functional printing, such as variable nozzle inclination angles, three-dimensional printhead kinematics, substrate heating, etc. These printers are equipped with advanced printing imaging and control features such as a fiducial camera and support the variation of the printing conditions, including the waveform and amplitude of the printhead actuating signal. The details of the printer in contact with the ink are chemically resistant, which allows the use of various organic solvents for the ink formulation. The imaging tools of professional printers allow direct observation of the jetting of the ink, which is very useful for the development of novel ink compositions with unknown jetting properties.

### 2.5. Substrates

Inkjet printing is capable of patterning the inks on a large variety of rigid and flexible substrates. The interaction of the ink droplet with the substrate surface mostly determines the shape and morphology of the resulting printed pattern, which means that the proper choice of the substrate is very important [38]. Substrates may be classified by their mechanical properties as follows: rigid solid, flexible solid, rigid absorbing, and flexible absorbing substrates. Absorbing substrates absorb the liquid from the droplet deposited on the surface, which may result in the increased dot size and distribution of the solute or suspended particles in the thickness of the substrate, while solid substrates retain the dot material on the surface. Drying of the droplets on the absorbing substrates proceeds via absorption followed by evaporation from the volume of the material, while on solid substrates, the only means of drying is evaporation from the droplet surface. Rigid absorbing substrates are rarely used for functional IJP and will not be considered below.

Glass is a great example of a rigid solid substrate for IJP [39]. Glass can be used as-is, as a neutral transparent carrier, or coated with an ITO or FTO conductive layer. ITO glass is widely used for the inkjet-based fabrication of electrooptic or photovoltaic devices. Both pristine and ITO-coated glasses are highly wettable by water and organic solvents if clean. Pristine glass is inert to almost all chemicals, while ITO may be damaged by strong acids and bases, which should be considered when choosing the ink formulation. Any metal or polymer substrate also becomes rigid at increased thickness, although usually, there is no reason for functional printing on such substrates.

Flexible solid substrates are represented by polymer films and metal foils with a thickness of tens to hundreds of micrometers [40]. Metal foils, mostly Al and Cu, widely used as conductive substrates, are highly wettable by water and organic solvents. Metal foils may be subjected to corrosion with improper inks. Films of PET, polyester, polyamide, and some other polymers employed for IJP are highly wettable by organic solvents, but much more by water. PTFE films are poorly wettable by any solvents or inks. These substrates are relatively inert, but can swell in some organic solvents.

Paper, the most popular printing substrate, belongs to the class of flexible absorbing substrates, along with fabrics and fibrous materials [41]. Untreated paper is highly wettable by both water and organic solvents and rapidly absorbs them from the droplets, although most paper contains some modifiers like kaolin, calcium carbonate, paraffins, etc., to decrease the water wettability and absorbing ability. Laminated paper like photopaper also has significantly decreased absorption ability. Paper and some other fibrous or microporous materials may exhibit the chromatographic effect, which affects the radial distribution of the solute. Fabrics made of different materials can be used as substrates for IJP. Their wettability and absorbing properties are determined by the nature of the material and the structure of the textile. For example, textiles made from carbon fibers or nanotubes are hydrophobic, but highly wettable by organic solvents, especially aromatics.

Since the substrate is large compared to the size of the inkjet droplet, the wetting capacity of the absorbing substrates can be considered sufficient in any case, and the patterns appear completely dry immediately after printing. In the case of solid substrates, the evaporation of the solvent from the dot occurs as an isothermal process due to the high

heat capacity of the substrate. The evaporation rate strongly depends on the boiling point of the solvent and the diameter of the dot, the latter one being determined by the wettability of the substrate. To improve the wettability of solid substrates, pre-treatment procedures such as degreasing, surface etching, plasma, or ion treatment could be employed [42].

Functional inks may be inkjet printed over other functional layers deposited by various methods. In this case, the surface properties of the previous layer should be considered. For example, the surface may be hydrophobized by silanization—the formation of the organosilane layer. Inkjet printing on microtextured surfaces such as a microelectrode array is also possible. A self-aligned approach may be used to increase the patterning accuracy and printing resolution [43]. This approach implies that the substrate is pre-patterned at a high resolution by another technique. While printing, the dispensed droplets are aligned in a certain position by the pattern of the substrate, improving the accuracy of the droplet positioning. Pre-patterning can also be used for the vertical engineering of multilayer printing constructs (Figure 2).

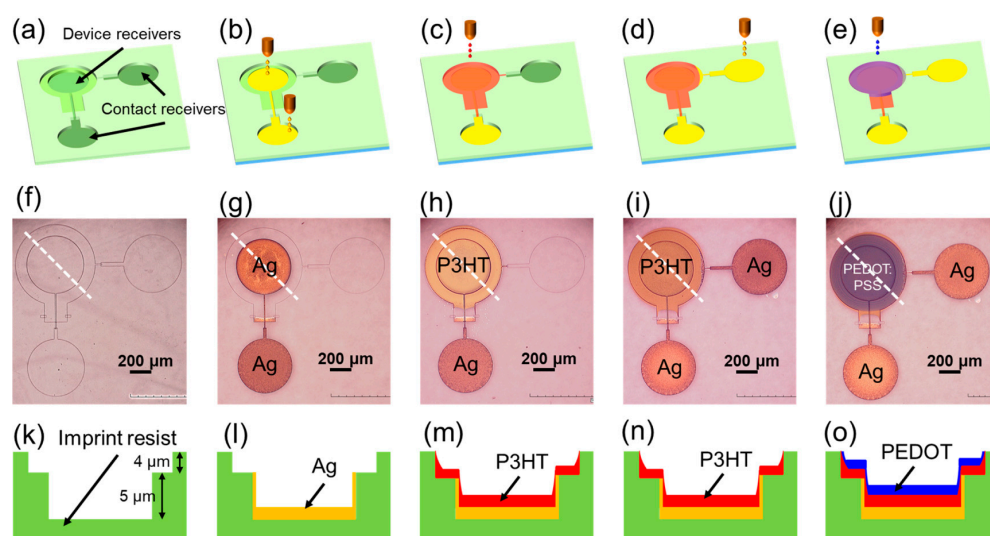


**Figure 2.** Vertical device fabrication on a pre-patterned substrate; (a–e) side view scheme, (f–j) top view microphotographs, (k–o) cross section scheme; reprinted with permission from [44].

One of the main advantages of IJP technology is the wide range of substrates suitable for printing. Due to the non-contact manner of the printing process, the thickness, density, and mechanical properties of the substrate do not affect the result. For rigid substrates, IJ printers provide the possibility for a planar feed analogous to 3D printers; for example, many home printers support the CD print option with a planar feeder. For flexible materials like papers or fabrics, a reel feed could be used.

### 3. Materials for Printing

Conjugated polymers (CPs) consist of macromolecules that are characterized by a backbone chain of alternating double- and single-bonds, forming a single  $\pi$ -system. Due to the high delocalization of the electrons along the conjugated chains, these polymers exhibit interesting electrical, electrochemical, and photophysical properties. But, at the same time, their rigid conjugated structure limits their solubility [44], and most of the CP-based inks, such as PEDOT:PSS, usually comprise nanoparticle dispersions. To make the CPs solution-processable, solubilizing groups are implemented on the side chain of the polymer. Long and/or branched alkyl chains provide solubility in aromatic or organochlorine solvents, which allows the preparation of the solution inks, but they require more sophisticated printing equipment. This approach is widely implemented for semiconducting CPs. Water-soluble CPs, which contain charged fragments, have been known for a long time, but they are rarely used for inkjet printing [45]. The solution processability of CPs can also be

achieved by employing a reactive printing approach, while a soluble precursor or reagent is inkjet printed.

A subclass of conductive polymers, which are characterized by high electrical conductivity, is distinguished from CPs. Due to their electrical and electrochemical properties, these polymers attract significant attention as functional materials for printed and miniaturized electronics [8]. Among the most popular conductive polymers are poly(ethylenedioxythiophene) (PEDOT), poly(3-hexylthiophene) (P3HT), polyaniline, polypyrrole, polyfluorenes, etc. Semiconducting CPs also meet their application in printed electronics, mostly in photovoltaics and light-emitting devices. The electrical conductivity and other functional properties of conductive polymers depend on their doping level, i.e., oxidation degree.

The main advantage of CPs over inorganic materials for IJP is their high stretchability and bendability, which is beneficial for their use in flexible and stretchable devices [46]. In addition, CPs combine distinctive electrical, photophysical, or electrochemical properties, which allows their utilization as multifunction materials [7].

The widely tunable electrical conductivity of CPs, ranging from nearly metallic conductivity to semiconductivity, allows their use as conductive and semiconductive parts in organic electronics. Due to the low band gap, CPs can efficiently absorb visible light, which, in combination with electronic conductivity, makes them suitable candidates for photovoltaic and photoconductive devices. Conversely, semiconducting CPs can be used in light-emitting devices for the same reasons. As redox-active materials, CPs are employed as catalysts and chemosensitive and energy storage materials.

When the electrical conductivity of pristine CPs remains insufficient for particular needs, ink formulations may be supplemented with metal particles [47] or carbon nanomaterials [48,49], affording composite material patterns. This approach can also be used for the introduction of functional particles to the printed composite.

### 3.1. Synthetic Approaches

Conjugated polymers for inkjet printing may be obtained using different synthetic approaches. Since many factors affect the properties of CPs, including the MM distribution, regioregularity, morphology, doping degree, etc., the same polymers obtained by different approaches may significantly differ in their properties [45]. Insoluble CPs such as PEDOT:PSS are poorly defined macromolecular objects since it is impossible to observe their individual macromolecules in solution. Thus, the characterization of such CPs is a challenging task and does not provide sufficient information on their macromolecular structure, and the reproducibility of the functional properties from sample to sample requires thorough evaluation of the synthetic procedure.

The most general approach to the synthesis of CPs is based on a metal-catalyzed coupling of aryl halides or their synthetic equivalents by the Yamamoto, Suzuki, Stille, Kumada, Heck, or Sonogashira coupling reactions [46]. However, due to the experimental complexity and high price of the reagents, this approach has limited implementation. The Yamamoto reaction affords homopolymers from different dihaloarenes using the reductive Ni(0) reagents (Figure 3a). Suzuki, Stille, and Negishi cross-couplings allow the bond formation between aryl halides with arylboronates, arylstannanes, or arylzinc halides, respectively, using Pd catalysts, which can be employed in the synthesis of polyarylenes (Figure 3b,c). The coupling of aryl halides with Grignard reagents with Ni-based catalysts, or Negishi coupling, can also be used for the synthesis of polyarylenes. Heck cross-coupling enables the synthesis of vinyl arenes via the Pd(0)-catalyzed coupling of aryl halides with terminal alkenes, which opens the route to poly(arylenevinylenes) (Figure 3d). The Sonogashira reaction results in the formation of arylacetylene from aryl halides and terminal acetylenes (Figure 3e).

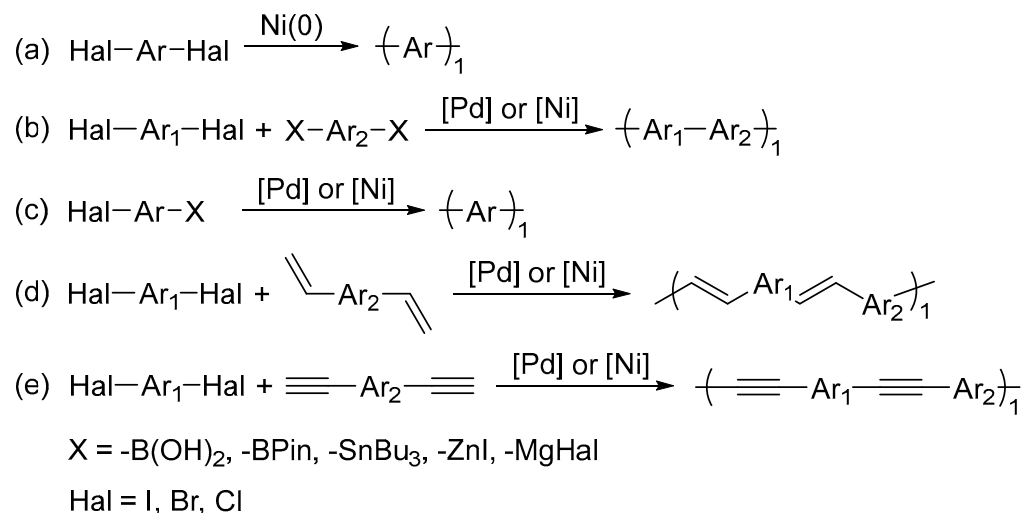


**Figure 3.** Variations of the metal-catalyzed coupling for the synthesis of conjugated polymers.

Cross-coupling reactions are widely used to prepare various conjugated polymers such as polythiophenes, polypyrroles, polyphenylenes, poly(phenylenevinylene)s, polyfluorenes, etc. These methods are suitable for the synthesis of highly regioregular CPs, for example, widely used in photovoltaics regioregular poly(3-hexylthiophene) (rr-P3HT), which are not available as such a regioregular by the oxidative polymerization approaches [47].

For the synthesis of the alkene-based conjugated polymers, some special approaches are employed [48]. Polyacetylenes can be prepared by the polymerization of acetylenes with the Ziegler–Natta or Luttinger catalysts (Figure 4a). In addition, polyacetylenes may be synthesized by elimination from poly(vinylhalides) or by retro-cycloaddition reactions [49]. The variety of synthetic methods provides control over the structure of polyacetylene: polymerization at lower temperatures affording polyacetylene with the predominating *cis*-configuration of the double-bond, while at temperatures closer to ambient, a more conductive all-*trans* polymer is formed.

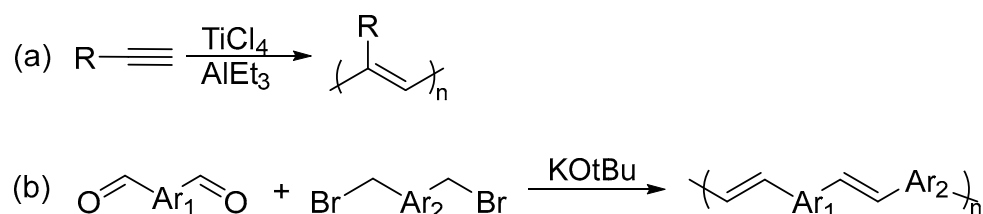


**Figure 4.** (a) Ziegler–Natta polyacetylene synthesis; (b) Wittig poly(arylenevinylene) synthesis.

As an alternative to Heck coupling, poly(arylenevinylene)s can be synthesized by the Wittig or Horner–Wadsworth–Emmons reaction between arylcarbaldehyde and arylmethylphosphonium ylide (Figure 4b). The alkene metathesis reaction can also be used for this purpose. Donor–acceptor polymers, consisting of alternating monomeric units with different properties, are mostly synthesized by the cross-coupling reactions of Wittig olefination.

The CPs obtained by the abovementioned methods are electroneutral and, thus, possess low electrical conductivity. If the polymers are required to be in the conductive state, oxidative doping is used, when the polymer is treated with an oxidative agent, for example with iodine vapors. The oxidation of the polymer leads to the formation of hole charge carriers (polarons) on the macromolecular chains, which enhance the electrical conductivity [50].

The most suitable approach for the synthesis of highly conductive polymers is based on oxidative polymerization. Benzene and a large variety of electron-rich aromatic molecules such as thiophene, pyrrole, or aniline undergo polymerization upon chemical or electrochemical oxidation (Figure 5). Commonly used oxidants are  $\text{FeCl}_3$ ,  $\text{Fe(OTf)}_3$ , or  $(\text{NH}_4)_2\text{S}_2\text{O}_8$ ,

but other oxidants like  $\text{Cu}^{2+}$  or  $\text{Ag}^+$  salts are also suitable [8]. The most popular commercial conductive polymers like PEDOT:PSS or polyaniline are produced by this method. Alternatively, the same monomers can be polymerized by electrochemical oxidation. Unfortunately, electrochemical oxidation affords the polymer as a film coating the electrode and is rarely suitable for the preparation of IJP inks. This approach affords oxidized polymers, which is beneficial for applications requiring high electrical conductivity.

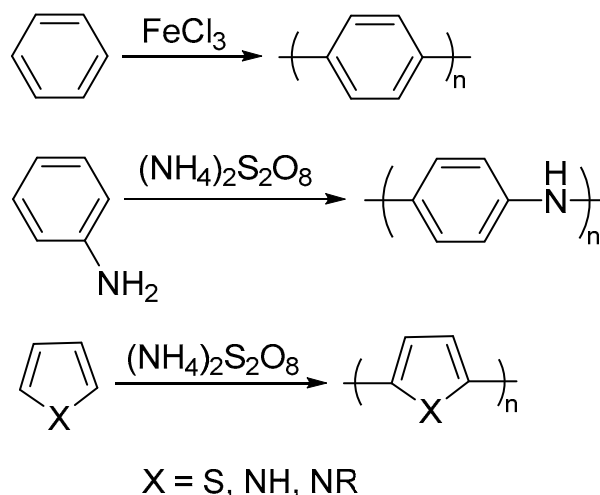


**Figure 5.** Oxidative polymerization of benzene and five-membered heterocycles.

To improve the conductivity of the polymers, polymerization may be conducted in the presence of anionic polyelectrolytes. For example, the electrical conductivity of PEDOT:PSS obtained from a solution containing poly(styrenesulfonate) (PSS) is several orders of magnitude higher compared with PEDOT polymerized with low-molecular anions [51]. The conductivity of PEDOT:PSS can be further improved by post-synthesis treatment with high-boiling-point solvents like DMSO or ethylene glycol and/or non-ionic surfactants.

Polycondensation and cross-coupling polymerization reactions afford the main chain-undoped semiconductor CPs; most of them are soluble in organic solvents like xylene and are suitable for inkjet printing as-is. These polymers have relatively high  $M_w$  values, and their macromolecular structure can be studied by solution-based techniques. To obtain conductive patterns from these CPs, the printed elements may be treated with an oxidant; for example, polyacetylene patterns exposed to  $\text{I}_2$  vapors turn from semiconductors to highly conductive materials. In contrast, CPs from oxidative polymerization are obtained in the doped state, which provides high electrical conductivity, but most of them are insoluble and form solid precipitates, which requires pre-treatment such as grinding and dispergation before being used as inks for IJP.

### 3.2. Polythiophenes

PEDOT:PSS is a workhorse of the organic electronics industry (Figure 6a), which is widely used in organic electronics, photovoltaics, electrocatalytic electrodes, etc. Commercial PEDOT:PSS inks represent 1–5% stable aqueous dispersions with a low fraction of particles larger than 100 nm in diameter, with a dynamic viscosity of ~10–30 cP, which makes them suitable for IJP as received as specified by the manufacturer [52]. However, to remove the aggregates that may form during storage, these inks should be filtered through a 0.22  $\mu\text{m}$  membrane or a syringe filter.

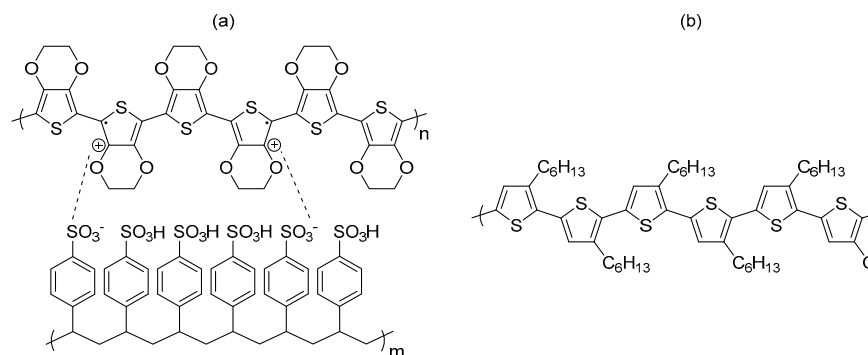


**Figure 6.** Structure of (a) PEDOT:PSS and (b) P3HT.

The electrical conductivity of PEDOT:PSS as obtained reaches the order of  $1 \text{ S cm}^{-1}$ , and can be further improved by a well-established procedure of post-treatment with high-boiling-point solvents or surfactants. The electrical conductivity of the treated PEDOT:PSS can reach  $\sim 100\text{--}200 \text{ S cm}^{-1}$ , which is only 1 order of magnitude lower than for graphite or 3.5 orders of magnitude lower than for graphene. The conductivity of the IJ-printed PEDOT:PSS patterns is sufficient for the fabrication of electrical circuits. PEDOT:PSS is a p-type conductive polymer with a band gap of  $\sim 3 \text{ eV}$ .

Another common thiophene-based p-type (semi)conductive polymer is P3HT (Figure 6) [53]. Regiorandom P3HT can be prepared via oxidative polymerization, but Negishi coupling or Kumada polycondensation, also called Grignard metathesis (GRIM), affords regioregular P3HT with low polydispersity and an  $\tilde{M}_w \sim 50\text{--}100 \text{ kDa}$  [54]. The resulting rr-P3HT is widely used in photovoltaics as a photoactive donor phase due to the high crystallinity, high p-type charge mobility, low band gap of 2 V, and highly lying HOMO, which fits with the LUMO of the common acceptors like PCBM. The conductivity of rr-P3HT in the neutral state is  $10^{-6}\text{--}10^{-7} \text{ S cm}^{-1}$ , which is three orders of magnitude higher compared with the regiorandom polymer, and a band gap of  $\sim 1.7 \text{ eV}$ . In the doped state, the conductivity may be increased to ca.  $10^3 \text{ S cm}^{-1}$ , which is comparable to PEDOT:PSS.

Since P3HT is soluble in some organic solvents [55], it can be printed from solution in chloroform, chlorobenzene, or another suitable organic solvent, preferably high-boiling-point aromatics. The concentration of the solutions is usually adjusted to maintain the viscosity of the ink within the printable range. P3HT is insoluble in water or alcohols. Typical solvents to prepare P3HT-based inks are xylene or chlorobenzene, which means the necessity of the professional IJP equipment to pattern this polymer. For photovoltaic purposes, the composite inks containing P3HT and fullerene or non-fullerene acceptors are widely used [56]. These inks afford blended patterns with a bulk heterojunction morphology suitable for solar cells. In the same manner, poly(3-octylthiophene) (P3OT) inks are also employed [57].

Inkjet inks with poly(3,3'-dipentoxybithiophene), poly(3,3'-dipentoxyterthiophene) [58], poly[5,5'-bis(3-dodecyl-2-thienyl)-2,2'-bithiophene (PQT-12)] [59], and some substituted poly(propylenedioxythiophenes) [60] have also been reported. The variation of the side chain substituents allows the fine-tuning of the morphology and the charge transport properties of the donor phase formed from these polymers. In addition, inkjet printing with the thiophenothiophen-containing polythiophenes [61] and polyselenophenes [62] with a distinctive electronic structure is described in the literature.

### 3.3. Polyanilines

Oxidative polymerization of aniline affords the conductive material called polyaniline (PANI). Although the most common oxidant for the polymerization of aniline is ammonium persulfate (APS), other oxidants such as  $\text{HAuCl}_4$  are employed [63]. Depending of the synthesis conditions, PANI specimens of different structure and oxidation degrees can be obtained. The most common PANI, including the commercial samples, consists of

linear polyaniline macromolecules in a semi-oxidized state called emeraldine (Figure 7). Protonated emeraldine or emeraldine salt (ES) possesses the highest electrical conductivity of up to  $10 \text{ S cm}^{-1}$  [64]. Deprotonation of the ES, usually with  $\text{NH}_4\text{OH}$ , affords the emeraldine base (EB) with 7–10 orders of magnitude lower conductivity. At the same time, EB is soluble in some polar organic solvents like NMP [65], while ES shows poor solubility. The band gap of PANI, which is a p-type CP, varies from  $\sim 2.8 \text{ eV}$  for ES to  $\sim 3.8 \text{ eV}$  for EB [66]. The most popular doping electrolyte for the synthesis of the ES polymer is dodecylbenzenesulfonic acid (DBSA) [67], but the same as PEDOT, PANI can also be doped with anionic polyelectrolytes such as PSS; the same as for PEDOT, such doping increases its conductivity, although the effect is much weaker [68].

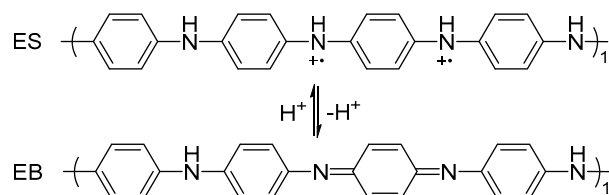


**Figure 7.** Structure of linear PANI base and salt.

Due to the high conductivity, low price, and diverse functional properties, PANI-based inks are widely used, especially in mass production. Printable ES PANI inks, including the commercial ones, are mostly water based and suitable for patterning by home IJ printers with both thermal and piezo nozzle chambers. The rheology of PANI inks prepared in certain conditions complies with the requirements of IJP and can be adjusted by SDS or other surfactants, which also stabilize the dispersion [69]. However, ES PANI inks based on organic solvents without any rheological modifiers are also available and suitable for IJP [70]. Solution inks based on the EB PANI, dissolved in polar organic or water-organic solvent systems, have also been reported [65].

### 3.4. Alkene-Based Polymers

Alkene-based CPs are mostly represented by poly(phenylenevinylene) (PPV) and its derivatives, which are accessible via Horner–Wadsworth–Emmons (HWE) polycondensation (Figure 8) [71]. The alkoxy-substituted derivative, MEH-PPV, is soluble in organic solvents such as chlorobenzene or toluene, and these solutions can be inkjet printed as-is [72]. Alternatively, an aqueous particle ink can be prepared from MEH-PPV using PEG and SDS stabilizers [73]. To obtain the aqueous solution inks based on the PPV polymer, water-soluble MPS-PPV polymer was synthesized [74]. Other PPV derivatives [75] including the heterocycle-based ones [76] are also used for inkjet printing.

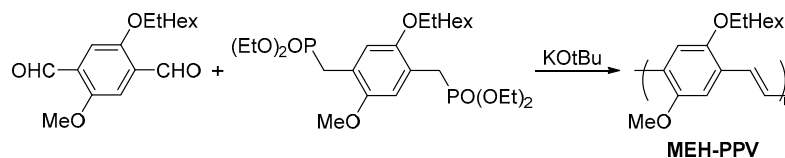


**Figure 8.** Scheme for the Horner–Wadsworth–Emmons synthesis of MEH-PPV.

Alkyne-containing CPs for inkjet printing are represented by poly(phenyleneethynylene)-*alt*-poly(phenylenevinylene) (PPE-*alt*-PPV), a copolymer with alternating phenyl rings with adjacent double- and triple-bonds accessible via Sonogashira cross-coupling [77]. This polymer is also printed as-is from the solutions in aromatic solvents [78]. Both the PPV and PPE-*alt*-PPV polymers behave as p-type semiconductors with a conductivity of  $10^{-11}$ – $10^{-8} \text{ S cm}^{-1}$  and a 2.2–2.4 eV band gap, which correspond to green light, and are highly beneficial for photovoltaic and light-emitting applications [77,79].

### 3.5. Donor–Acceptor Polymers

The next generation of low-band-gap semiconducting polymers is represented by conjugated copolymers consisting of alternating electron-donating and electron-withdrawing fragments, namely donor–acceptor (DA) polymers [80]. To date, a large variety of n- and p-type DA polymers is known, and plenty of them meet their application in inkjet-printed electronics. The donor and acceptor fragments of different structures are used for the design of the DA polymers with desired energy levels, band gaps, and charge carrier types (Figure 9).

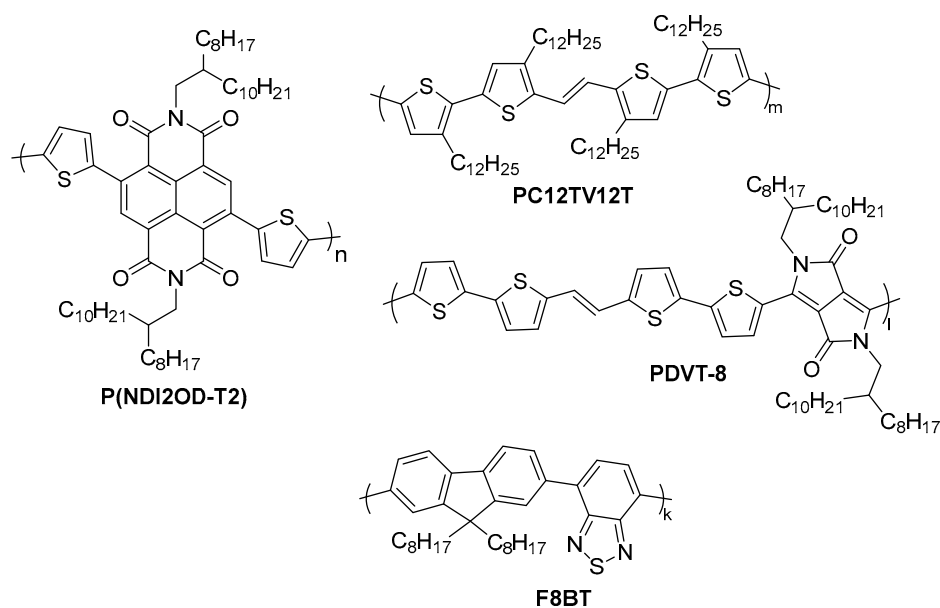


**Figure 9.** Structures of P(NDI2OD-T2), PC12TV12T, PDVT-8, and F8BT.

One of the frequently used commercially available n-type semiconducting DA polymers is poly([N,N'-bis(2-octyldodecyl)-naphthalene-1,4,5,8-bis(dicarboximide)-2,6-diyl]-alt-5,5'-(2,2'-bithiophene)) (P(NDI2OD-T2)), which consists of alternating naphthalenediimide and bithiophene fragments. The preparation of P(NDI2OD-T2) is possible by means of either Stille or Yamamoto coupling starting from different monomers, affording polymers with a broad  $\tilde{M}_w$  range of 10–300 kDa [81]. The conductivity of the undoped polymer is  $10^{-8} \text{ S cm}^{-1}$  [82], while for heavily n-doped samples, it increases up to  $10^{-3} \text{ S cm}^{-1}$ . Due to the narrow (1.6 eV) band gap and high charge mobility (up to  $\sim 10^{-1} \text{ cm}^2 \text{ V}^{-1} \text{ s}^{-1}$ ), this polymer is widely used in photovoltaics and organic electronics [83]. The solubility of P(NDI2OD-T2) in aromatic solvents such as xylene or *o*-dichlorobenzene allows the formulation of solution inks for IJP.

The variety of p-type DA polymers used for inkjet printing is represented by several classes of complex copolymers tailored like a DNA sequence from the limited set of monomeric units. Such polymers are mostly prepared by the metal-catalyzed cross-couplings except the vinylene-containing ones, which are accessible via the Horner–Wadsworth–Emmons reaction. The resulting substances are soluble in chlorinated and aromatic solvents, and the resulting solutions are suitable for IJP as-is [84–86].

The family of polymers based on thiophene and thiazole monomeric units include the commercially available PC12TV12T [84] and some other polymers [85,86]. The diketopyrrole pyrrole-based family of DA polymers includes commercial PDVT-8 with thiophene and ethylene co-monomeric units [87] and other copolymers containing fluorene [88], thiazole [89], or azine [90] units. The benzothiadiazole-based family of DA polymers, besides the commercial F8BT [91], which also contains the fluorene units, comprises polymers containing more complex co-monomers [92–95]. Advanced donor–acceptor conjugated

polymers provide a versatile platform for the fine-tuning of their band gaps and charge mobility and, thus, are employed as semiconductors in transistors and photovoltaic devices.

### 3.6. Miscellaneous Polymers

Although polypyrroles (PPy, Figure 10), along with polythiophenes and polyanilines, are the best discovered conductive polymers, they have met only a limited utilization for IJP. PPy is a p-type conductor with a moderate band gap of  $\sim 2.25$  eV [96]. These CPs exhibit high electrical conductivity up to  $2000 \text{ S cm}^{-1}$  [97] and are in general more electron-rich in comparison with thiophenes or anilines, which is reflected in the high lying energy levels and lower oxidation potentials.

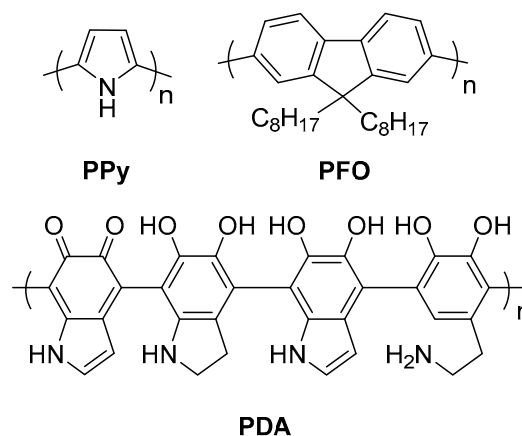


**Figure 10.** Structures of the PPy, PFO, and PDA.

Polypyrrole, accessible from the polymerization of 1H-pyrrole by chemical oxidants, is the N-containing structural analog of polythiophene, but it has found only a limited application in printing electronics. Oxidative polymerization with ferric salts using the gemini surfactant as the dopant and PVA as the stabilizer affords printable PPy [98]. The PPy particles are poorly stable in aqueous dispersions and need to be stabilized by polyvinyl alcohol or low-molecular-weight surfactants in the ink formulation [99].

Inks based on polyfluorenes, which can be synthesized via the Suzuki reaction, are also employed for inkjet printing. Commercial poly(9,9-dioctylfluorene) (PFO, Polymer 196, Figure 10) and poly(9,9-dihexylfluorene) (PF6) with an  $\tilde{M}_w$  of 20–50 kDa are soluble in chlorinated and aromatic solvents and can be printed as-is [100,101]. Alternating copolymer of fluorene derivatives with phenylene co-monomeric units [102] and polymeric spirobifluorenes [103] are also known to be inkjet printed. PFO and PF6 have a moderate band gaps of 2.8–3.0 eV, which corresponds to blue or violet light, and thus, are used as the blue emitters in OLEDs.

Dopamine (3,4-dihydroxyphenethylamine) undergoes self-polymerization in air in aqueous Tris buffer, affording a stable dispersion of polydopamine (PDA, Figure 10) polymer nanoparticles [104]. An aqueous dispersion of PDA can be employed as IJ inks as-is. The structure of the polymer is poorly discovered. Several reports are known describing IJP with triarylamine-based inks [105]. The electrical properties of PDA are close to those of PANI or poly(2-aminophenol), but polydopamine exhibits some distinctive adhesion properties and shows better flexibility and stretchability.

The choice of the polymer for a certain task depends on the required electrical, electrochemical, or optical properties. In addition, the formulation may be chosen for the reason of compatibility with the substrate or other printed layers. A brief overview of the most common types of the CPs and their inks is presented below (Table 1).

**Table 1.** Overview of CPs and inks for inkjet printing.

Polymer	Electrical Conductivity	p/n	Polymerization Method	Form <sup>1</sup>	Applications <sup>2</sup>
PEDOT:PSS	High/medium	p	Oxidative	AqD	WC, LE, PV, SA, ES
PANI	High/medium	p	Oxidative	AqD, OS	WC, LE, PV, SA
PPy	High/medium	p	Oxidative	AqD	WC, SA
P3HT/P3OT	Medium	p	Cross-coupling Oxidative	OS	SC, PV, LE
PVVs	Low	p	HWE Cross-coupling	OS, AqS	SC, LE
DA polymers	Medium/low	p/n	Cross-coupling	OS	SC, PV, LE, SA
Polyfluorenes	Medium/low	p	Cross-coupling	OS	SC, LE, PV

<sup>1</sup> AqS—aqueous solutions, AqD—aqueous dispersions, OS—solutions in organic solvents, <sup>2</sup> WC—wiring and conductive elements of devices, SC—semiconductor devices, LE—light-emitting devices, PV—photovoltaic devices, SA—sensors or actuators, ES—energy storage.

#### 4. Applications

The chemical diversity of (semi)conductive polymers forms a large pool of functional materials with different electrical, photophysical, and electrochemical properties, offering functional materials for various applications. The ability of inkjet printing technology for the patterning of the micrometer and sub-micrometer layers of CPs makes it a perfect tool for the patterning of thin film and planar elements and devices. Plenty of planar semiconductor devices and circuits, photovoltaic elements, light-emitting devices, sensors, and actuators employing inkjet-printed CP elements are reported in the literature. In this section, the applications of inkjet patterned (semi)conductive polymers and the relation of their properties to the functional characteristics of the resulting devices are overviewed.

CPs for inkjet printing could be divided into two types: highly conductive polymers and semiconductive polymers. Highly conductive polymers, namely PEDOT, PANI, and PPy, are mostly considered in device engineering as a replacement for the metallic elements due to their conductivity of up to 1000 S cm<sup>-1</sup> [106]. However, in contrast to metallic conductors, these polymers have dominant p-type conductivity and, thus, form junctions in contact with n-type semiconductors. This peculiarity enables the use of these polymers as an electron-blocking conductive layer, e.g., in solar cells. Semiconductive polymers with various structures are used as an alternative to inorganic semiconductors in various semiconductor devices. The easy tuning of the energy of frontier orbitals (semiconductor zone boundaries), the band gap value, and the concentration and mobility of the charge carriers make these materials a valuable replacement for the convenient semiconductors [107]. Inkjet deposition provides significant facilitation of the patterning process in comparison with vapor deposition and other techniques for the deposition of inorganic materials.

##### 4.1. Semiconductor Devices

Inkjet printing of (semi)conductive polymers is a versatile tool for the maskless prototyping and manufacturing of semiconductor devices. The patterning resolution of IJP allows the low-cost and material-economic maskless deposition of thin films of (semi)conductive polymers for the fabrication of miniaturized semiconductor devices [7,12]. Inkjet printing secures the effective contact between the printed layer, minimizing the contact resistance and increasing the efficiency of semiconductor devices. CPs with medium conductivity such as rr-P3HT, polyfluorenes, or DA polymers are employed in printed semiconductor layers due to the low concentration of the minority charge carriers. Highly conductive CPs like PEDOT:PSS or PANI can be used for the patterning of the contacts of semiconductor devices or act as p-type materials in the junctions of bipolar devices. Al-

though both the horizontal and vertical alignments of semiconductor devices are accessible via IJP, the latter one is preferable.

The IJP technique was implemented for the first time to manufacture a vertically stacked Schottky diode, in which the rr-P3HT layer was inkjet printed on the surface of a gold bottom contact, followed by the deposition of an aluminum top contact [108]. Using the imprinted substrates, fully printed vertically stacked Schottky Ag/rr-P3HT/PEDOT:PSS diodes with a rectifying ratio of up to  $10^4$  were obtained [44]. The fabrication of p-n diodes is also possible by means of IJP; for example, horizontal diodes based on PEDOT/PPV and PPy/PPV junctions were printed on patterned ITO microelectrodes [109]. Vertical p-n diodes based on the PEDOT:PSS/TIPS-pentacene junction were also reported [110]. An inkjet-printed PEDOT:PSS top contact was also employed for vertically stacked  $\text{In}_2\text{O}_3/\text{CuO}$  and  $\text{In}_2\text{O}_3/\text{NiO}$  diodes [111]. Metal–insulator–semiconductor diodes based on Ag and PEDOT:PSS as contacts, PMMA-PMMA as the insulator, and polytriarylamine as the semiconductor were manufactured by means of inkjet printing [112]. Electromechanical devices, i.e., membrane actuators based on inkjet-printed PEDOT:PSS [113] or PEDOT:PSS/carbon aerogel [114,115], electroactive layers are known. Artificial muscle actuators can also be inkjet printed with PEDOT:PSS inks [116].

Extensive efforts have been made towards the IJP manufacturing of organic field-effect transistors (FETs). FET are unipolar semiconductor devices with the gate (G) isolated from the rest of the device by the insulating (I) layer, which controls the current in the semiconductor (SC) between the source and drain (S/D) by an electric field (Figure 11). The main characteristic parameters of FETs that are most frequently reported in the literature are the charge mobility of the semiconductor  $\mu$  and  $I_{\text{on}}/I_{\text{off}}$  ratio. The charge mobility  $\mu$  ( $\text{cm}^2 \text{V}^{-1} \text{s}^{-1}$ ) reflects the average velocity of the charge carriers in proportion to the applied electric field and is connected to the conductivity  $\sigma$ , charge carrier charge  $q$ , and concentration  $n$ :

$$\sigma = \mu q n \quad (2)$$

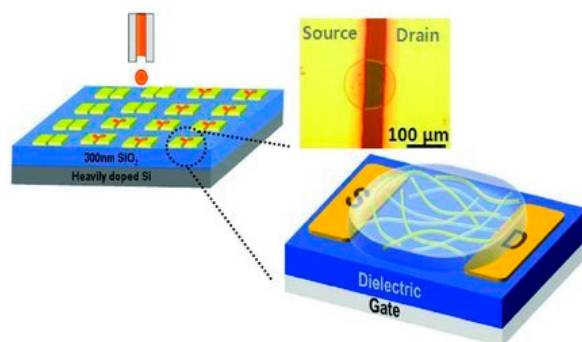


**Figure 11.** Schematic representation of the IJP of a bottom gate FET, with permission from [117].

Practically, lower  $\mu$  values mean lower power consumption and thermal power dissipation of the element based on this semiconductor. The  $I_{\text{on}}/I_{\text{off}}$  is the dimensionless value, which is connected to the leakage current of the transistor.

The transistors can be printed on different rigid and flexible substrates using either top gate or bottom gate configurations. Inkjet printing with highly conductive PEDOT:PSS may be employed for the fabrication of S, D, and G electrodes, while the semiconductor layer may be printed with rr-P3HT or other semiconductive CPs. IJP technology is a powerful tool for the fabrication of transistors for various demands, for example megahertz-class transistors with an operating frequency of up to 22 MHz, which complies with high-frequency RFID [118]. Horizontally aligned FETs with side-gate configurations were fabricated using an inkjet-printed P3HT semiconductor layer [119]. Using the inks containing light-sensitive CPs PDPP-DBTE [120] and PDPPTzBT [121], phototransistors can be printed. The detailed information of the scope, materials, and key parameters of inkjet-printed FETs is summarized below in Table 2.

Table 2. Summary of inkjet-printed FETs. Inkjet-printed components are highlighted with bold.

Channel <sup>1</sup>	Gate	Insulator <sup>2</sup>	Source/ Drain	Substrate <sup>3</sup>	$\mu$ , $\text{cm}^2 \text{V}^{-1} \text{s}^{-1}$	$I_{\text{on}}/I_{\text{off}}$	Configuration <sup>4</sup>	Ref.
P3OT	Si+Al-RS	SiO <sub>2</sub>	Au	Si	$2 \times 10^{-3}$	$2 \times 10^4$	BG	[122]
F8T2	<b>Ag</b> <b>PEDOT:PSS</b>	PVP	<b>PEDOT:PSS</b>	Glass	$2 \times 10^{-2}$	$10^5$	TG	[123]
PPy	<b>PEDOT:PSS</b>	K60	<b>PEDOT:PSS</b>	SiO <sub>2</sub>	$10^{-1}$	$3 \times 10^3$	BG	[124]
F8T2	<b>PEDOT:PSS</b>	PVP	<b>PEDOT:PSS</b>	SiO <sub>2</sub>	$10^{-3}$	$10^4$	TG	[125]
P3HT	<b>PEDOT:PSS</b>	PVP	Ag	PE	-	$10^2$	TG	[126]
TIPS	ITO	Al <sub>2</sub> O <sub>3</sub>	<b>PEDOT:PSS</b>	Glass	$3 \times 10^{-1}$	$10^5$	BG	[127]
P3HT	Doped Si	SiO <sub>2</sub>	Au/Ti	Si	$6 \times 10^{-3}$	$10^6$	BG	[117]
pBTBT	Doped Si	SiO <sub>2</sub>	Au	Si	$10^{-1}$	$10^7$	BG	[61]
P3HT/C	Au	SiO <sub>2</sub>	Au	Si	$6 \times 10^{-3}$	$10^4$	BG	[128]
<b>PQT12</b> <b>P3HT</b> <b>F8T2</b>	Al	PMMA PVP	Au/Ni	Glass	$8 \times 10^{-2}$	$5 \times 10^3$	TG	[129]
TIPS	<b>PEDOT:PSS</b>	PMMA	<b>PEDOT:PSS</b>	-	$10^{-1}$	$10^2$	BG	[130]
PHTBTz-C8	Mo	SiO <sub>2</sub>	Au	SiO <sub>2</sub>	$2.5 \times 10^{-1}$	$10^7$	BG	[86]
TIPS/triarylamine	Cu	CYTOP	<b>PEDOT:PSS</b>	PET	$2 \times 10^{-1}$	$3 \times 10^2$	TG	[131]
<b>P3HT</b> <b>PC12TV12F</b> <b>P(NDI2OD-T2)</b> <b>PTVPhI-Eh</b> <b>F8BT</b> <b>PDTTDPP</b> <b>DPPT-TT</b>	Al	PMMA P(VDF-TrFE)	Au/Ni	PEN	2.3	$10^5$	TG	[132]
<b>P(NDI2OD-T2)</b>	Al	PMMA	Au/Cr	Glass	6.4	$10^7$	TG	[133]
<b>PQBTz-C12</b> <b>PQBTz-C12/PS</b>	-	SiO <sub>2</sub>	Au/Ti	Si	$4.6 \times 10^{-2}$	-	BG	[134]
<b>PDVT-8/PS</b>	Doped Si	SiO <sub>2</sub>	Au	Si	$5.8 \times 10^{-1}$	$2 \times 10^3$	BG	[135]
<b>DPPT-TT</b> <b>P(NDI2OD-T2)</b>	-	-	-	-	-	-	-	[136]
<b>PDVT-8/PS</b>	Doped Si	SiO <sub>2</sub>	Au	Si	1.5	$10^5$	BG	[137]
P(NDI2OD-T2)	<b>PEDOT:PSS</b>	PMMA	Ag	Glass	$9 \times 10^{-1}$	-	TG	[138]
TIPS	Ag	PVP	<b>PEDOT:PSS</b>	PEN	1	$3 \times 10^3$	BG	[139]
<b>P3DT/CNT</b>	<b>PEDOT:PSS</b>	PMMA	Au/Cr	Glass	15	$10^7$	TG	[140]
TIPS	Ag	Parylene C	<b>PEDOT:PSS</b>	PI	$4 \times 10^{-1}$	$10^5$	BG	[141]
<b>P(NDI2OD-T2)</b> <b>IDTBT</b>	Al	PMMA/ Parylene C	Au/Ni	Glass	$5 \times 10^{-1}$	-	TG	[95]
<b>P(NDI2OD-T2)</b>	<b>PEDOT:PSS</b>	PMMA	<b>PEDOT:PSS</b>	PEN	$2.5 \times 10^{-1}$	$10^4$	TG	[142]
<b>P12CPDTBT/CNT</b>	Al	PMMA	Au/Cr	Glass	20	$10^7$	TG	[92]
DPPT-TT	<b>PEDOT:PSS</b>	PS	Ag	Glass PEN	1.6	$10^3$	TG	[118]
<b>P(8T2Z-co-6T2Z)-12</b>	Mo	SiO <sub>2</sub>	Au	Glass	$2 \times 10^{-1}$	$10^7$	BG	[143]
<b>P(NDI2OD-T2)</b>	<b>PEDOT:PSS</b>	Parylene C	<b>PEDOT:PSS</b>	Master-Bi	$10^{-2}$	$10^5$	TG	[144]

<sup>1</sup> TIPS—6,13-bis(triisopropylsilyl)ethynylpentacene, <sup>2</sup> PS—polystyrene, PVP—poly(vinylphenol), PMMA—poly(methylmethacrylate), K60—poly(N-vinylpyrrolidone), <sup>3</sup> PE—polyester, PI—polyimide, PEN—polyethylene naphthalate, <sup>4</sup> TG—top gate configuration, BG—bottom gate configuration.

Organic TFT, a special kind of planar FET characterized by low thickness and, thus, a high aspect ratio, can also be manufactured by means of IJP. As thin-film elements, TFT

transistors are vertically aligned, which allows their facile manufacturing by the inkjet printing technique. The same as for FETs, any component of the TFT transistor, namely semiconductor film, insulator film, and electrodes, can be applied by the printing procedure. Inkjet printing can easily afford sub-micrometer organic films, which opens the possibility to produce flexible sub-2 V-operating TFT transistors [145]. More detailed data for inkjet-printed TFTs is presented in Table 3.

**Table 3.** Summary of inkjet-printed TFT transistors. Inkjet-printed components are highlighted with bold.

Channel <sup>1</sup>	Gate	Insulator	Source/ Drain	Substrate	$\mu$ , $\text{cm}^2 \text{V}^{-1} \text{s}^{-1}$	$I_{\text{on}}/I_{\text{off}}$	Configuration	Ref.
<b>P3HT F8T2</b>	Doped Si	SiO <sub>2</sub>	Au/Cr	Si	10 <sup>-1</sup>	10 <sup>6</sup>	BG	[20]
<b>P3HT F8T2 poly(vinylene thiophene)</b>	<b>PEDOT:PSS</b>	PVP	<b>PEDOT:PSS</b>	Glass	2 × 10 <sup>-3</sup>	10 <sup>5</sup>	TG	[76]
p3HT	Doped Si	SiO <sub>2</sub>	<b>PEDOT:PSS</b>	Si	1.2 × 10 <sup>-2</sup>	2.9 × 10 <sup>3</sup>	BG	[146]
p3HT	Doped Si	SiO <sub>2</sub>	<b>PEDOT:PSS</b>	Si	6 × 10 <sup>-3</sup>	10 <sup>3</sup>	BG	[147]
F8T2	<b>Al PEDOT:PSS</b>	PMMA	<b>PEDOT:PSS ITO</b>	Glass ITO	4.5 × 10 <sup>-3</sup>	10 <sup>4</sup>	BG TG	[148]
P3HT	ITO	SiO <sub>2</sub>	ITO	ITO	2.3 × 10 <sup>-3</sup>	10 <sup>5</sup>	BG	[149]
PQT12	Doped Si	SiO <sub>2</sub>	<b>Ag/ PEDOT:PSS</b>	Si	2.5 × 10 <sup>-2</sup>	2 × 10 <sup>7</sup>	BG	[150]
<b>PQT12/CNT</b>	Doped Si	SiO <sub>2</sub>	Au/Cr	Si	2.3 × 10 <sup>-1</sup>	10 <sup>6</sup>	BG	[59]
<b>P(NDI2OD-T2)</b>	Au	Cytop PS PMMA PTBS	Au	PET Glass	8.5 × 10 <sup>-1</sup>	10 <sup>6</sup>	TG	[151]
TIPS	<b>PEDOT:PSS</b>	PVP	<b>PEDOT:PSS</b>	-	1.3 × 10 <sup>-1</sup>	5.6 × 10 <sup>6</sup>	TG BG	[152]
TIPS N1400	<b>PEDOT:PSS</b>	Parylene C	<b>PEDOT:PSS</b>	PET	7.8 × 10 <sup>-3</sup>	10 <sup>4</sup>	BG	[153]
F8T2	<b>PEDOT:PSS</b>	PVP	<b>PEDOT:PSS</b>	PI	2 × 10 <sup>-2</sup>	10 <sup>5</sup>	TG	[154]
<b>P3HT</b>	Doped Si	SiO <sub>2</sub>	Au	Si	8.1 × 10 <sup>-3</sup>	10 <sup>3</sup>	BG	[155]
<b>pBTTT</b>	<b>Ag</b>	<b>PVP</b>	<b>Ag</b>	PVP on paper	10 <sup>-1</sup>	3.2 × 10 <sup>4</sup>	BG	[156]
<b>TAA</b>	<b>Ag</b>	<b>PVP</b>	<b>Ag</b>	PEN	10 <sup>-1</sup>	5 × 10 <sup>1</sup>	BG	[157]
<b>P3HT</b>	Doped Si	SiO <sub>2</sub>	Au	Si	6 × 10 <sup>-2</sup>	10 <sup>3</sup>	BG	[158]
CNT	<b>PEDOT:PSS</b>	PVP	<b>PEDOT:PSS</b>	PEN	7	10 <sup>5</sup>	BG	[159]
pBTCT	<b>PEDOT:PSS</b>	-	<b>Ag</b>	Glass	2.5 × 10 <sup>-3</sup>	1.8 × 10 <sup>2</sup>	TG	[160]
<b>PQT-12</b>	Doped Si	SiO <sub>2</sub>	<b>Ag</b>	Si	10 <sup>-1</sup>	10 <sup>6</sup>	BG	[161]
<b>CNT/P3HT</b>	<b>PEDOT:PSS</b>	<b>PVP</b>	<b>PEDOT:PSS</b>	PI	5.3 × 10 <sup>-2</sup>	10 <sup>4</sup>	BG	[162]
<b>P3HT</b>	<b>PEDOT:PSS</b>	<b>PVP P(VDF- HPF)</b>	<b>PEDOT:PSS</b>	PI	5 × 10 <sup>-3</sup>	5.9 × 10 <sup>6</sup>	BG	[163]
<b>PDVT-8</b>	Mo	Al <sub>2</sub> O <sub>3</sub>	Au/Mo	PI	2.4	10 <sup>6</sup>	BG	[164]
<b>PDVT-8</b>	Doped Si	PVP/ Al <sub>2</sub> O <sub>3</sub> SiO <sub>2</sub>	Au	Si	6.5 × 10 <sup>-1</sup>	1.6 × 10 <sup>4</sup>	BG	[165]
<b>P3HT PQT-12 P(8T2Z-co- 6T2Z)-12</b>	Mo	SiO <sub>2</sub>	Au	Glass	10	-	BG	[166]
<b>P(NDI2OD-T2)</b>	Al	Cytop Al <sub>2</sub> O <sub>3</sub>	Au	Glass	10 <sup>-1</sup>	-	TG	[167]

<sup>1</sup> TAA—triarylamine, CNT—carbon nanotube.

Electrolyte-based transistors, electrolyte-gated FET (EGFETs), and electrochemical transistors (ECTs) are also accessible via inkjet printing (Figure 12a). Electrolyte-gated transistors are FETs with a liquid or gel electrolyte to separate the gate from the channel instead of a solid insulator, and the field effect acts by the formation of electrical double-layers on the interphases of the electrolyte with the gate and channel (Figure 12b). Electrochemical transistors are constructively similar to EGFETs, but they are governed by an electrochemical redox reaction of the channel material accompanied by the injection of the electrolyte ions, and thus, ECTs are not truly field-effect devices (Figure 12c).

For example, the block-copolymer of 3-hexylthiophene with *N,N*-dimethylaminoethyl methacrylate was used to improve the adhesion between the electrolyte gate and rr-P3HT semiconductor [168]. EGFETs with a device mobility of up to  $16 \text{ cm}^2 \text{ V}^{-1} \text{ s}^{-1}$  and an on/off ratio  $10^2$  with a printed PEDOT:PSS gate electrode were reported [169]. ECTs printed with PEDOT:PSS as the conductive material and different polyelectrolytes were reported [170,171].

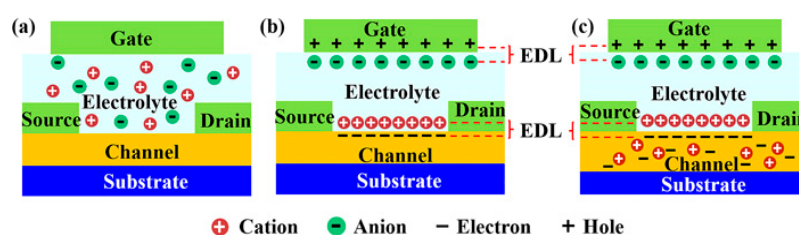


**Figure 12.** Schematic representation of (a) electrolyte-based transistor construction and action of the (b) electrolyte-gated and (c) electrochemical transistor; reprinted with permission from [172].

Large arrays of FETs [173] and TFT [174] transistors with PEDOT:PSS inkjet-printed contacts are reported, as well as vertical FETs with a PDVT semiconductor layer [87] and stretchable FETs with inkjet-printed PEDOT:PSS contacts [175]. The backplane TFT matrices for different types of displays, containing inkjet-printed PEDOT:PSS contacts [176], as well as a PQT-12 [177,178] or P(8T2Z-co-6T2Z)-12 [179] semiconductor layer are reported. In addition, the ECT backplane matrices with IJP PEDOT:PSS contacts were manufactured [180].

Inkjet printing technology perfectly fits the requirements for the fabrication of film-based electronic components and integrated devices, since its multilayer printing ability enables the application of multiple layers of different materials on a single printer. For the fabrication of the electrodes and current collectors, PEDOT:PSS and other highly conductive CPs are used. Semiconducting polymers such as rr-P3HT, PVVs, or D-A polymers serve as a semiconductor layer in diodes or transistors. In combination with inkjet-printable insulating polymers, the all-IJ fabrication of semiconductor devices is possible.

#### 4.2. Circuits

Inkjet printing, capable of freeform multicomponent multilayer patterning at once, is a perfect method for manufacturing microscopic-scale circuits for various purposes [181]. Inkjet printing of CPs is widely employed in the manufacturing of various integrated circuits and their components, including wiring and passive and active elements.

Due to the high electrical conductivity of some CPs, they are employed for the inkjet printing of conductive tracks, which are suitable for the wiring of flexible, wearable, and stretchable electronics [182]. Inkjet-printed tracks of high-boiling-point solvent and surfactant-treated PEDOT:PSS exhibit a conductivity of up to  $700 \text{ S cm}^{-1}$  and tolerate 100% strain [183]. Composite PEDOT:PSS patterns with the addition of Au clusters has a conductivity of more than two orders of magnitude higher, approaching the conductivity of monolithic Ag [184]. The patterning of composite PEDOT:PSS inks with carbon nanotubes results in highly transparent conductive wires [185]. Inkjet-printed tracks made of PANI:PSS, which is able to form highly conductive crystalline nanofibers, are also known [186]. Several reports describe the manufacturing of PEDOT:PSS printed passive components [187,188] and integrated passive circuits, e.g., RC-filters, via the inkjet pattern-

ing of PEDOT:PSS resistive elements [189] and, moreover, printed PEDOT:PSS or PANI resistive electrodes of a capacitor [190].

Much more attention has been drawn by the possibility of the IJP manufacturing of active electric circuits with CP-based inks. There have been 13.56 MHz rectifiers based on Schottky diodes with an inkjet-printed P(NDI2OD-T2) semiconducting layer reported [191], as well as high-frequency rectifiers based on FETs [192] and EGFETs with IJP PEDOT:PSS gates [193]. Ring oscillators with a gain up to 20 based on FETs [194,195] and EGFETs [196,197] with inkjet-printed elements were manufactured.

Numerous studies are devoted to the development of logic elements with transistors based on inkjet-printed CPs, such as latches [198] and logic gates, including inverters. The data on the inverters (Table 4) and other logic gates (Table 5) are summarized in the tables. More sophisticated logic devices like twilight switches [199] and calculation modules can also be inkjet printed with CPs [200,201].

**Table 4.** Summary of inverters based on transistors with inkjet-printed elements. Only inkjet-printed materials are indexed.

Type <sup>1</sup>	Channel	Gate	Source/Drain	Gain	Substrate <sup>2</sup>	Ref.
EGT	-	PEDOT:PSS	-	-	Glass	[202]
FET	pBTTT	-	-	16	Si	[61]
EGT	-	PEDOT:PSS	-	-	ITO	[203]
EGT	-	PEDOT:PSS	-	9.6	ITO	[204]
FET	PDBD PDBD-Se	-	-	80	PET	[89]
FET	P(NDI2OD-T2) DPPT-TT	-	-	28	Plastic	[205]
FET	P(NDI2OD-T2)	-	-	22.8	Glass	[206]
FET	P(NDI2OD-T2) DPPT-TT	PEDOT:PSS	PEDOT:PSS	17	PEN	[207]
FET	P(NDI2OD-T2) PC12TV12T	-	-	25	PEN	[208]
TFT	F8T2	PEDOT:PSS	PEDOT:PSS	7	Glass	[181]
FET	P3HT P2100 P(NDI2OD-T2)	-	-	30	PEN Glass	[209]
TFT	PQT	-	-	6.6	Glass	[210]
TFT	P(NDI2OD-T2) PQT12	PEDOT:PSS	-	6.2	Glass	[211]
FET	P(NDI2OD-T2) PC12TV12T	-	-	25	Glass	[212]
FET	P(NDI2OD-T2) P3HT P3Se P5Se	-	-	10	Glass	[62]
FET	PDBTAZ	-	-	20	Glass	[90]
TFT	PHTBTz-C8	-	-	35	PET	[213]
TFT	-	PEDOT:PSS	PEDOT:PSS	7.2	PE	[214]
FET	P(NDI2OD-T2) 29-DPP-TVT	PEDOT:PSS	-	17	PEN	[215]
FET	P(NDI2OD-T2) DPPT-TT	PEDOT:PSS	PEDOT:PSS	21	Glass	[216]
EGT	-	PEDOT:PSS	-	3.5	PI	[217]
TFT	DPPDTT P3HT	-	-	-	PEN	[218]
EGT	-	PEDOT:PSS	-	329	Glass	[219]

<sup>1</sup> EGT—electrolyte-gated transistor, FET—field-effect transistor, TFT—thin-film transistor, <sup>2</sup> ITO—indium tin oxide, PET—polyethylene terephthalate, PI—polyimide, PEN—polyethylene naphthalate.

**Table 5.** Summary of logic gates based on transistors with inkjet-printed elements.

Type <sup>1</sup>	Printed	IJP Materials	NOT	AND	OR	NOR	XOR	NAND	Gain	Substrate	Ref.
EGT	G	PEDOT:PSS	+			+		+	-	Glass	[202]
FET	SC	pBTTT	+						16	Si	[61]
EGT	G	PEDOT:PSS	+	+		+	+	+	-	ITO	[203]
EGT	G	PEDOT:PSS				+	+	+	9.6	ITO	[204]
FET	SC	PDBD PDBD-Se	+					+	80	PET	[89]
FET	SC	P(NDI2OD-T2) DPPT-TT				+		+	28	Plastic	[205]
FET	SC	P(NDI2OD-T2)	+					+	22.8	Glass	[206]
FET	S/D, G; SC	PEDOT:PSS; P(NDI2OD-T2) DPPT-TT	+						17	PEN	[207]
FET	SC	P(NDI2OD-T2) PC12TV12T			+	+	+	+	25	PEN	[208]
TFT	S/D, G; SC	PEDOT:PSS; P3HT	+					+	7	PEN	[145]
FET	G	PEDOT:PSS	+			+		+	14	Glass	[220]
FET	S/D, G	PEDOT:PSS	+	+	+	+		+	14	Paper	[221]
FET	SC	P(NDI2OD-T2)	+			+		+	-	Glass	[200]

<sup>1</sup> EGT—electrolyte-gated transistor, FET—field-effect transistor, TFT—thin-film transistor.

Inkjet printing of CPs is also widely employed for the fabrication of semiconductor memory devices with different working principles and based on passive and active inkjet-printed elements. Resistive horizontally [222,223] and vertically [224] stacked read-only memory devices based on inkjet-printed PEDOT:PSS resistive elements have been produced. The introduction of semiconductors [225] or spin-on-glass [226,227] materials affords rewritable resistive memories with PEDOT:PSS electrodes. Other memory devices with inkjet-printed elements such as ferroelectric memory devices with an inkjet-printed PC12TV12T semiconductor layer [228] or PEDOT:PSS electrodes [229] and floating-gate memory transistors based on PC12TV12T [84] and P(NDI2OD-T2) [230] semiconductor layers and PEDOT:PSS contacts [231] are reported. IJP patterned PC12TV12T [232], PQT-12 [233], and P(NDI2OD-T2) [234] semiconductor layers are also employed in capacitor-antifused memory transistors.

Due to the high electrical conductivity, printed PEDOT:PSS and PANI wiring may replace metal wiring in applications demanding the transparency, flexibility, or stretchability of the printed element, preserving a sufficiently low thickness of the wire. Inkjet printing technology allows the fabrication of complex electrical circuits for different purposes due to the ability of freeform and multimaterial patterning. The semiconductor devices printed by inkjet technology can be combined with various passive components to form logic and memory circuits, passive devices, etc.

#### 4.3. Displays and Indicating Devices

Printing technologies are widely used for the manufacturing of light-emitting and display devices such as electrochromic and electroluminescent elements, (O)LEDs, LCD and AMOLED matrices, etc. The emerging role of organic materials in the design and production of display devices leads to the wide employment of inkjet-printable conjugated polymers. Inkjet printing provides the possibility for the fabrication of freeform display devices like luminous tracks, tags, or graphics on demand. Inkjet technology affords

facile translation from a single element to a high-resolution display matrix on the same printing equipment.

IJP can be used for the fabrication of electrochromic elements. Most of the conductive polymers exhibit strong electrochromic behavior due to the dependence of the population of the delocalized charge carriers (polarons) on the oxidation degree. Inkjet-printed PEDOT:PSS [235] and PANI [236] films are used as active layers, or as conductive binders for other electrochromic materials [237]. A full-color CMY electrochromic device was also manufactured by the inkjet printing of three thiophene-containing CPs [60]. Several reports describe the manufacturing of multipixel electrochromic displays based on an IJP PEDOT:PSS [238] electrochromic layer.

IJP is also suitable for the manufacturing of light-emitting devices. Due to the high conductivity, optical transparency, low work function, and p-type charge transport, inkjet-printed PEDOT:PSS patterns are widely used as the hole injection layers in electroluminescent devices such as LEDs [239–241]. The addition of carbon nanotubes to the PEDOT:PSS inkjet ink enhances the conductivity of the printed hole injection layer [242]. The scope of IJP technology is not limited by the patterning of the hole injection layer; active electroluminescent layers can also be deposited by means of inkjet printing. For the inkjet printing of such layers, inks based on different semiconductive polymers are employed. Semiconductive homopolymers such as polyfluorenes PFO [243,244] or PF6 [245,246], or polyphenylenes [247], as well as various DA polymers (poly(phenylenevinylene) [73,248], poly(fluorenephenylenes) [249]), or more complex copolymers [91,250,251] can be inkjet printed as active layers of electroluminescent devices. An interesting example of inkjet printing with water-soluble cationic polyphenylene or its interpolymer complex with anionic poly(phenylenevinylene) was demonstrated [74].

Inkjet patterned (semi)conductive polymers may serve as hole injection or light-emitting layers for OLED displays. Almost all TFE OLED displays (flexible OLED) are manufactured using inkjet printing, which clearly illustrates the prospects of IJP technology in this field. The same as for single LEDs, hole injection layers for LED displays can be deposited by the inkjet printing of PEDOT:PSS inks (Figure 13) [252,253]. Inkjet-printed light-emitting layers based on PPV [254,255], PFO [256], F8T2 [257], and some more complicated DA polymers [93,258] are also reported.

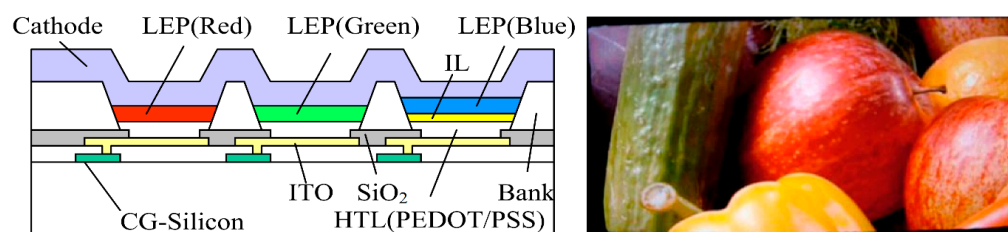


**Figure 13.** Device structure of full-color AMPLD display pixel and full color image on this display; adopted with permission from [252].

#### 4.4. Photovoltaics

Inkjet printing is one of the emerging manufacturing techniques for photovoltaic devices. The working principle of the photovoltaic element is based on the charge separation between the contacting donor and acceptor materials, which compose an active layer (AL), caused by the absorption of the light. To collect the separated charge carriers before their recombination and produce the electromotive force, the active layer is separated from the electrode by barrier layers: the hole injection layer (HIL) and/or sometimes the electron injection layer. Depending on the morphology of the interphase between the donor and acceptor materials, active layers are classified as planar, bulk, or pseudoplanar heterojunctions (Figure 14).

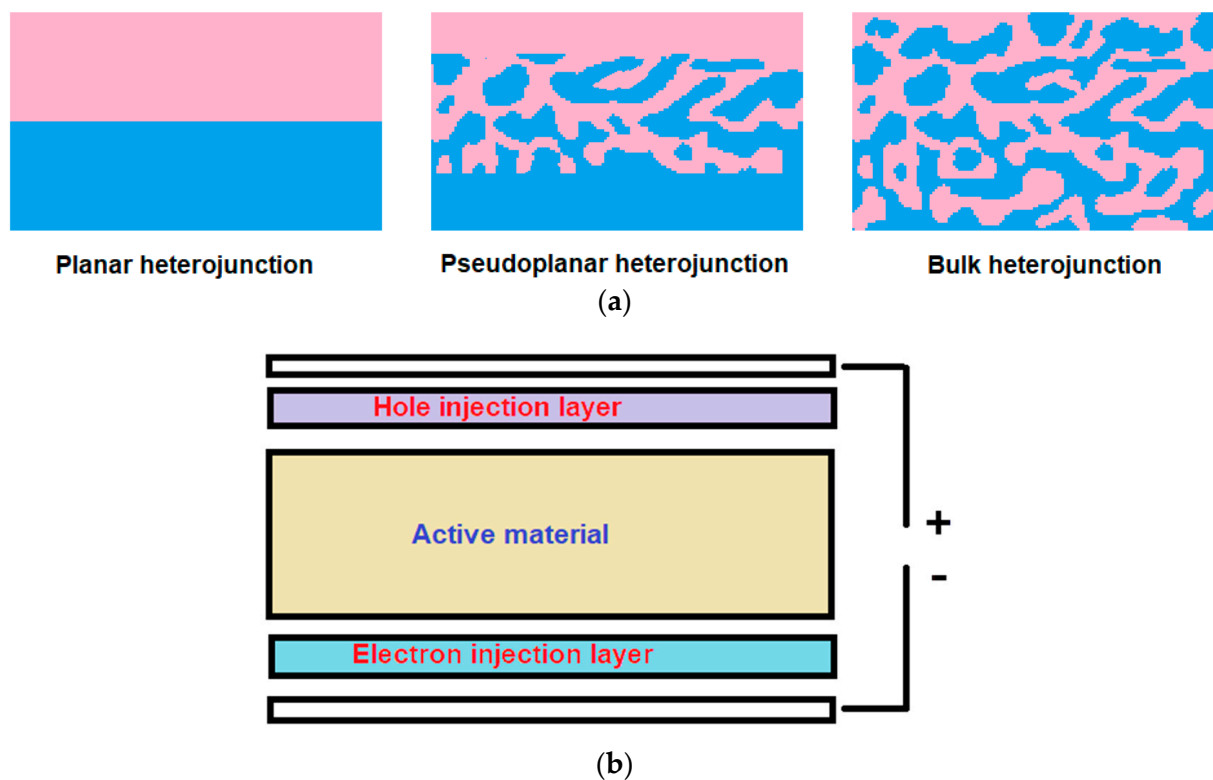


**Figure 14.** Schematic representation of (a) heterojunction morphologies and (b) the structure of the thin-film photovoltaic element.

Both the HIL and AL of a bulk heterojunction solar cell may be patterned using the inkjet printing technology. Inkjet printing of HILs using inks based on PEDOT:PSS, PEDOT:PSS composites with graphene or silver nanoparticles, as well as PANI was reported. Blended inks containing different semiconductive polymers and fullerene or non-fullerene acceptors are employed for the patterning of active bulk heterojunction layers. Pseudoplanar heterojunction solar cells are also accessible via inkjet printing using sequentially miscible donor and acceptor inks [259]. The materials and performance characteristics of inkjet-printed photovoltaic devices are summarized below (Table 6).

**Table 6.** Summary of inkjet-printed photovoltaic devices. Inkjet-printed components are highlighted with bold.

Hole Transport Layer	Active Layer	PCE <sup>1</sup> , %	OCV <sup>2</sup> , V	SCC <sup>3</sup> , mA cm <sup>-2</sup>	Ref.
		2.28	0.61	6.92	[260]
		0.08	0.31	0.82	[259]
		3.71	0.63	10.7	[261]
		2.25	0.57	9.49	[262]
<b>PEDOT:PSS</b>	<b>P3HT:PCBM</b>	1	0.56	6.8	[263]
		0.18	0.48	0.33	[264]
		2.28	0.61	6.92	[260]
		0.08	0.31	0.82	[259]
					[265,266]

Table 6. Cont.

Hole Transport Layer	Active Layer	PCE <sup>1</sup> , %	OCV <sup>2</sup> , V	SCC <sup>3</sup> , mA cm <sup>-2</sup>	Ref.
PEDOT:PSS	P3HT:PCBM	3	0.45	4.7	[267]
		1.4	0.66	4.67	[268]
		4.05	0.58	11.2	[269]
		3.5	0.54	10.1	[270]
		3.8	0.68	9.05	[271]
		2.4	0.57	9.34	[272]
		1.3	0.45	4.73	[273]
		2.83	0.62	8.6	[274]
		1.99	0.54	7.9	[275]
		3.07	0.53	12.12	[276]
		2.6	0.53	7.6	[277]
		2.2	0.6	8.3	[278]
		0.6	0.46	3	[279]
		3	0.45	4.7	[267]
		1.4	0.66	4.67	[268]
			[280]		
PEDOT:PSS	P3HT:PCBM	3.2	0.6	9.6	[281]
		3.3	0.62	9.78	[282]
		1.5	0.61	6.6	[283]
		2.5	0.55	7.25	[284]
		2.53	0.56	10.8	[52]
		0.19	0.56	5.6	[285]
-	P3HT:PCBM	0.35			[286]
		3.2	0.6	9.8	[287]
PEDOT:PSS	PCPDTBT or PSBTBT:PCBM or bis-PCBM	1.48	0.67	5.29	[288]
-	P3OT:PC71BM	6.5			[289]
		0.03	0.9	$2.3 \times 10^{-3}$	[290]
			0.9	$4.73 \times 10^{-3}$	[291]
PEDOT:PSS	P3HT:PCBM or PC71BM	2.22	0.61	9.49	[292]
PEDOT:PSS	PFDTBTP:PCBM	3	0.83	6	[293]
-	NK-1952:PEDOT:PSS	0.13	0.4		[294]
PEDOT:PSS	PFDTBTP:PCBM or PC71BM	3.5	0.9	6.71	[295]
PEDOT:PSS	PCPDTBTP:PCBM	3.7	0.9	8.65	[296]

Table 6. Cont.

Hole Transport Layer	Active Layer	PCE <sup>1</sup> , %	OCV <sup>2</sup> , V	SCC <sup>3</sup> , mA cm <sup>-2</sup>	Ref.
PEDOT:PSS	PCDTBT:PC71BM	5.1	0.89	9.95	[297]
PEDOT:PSS	Si-PCPDTBT or PCPDTBT: PC71BM	5.66	0.61	16.8	[94]
PEDOT:PSS	PV2000	7	0.78	13.4	[298]
PEDOT:PSS	PS:P3HT:PCBM	2	0.51	7.38	[299]
PEDOT:PSS	P3HT:ICBA	2.9	0.81	7.1	[300]
Poly-PT PEDOT:PSS	P3HT:PCBM				[301]
Ag:PEDOT	P3HT:PCBM	2.94		8.82	[302]
PANI:PAMPSA	P3HT:PC71BM	2.53	0.63	7.72	[303]
PEDOT:PSS	O-IDTBR or PV2000: PC71BM	5			[304]
-	P3HT:O- IDTBR	6.47	0.71	13.8	[305]
-	P3HT:ICBA	4.7	0.83	9.57	[306]
PANI:PAMPSA	-	10.6	0.94	18.4	[307]
PEDOT:PSS	PTB7- Th:IEICO-4F	12.5	0.71	27	[308]
PEDOT:PSS	P3HT:O- IDTBR	6.47	0.71	13.8	[309]
-	PM6:ITIC-4F	10.8	0.88	19.9	[310]
PEDOT:PSS	-	16.8	1.02	22	[311]
-	PBDB-T:ITIC or PBDB-T-2F: BTP-BO-4Cl	13.6	0.83	23.9	[312]
Graphene/PEDOT:PSS	PTB7:PCBM	1.12	0.65	3.16	[313]

<sup>1</sup> Power conversion efficiency, <sup>2</sup> open-circuit voltage, and <sup>3</sup> short-circuit current.

#### 4.5. Sensors

Due to the miniaturization of analytical devices and sensors, micromachining techniques replace macroscopic fabrication processes. Inkjet printing technology is a powerful tool for the fabrication of sensors and analytical devices with different working principles.

The very basic working principle for inkjet-printed analytical devices is the resistive sensing, when the variation of the measured parameter such as temperature, elongation, the concentration of the chemical, etc., changes the resistance of the conductive element. This method is highly suitable for the detection of basic chemicals like gaseous ammonia or volatile organic compounds. The irreversible kind of resistive chemosensor, the so-called chemical fuse, is used for safety purposes. In the same manner, impedimetric sensors are employed. Active sensing elements such as transistors or resonating circuits can also be used for the detection of these parameters. For the detection of more complex, especially biorelevant, chemicals such as glucose or ascorbic acid, amperometric and voltametric-based sensors, especially with enzymatic active materials, are used. pH sensors are based on the potentiometric principle. The data for the reported chemical sensors with inkjet-printed elements are summarized in the table below (Table 7).

**Table 7.** Summary of the inkjet-printed chemical sensors.

Inkjet-Printed Polymer	Sensing Principle	Analyte <sup>1</sup>	Ref.
PANI	Electrochemical	Ascorbic acid	[314]
PEDOT:PSS	Amperometric	H <sub>2</sub> O <sub>2</sub>	[315]
DPP-DTT	Transistor	DNA	[316]
PANI	Amperometric	Biomolecules	[317,318]
PANI	Electrochemical	Antioxidants	[319]
PEDOT:PSS	Electrochemical	Salbutamol	[320]
PEDOT:PSS	Resistive	CO <sub>2</sub>	[321,322]
PEDOT:PSS	Amperometric	Glucose	[323–325]
PPy	Amperometric	Glucose	[326]
PANI	Amperometric	Glucose	[327]
PANI	Resistive	Glucose	[328]
PEDOT:PSS	Transistor	Glucose	[329]
PEDOT:PSS	Electrochemical	H <sub>2</sub> O <sub>2</sub> , NADH, Fe(III)	[330]
PANI	Resistive	H <sub>2</sub> S	[331]
PEDOT:PSS	Electrochemical	N <sub>2</sub> H <sub>4</sub>	[332]
PANI	Amperometric	NH <sub>3</sub> , amines	[333,334]
PEDOT:PSS	CMOS	NH <sub>3</sub>	[335]
PANI	Impedancimetric	NH <sub>3</sub>	[336–338]
PANI	Resistive	NH <sub>3</sub>	[68,339–342]
PEDOT:PSS	Resistive	NH <sub>3</sub>	[343–347]
PANI	Impedancimetric	NH <sub>3</sub> (aq)	[348]
PANI	Impedancimetric	NH <sub>3</sub> (aq)	[348]
PANI	Potentiometric	pH	[69]
PPy	Potentiometric	pH	[349]
PEDOT:PSS	Transistor	pH, Na, K	[350,351]
PEDOT:PSS	Chemical fuse	VOC	[352]
Poly(vinylacetylene)	Indicator paper	VOC	[353]
PPy	Resistive	VOC	[354]
PEDOT:PSS	Resistive	VOC	[355–358]
PEDOT:PSS	RFID	VOC	[359]
P3HT	Transistor	VOC	[360]
PEDOT:PSS	Transistor	VOC	[361]

<sup>1</sup> VOC—volatile organic compound.

Touch sensors based on the capacitive sensing principle can be manufactured. Examples of inkjet-printed thermocouple-like temperature sensors [362] or strain-sensitive matrices [363] are also known. Inkjet printing allows the fabrication of freeform flexible [364], stretchable [365], wearable [366], transparent [104], and tattoo-like [367] sensors. Photoresponsive semiconductor sensors may be manufactured with the aid of inkjet printing in the same manner as photovoltaic devices. Photodiodes based on inkjet-printed CPs, PEDOT:PSS conductive layers, various photoresponsive layers (P3HT:PCBM [368], PCDTPT:PC71BM [369], P3HT:IDTBR [370], PEDOT:PSS:cyanine), and more complex bulk heterojunction donor–acceptor blends [371] have been produced. A phototransistor with inkjet-printed PEDOT:PSS contacts was reported [372]. Finally, RGB photoresponsive matrices with the combination of inkjet-printed PEDOT:PSS:cyanine active subpixels are accessible. Inkjet-printed sensors are listed in Table 8.

**Table 8.** Summary of inkjet-printed physical sensors.

Inkjet-Printed Polymer	Sensing Principle	Measured Property	Ref.
PEDOT:PSS	Resistive	Health monitoring	[365]
PANI	Impedancimetric	Humidity	[65]
PANI	Resistive	Humidity	[373,374]
PEDOT:PSS	Resistive	Humidity	[364,375]
PEDOT:PVMA	Resistive	Humidity	[376]
PEDOT:PSS	Resistive	Humidity	[377]
PANI	Resistive	Humidity	[377]
PEDOT:PSS	Transistor	Humidity	[378]
P3HT	Diode	Magnetic field	[379]
PEDOT:PSS	Piezoelectric	Mechanical	[380]
PEDOT:PSS	Capacitive	Pressure	[381]
PEDOT:PSS	Resistive	Pressure	[362]
PEDOT:PSS	Transistor	Pressure	[382]
P3HT	Resistive	Strain	[383]
P3HT	Resistive	Strain	[384–386]
PEDOT:PSS	Resistive	Strain	[384–386]
P3HT:PC61BM	Transistor	Strain	[363]
PEDOT:PSS	Resistive	Temperature	[366,387,388]
Polydiacetylene	Thermochromic	Temperature	[389]
PEDOT:PSS	Capacitive	Touch panel	[390,391]
Polydopamine	Capacitive	Touch panel	[104]

#### 4.6. Miscellaneous

Inkjet printing technology can be employed for the manufacturing of freeform electrochemical energy-storage devices. Inkjet-printed electrodes for flexible supercapacitors based on PEDOT:PSS have been produced [392–394]. The addition of carbon nanomaterials to PEDOT:PSS [395] or PANI [396,397] inks increases the conductivity and capacitance of the printed supercapacitors. Reactive printed polypyrrole electrodes are also employed for the manufacturing of flexible supercapacitors [398]. A rare example of the IJP-aided fabrication of the silicone anode for a lithium-ion battery using Si/PEDOT:PSS inks was reported, where the PEDOT:PSS acts as a conductive binder [399].

Conductive polymers deposited on membranes by means of inkjet printing improve their performance due to their poor wettability. Nanofiltration and Janus filtration membranes, modified with reactive inkjet-printed self-polymerized dopamine layers, show enhanced separation and anti-fouling properties [400–402]. Acoustic absorbing membranes based on inkjet-printed PEDOT:PSS were also reported [403].

Inkjet-printed conductive polymer patterns have a couple of biologic applications. The individual features of living bodies require the individual fabrication of biocompatible devices, and IJP technology perfectly fulfills these needs due to the ability of custom freeform manufacturing. Inkjet printing is used for the fabrication of conductive PEDOT:PSS neurointerfaces [404], muscle tissue stimulation [405], and myography [406], as well as polypyrrole-printed cell-compatible electrodes capable of the stimulation of PC12 cells [407,408]. PANI printed patterns on the biocompatible scaffolds are proposed to be used for bone tissue engineering [409].

## 5. Outlook and Challenges

The discussed number of works highlight the particular benefits of inkjet printing with CP-based inks for the development and fabrication of organic and polymeric electronics. Inkjet printing appears to be a powerful tool for the patterning of miniaturized freeform and complex structures for electronic devices for a broad range of applications: semiconductor devices, electrical circuits, light-emitting and display devices, sensors, energy-storage devices, and healthcare gadgets. The employment of inkjet inks based on conjugated

(semi)conductive polymers provides the possibility to fabricate flexible, stretchable, and bendable microelectronic devices.

As demonstrated by the discussed works, any (semi)conductive polymer may be adopted for IJP technology either in dispersion or in solution after some pre-treatment. Submicrometer particles of insoluble CPs can be easily stabilized in dispersion by their own surface charge or external charged surfactants, showing significant benefit over the much more poorly dispersible inorganic particles in inkjet printing. In addition, due to their softness and cohesion, CPs show, to some extent, film-forming ability, in contrast to inorganic particles. Inkjet printing is highly tolerant to the nature, size, and mechanical properties of the printing substrate, including those with rough and porous surfaces. At the same time, inkjet patterning shows a unique combination of high resolution and precision, low price, and perfect scalability, which makes it a promising tool for thin-film microelectronics. Inkjet printing equipment allows multilayer deposition in one setup or, in particular, in a single run. Of particular interest is the material effectiveness of IJP: the utilization of the inks in this technology closely approaches 100%.

The major drawback of IJP technology is the extremely low thickness of the single deposited layer, which rarely exceeds one micrometer. Owing to this inherent limitation of the inkjet printing method, the greatest effort is focused on the fabrication of thin-film devices, e.g., FETs, photovoltaic devices, and film-based sensors. Strict requirements for the inks for IJP also limit the feasibility of this technology to some extent, although these requirements can be satisfied for most of the CP-based inks. Bulk deposition technologies such as screen or reel-to-reel printing economically surpass inkjet printing on the larger scales, but the latter technology is also applicable on an industrial scale.

Further development of functional inkjet printing with conjugated polymers is mostly directed toward the fabrication of thin-film integrated circuits for stretchable, wearable electronics, highly autonomous devices such as sticker sensors, and electrochromic laminates. Among the emerging fields for the application of the inkjet printing of CPs are miniaturized electrochemical power sources, sensors, and artificial muscles. On-demand digital fabrication of the devices for personalized medicine and other custom printable elements may be a prospective niche for IJP technology since it allows easily customizable freeform printing. IJP can be easily combined with other manufacturing techniques such as 3D printing, by printing 2D functional patterns between the 3D layers. IJP could also solve a customization problem typical of high-throughput techniques such as intaglio printing, which is a relevant task in light of the trends in custom manufacturing in industry.

To date, the patterning resolution accessible via IJP technology is close to the theoretical maximum, which is limited by the physical restrictions of droplet dynamics. Future development of inkjet printing with conductive polymers as a fabrication technique may be focused on the improvement of the functional properties of the deposited materials through molecular engineering. Experts in this field expect a new generation of conjugated (semi)conducting polymers to emerge, with truly metallic conductivity, tunable magnetic properties, and a high electromechanical response, which may open the possibilities for the inkjet printing of active elements that can convert the electric current into motion directly or using a magnetic field. Most of the discussed printed devices are quite simple in the circuit design sense and usually comprise one or few elements, and one may expect the improvement of the complexity of printed devices, including the multistage architecture with multiple layers of elements printed one over another.

Like filament 3D printing, functional inkjet printing is expected to spread as an affordable technique for microelectronics fabrication for domestic use and small business, if supported by sufficient software and the assortment of substrates and water-based functional inks, and conjugated polymers can be considered as an optimal class of materials to fulfill this need. At this stage, the development of the drivers and printing software, which may help to convert home printers to fully functional additive manufacturing devices, is strongly demanded. There is a wide gap in the price and functionality between home inkjet printers and R&D machines like Dimatix, and filling this gap with the family of inkjet

printing devices within the USD 1000–1500 price range, which would be supplemented with some “CNC-like” features such as improved planar kinematics, heating of the substrate, and special software, can boost the rise of home inkjet printing manufacturing, as occurred before with home 3D printing. At the same time, functional inkjet printing appears to be a perfect tool for the fast prototyping of microelectronics for R&D purposes due to its customizability and low operational cost.

Summarizing the review, CP-based inks show particular advantages over inorganic inks due to the unique properties of these materials. The exploitation of conjugated polymers as functional materials for inkjet printing allows significant broadening of the scope of functional IJP and, in our opinion, will boost the implementation of inkjet printing as a device fabrication technology.

**Author Contributions:** Investigation, D.A.L.; writing—original draft preparation, D.A.L.; writing—review and editing, D.A.L. and O.V.L.; visualization, D.A.L.; supervision, O.V.L.; funding acquisition, D.A.L. All authors have read and agreed to the published version of the manuscript.

**Funding:** This research was funded by the Russian Science Foundation (RSF), grant number 22-73-00316.

**Conflicts of Interest:** The authors declare no conflicts of interest. The funders had no role in the design of the study; in the collection, analyses, or interpretation of the data; in the writing of the manuscript; nor in the decision to publish the results.

## References

1. Wang, X.; Zhang, M.; Zhang, L.; Xu, J.; Xiao, X.; Zhang, X. Inkjet-printed flexible sensors: From function materials, manufacture process, and applications perspective. *Mater. Today Commun.* **2022**, *31*, 103263. [[CrossRef](#)]
2. Hussain, A.; Abbas, N.; Ali, A. Inkjet Printing: A Viable Technology for Biosensor Fabrication. *Chemosensors* **2022**, *10*, 103. [[CrossRef](#)]
3. Sztymela, K.; Bienia, M.; Rossignol, F.; Mailley, S.; Ziesche, S.; Varghese, J.; Cerbelaud, M. Fabrication of modern lithium ion batteries by 3D inkjet printing: Opportunities and challenges. *Heliyon* **2022**, *8*, e12623. [[CrossRef](#)] [[PubMed](#)]
4. Lin, Y.; Chen, J.; Tavakoli, M.M.; Gao, Y.; Zhu, Y.; Zhang, D.; Kam, M.; He, Z.; Fan, Z. Printable Fabrication of a Fully Integrated and Self-Powered Sensor System on Plastic Substrates. *Adv. Mater.* **2019**, *31*, e1804285. [[CrossRef](#)] [[PubMed](#)]
5. Teichler, A.; Perelaer, J.; Schubert, U.S. Inkjet printing of organic electronics—Comparison of deposition techniques and state-of-the-art developments. *J. Mater. Chem. C* **2013**, *1*, 1910–1925. [[CrossRef](#)]
6. Yin, Y.; Zeng, Y.; Chen, X.; Fan, Y. The internet of things in healthcare: An overview. *J. Ind. Inf. Integr.* **2016**, *1*, 3–13. [[CrossRef](#)]
7. Chung, S.; Cho, K.; Lee, T. Recent Progress in Inkjet-Printed Thin-Film Transistors. *Adv. Sci.* **2019**, *6*, 1801445. [[CrossRef](#)] [[PubMed](#)]
8. Swager, T.M. 50th Anniversary Perspective: Conducting/Semiconducting Conjugated Polymers. A Personal Perspective on the Past and the Future. *Macromolecules* **2017**, *50*, 4867–4886. [[CrossRef](#)]
9. Weng, B.; Shepherd, R.L.; Crowley, K.; Killard, A.J.; Wallace, G.G. Printing conducting polymers. *Analyst* **2010**, *135*, 2779–2789. [[CrossRef](#)]
10. Zub, K.; Hoepfener, S.; Schubert, U.S. Inkjet Printing and 3D Printing Strategies for Biosensing, Analytical, and Diagnostic Applications. *Adv. Mater.* **2022**, *34*, e2105015. [[CrossRef](#)]
11. Du, X.; Wankhede, S.P.; Prasad, S.; Shehri, A.; Morse, J.; Lakal, N. A review of inkjet printing technology for personalized-healthcare wearable devices. *J. Mater. Chem. C* **2022**, *10*, 14091–14115. [[CrossRef](#)]
12. Mattana, G.; Loi, A.; Woytasik, M.; Barbaro, M.; Noël, V.; Piro, B. Inkjet-Printing: A New Fabrication Technology for Organic Transistors. *Adv. Mater. Technol.* **2017**, *2*, 1700063. [[CrossRef](#)]
13. Sumaiya, S.; Kardel, K.; El-Shahat, A. Organic Solar Cell by Inkjet Printing—An Overview. *Technologies* **2017**, *5*, 53. [[CrossRef](#)]
14. Deiner, L.J.; Reitz, T.L. Inkjet and Aerosol Jet Printing of Electrochemical Devices for Energy Conversion and Storage. *Adv. Eng. Mater.* **2017**, *19*, 1600878. [[CrossRef](#)]
15. Li, C.; Bu, F.; Wang, Q.; Liu, X. Recent Developments of Inkjet-Printed Flexible Energy Storage Devices. *Adv. Mater. Interfaces* **2022**, *9*, 2201051. [[CrossRef](#)]
16. Rosario, T.N. Concepts and Strategies to Adapt Inkjet Printing to Industrial Application Requirements. In *Handbook of Industrial Inkjet Printing*; Wiley: Hoboken, NJ, USA, 2017; pp. 239–252. [[CrossRef](#)]
17. Zapka, W. Pros and Cons of Inkjet Technology in Industrial Inkjet Printing. In *Handbook of Industrial Inkjet Printing*; Wiley: Hoboken, NJ, USA, 2017; pp. 1–6. [[CrossRef](#)]
18. Uddin, M.J.; Hassan, J.; Douroumis, D. Thermal Inkjet Printing: Prospects and Applications in the Development of Medicine. *Technologies* **2022**, *10*, 108. [[CrossRef](#)]
19. Shah, M.A.; Lee, D.-G.; Lee, B.-Y.; Hur, S. Classifications and Applications of Inkjet Printing Technology: A Review. *IEEE Access* **2021**, *9*, 140079–140102. [[CrossRef](#)]

20. Paul, K.E.; Wong, W.S.; Ready, S.E.; Street, R.A. Additive jet printing of polymer thin-film transistors. *Appl. Phys. Lett.* **2003**, *83*, 2070–2072. [[CrossRef](#)]
21. Driessen, T.; Jeurissen, R. Drop Formation in Inkjet Printing. In *Fundamentals of Inkjet Printing*; Wiley: Hoboken, NJ, USA, 2016; pp. 93–116. [[CrossRef](#)]
22. Yoo, H.; Kim, C. Generation of inkjet droplet of non-Newtonian fluid. *Rheol. Acta* **2013**, *52*, 313–325. [[CrossRef](#)]
23. Tuladhar, T. Measurement of Complex Rheology and Jettability of Inkjet Inks. In *Handbook of Industrial Inkjet Printing*; Wiley: Hoboken, NJ, USA, 2017; pp. 409–430. [[CrossRef](#)]
24. Derby, B.; Reis, N. Inkjet Printing of Highly Loaded Particulate Suspensions. *MRS Bull.* **2011**, *28*, 815–818. [[CrossRef](#)]
25. Wijshoff, H. The dynamics of the piezo inkjet printhead operation. *Phys. Rep.* **2010**, *491*, 77–177. [[CrossRef](#)]
26. Rembe, C.; aus der Wiesche, S.; Hofer, E.P. Thermal ink jet dynamics: Modeling, simulation, and testing. *Microelectron. Reliab.* **2000**, *40*, 525–532. [[CrossRef](#)]
27. Abd El-Rahman Elsayed Saad, A.; Aydemir, C.; Ayhan Özsoy, S.; Yenidoğan, S. Drying methods of the printing inks. *J. Graph. Eng. Des.* **2021**, *12*, 29–37. [[CrossRef](#)]
28. Kaçar, R.; Serin, R.B.; Uçar, E.; Ülkü, A. A review of high-end display technologies focusing on inkjet printed manufacturing. *Mater. Today Commun.* **2023**, *35*, 105534. [[CrossRef](#)]
29. Deegan, R.D.; Bakajin, O.; Dupont, T.F.; Huber, G.; Nagel, S.R.; Witten, T.A. Capillary flow as the cause of ring stains from dried liquid drops. *Nature* **1997**, *389*, 827–829. [[CrossRef](#)]
30. Mampallil, D.; Eral, H.B. A review on suppression and utilization of the coffee-ring effect. *Adv. Colloid Interface Sci.* **2018**, *252*, 38–54. [[CrossRef](#)]
31. Song, O.; Rhee, D.; Kim, J.; Jeon, Y.; Mazánek, V.; Söll, A.; Kwon, Y.A.; Cho, J.H.; Kim, Y.-H.; Sofer, Z.; et al. All inkjet-printed electronics based on electrochemically exfoliated two-dimensional metal, semiconductor, and dielectric. *Npj 2d Mater. Appl.* **2022**, *6*, 64. [[CrossRef](#)]
32. Kim, J.; Kumar, R.; Bandodkar, A.J.; Wang, J. Advanced Materials for Printed Wearable Electrochemical Devices: A Review. *Adv. Electron. Mater.* **2016**, *3*, 1600260. [[CrossRef](#)]
33. Wilson, M.C.; Castrejón-Pita, J.R.; Castrejón-Pita, A.A. *Reactive Inkjet Printing: A Chemical Synthesis Tool*; The Royal Society of Chemistry: London, UK, 2017. [[CrossRef](#)]
34. Cho, J.; Shin, K.-H.; Jang, J. Polyaniline micropattern onto flexible substrate by vapor deposition polymerization-mediated inkjet printing. *Thin Solid Film.* **2010**, *518*, 5066–5070. [[CrossRef](#)]
35. Cho, J.; Shin, K.-H.; Jang, J. Micropatterning of conducting polymer tracks on plasma treated flexible substrate using vapor phase polymerization-mediated inkjet printing. *Synth. Met.* **2010**, *160*, 1119–1125. [[CrossRef](#)]
36. Calvert, P. Inkjet Printing for Materials and Devices. *Chem. Mater.* **2001**, *13*, 3299–3305. [[CrossRef](#)]
37. Morita, N.; Khalate, A.A.; Buul, A.M.v.; Wijshoff, H. Inkjet Printheads. In *Fundamentals of Inkjet Printing*; Wiley: Hoboken, NJ, USA, 2016; pp. 57–92.
38. Magdassi, S. *The Chemistry of Inkjet Inks*; World Scientific Pub Co Pte Ltd.: Singapore, 2009.
39. Parthier, L.; Wiegel, T.; Ottermann, C.; Prince, F. Glass Substrates for Industrial Inkjet Printing Applications. In *Handbook of Industrial Inkjet Printing*; Wiley: Hoboken, NJ, USA, 2017; pp. 391–408. [[CrossRef](#)]
40. Sílvia Manuela Ferreira, C.; Luís, A.R.; Júlio, C.V. Printing Technologies on Flexible Substrates for Printed Electronics. In *Flexible Electronics*; Simas, R., Ed.; IntechOpen: Rijeka, Croatia, 2018; Chapter 3.
41. Wang, Y.; Guo, H.; Chen, J.J.; Sowade, E.; Wang, Y.; Liang, K.; Marcus, K.; Baumann, R.R.; Feng, Z.S. Paper-Based Inkjet-Printed Flexible Electronic Circuits. *ACS Appl. Mater. Interfaces* **2016**, *8*, 26112–26118. [[CrossRef](#)]
42. Biswas, T.; Yu, J.; Nierstrasz, V. Effective Pretreatment Routes of Polyethylene Terephthalate Fabric for Digital Inkjet Printing of Enzyme. *Adv. Mater. Interfaces* **2021**, *8*, 2001882. [[CrossRef](#)]
43. Mahajan, A.; Hyun, W.J.; Walker, S.B.; Rojas, G.A.; Choi, J.-H.; Lewis, J.A.; Francis, L.F.; Frisbie, C.D. A Self-Aligned Strategy for Printed Electronics: Exploiting Capillary Flow on Microstructured Plastic Surfaces. *Adv. Electron. Mater.* **2015**, *1*, 1500137. [[CrossRef](#)]
44. Cao, M.; Hyun, W.J.; Francis, L.F.; Frisbie, C.D. Inkjet-printed, self-aligned organic Schottky diodes on imprinted plastic substrates. *Flex. Print. Electron.* **2020**, *5*, 015006. [[CrossRef](#)]
45. Namsheer, K.; Rout, C.S. Conducting polymers: A comprehensive review on recent advances in synthesis, properties and applications. *RSC Adv.* **2021**, *11*, 5659–5697. [[CrossRef](#)]
46. Yamamoto, T.; Koizumi, T.-a. Synthesis of  $\pi$ -conjugated polymers bearing electronic and optical functionalities by organometallic polycondensations and their chemical properties. *Polymer* **2007**, *48*, 5449–5472. [[CrossRef](#)]
47. Wu, P.-T.; Xin, H.; Kim, F.S.; Ren, G.; Jenekhe, S.A. Regioregular Poly(3-pentylthiophene): Synthesis, Self-Assembly of Nanowires, High-Mobility Field-Effect Transistors, and Efficient Photovoltaic Cells. *Macromolecules* **2009**, *42*, 8817–8826. [[CrossRef](#)]
48. Masuda, T. Substituted Polyacetylenes: Synthesis, Properties, and Functions. *Polym. Rev.* **2016**, *57*, 1–14. [[CrossRef](#)]
49. Saxman, A.M.; Liepins, R.; Aldissi, M. Polyacetylene: Its synthesis, doping and structure. *Prog. Polym. Sci.* **1985**, *11*, 57–89. [[CrossRef](#)]
50. Scheunemann, D.; Järsvall, E.; Liu, J.; Beretta, D.; Fabiano, S.; Caironi, M.; Kemerink, M.; Müller, C. Charge transport in doped conjugated polymers for organic thermoelectrics. *Chem. Phys. Rev.* **2022**, *3*, 021309. [[CrossRef](#)]

51. Gueye, M.N.; Carella, A.; Faure-Vincent, J.; Demadrille, R.; Simonato, J.-P. Progress in understanding structure and transport properties of PEDOT-based materials: A critical review. *Prog. Mater. Sci.* **2020**, *108*, 100616. [[CrossRef](#)]
52. Singh, A.; Katiyar, M.; Garg, A. Understanding the formation of PEDOT:PSS films by ink-jet printing for organic solar cell applications. *RSC Adv.* **2015**, *5*, 78677–78685. [[CrossRef](#)]
53. Kleinschmidt, A.T.; Root, S.E.; Lipomi, D.J. Poly(3-hexylthiophene) (P3HT): Fruit fly or outlier in organic solar cell research? *J. Mater. Chem. A* **2017**, *5*, 11396–11400. [[CrossRef](#)]
54. Chen, T.-A.; Wu, X.; Rieke, R.D. Regiocontrolled Synthesis of Poly(3-alkylthiophenes) Mediated by Rieke Zinc: Their Characterization and Solid-State Properties. *J. Am. Chem. Soc.* **2002**, *117*, 233–244. [[CrossRef](#)]
55. Roesing, M.; Howell, J.; Boucher, D. Solubility characteristics of poly(3-hexylthiophene). *J. Polym. Sci. Part B Polym. Phys.* **2017**, *55*, 1075–1087. [[CrossRef](#)]
56. Dang, M.T.; Hirsch, L.; Wantz, G. P3HT:PCBM, best seller in polymer photovoltaic research. *Adv. Mater.* **2011**, *23*, 3597–3602. [[CrossRef](#)] [[PubMed](#)]
57. Teichler, A.; Perelaer, J.; Schubert, U.S. Screening of Film-Formation Qualities of Various Solvent Systems for  $\pi$ -Conjugated Polymers Via Combinatorial Inkjet Printing. *Macromol. Chem. Phys.* **2013**, *214*, 547–555. [[CrossRef](#)]
58. Pede, D.; Serra, G.; De Rossi, D. Microfabrication of conducting polymer devices by ink-jet stereolithography. *Mater. Sci. Eng. C* **1998**, *5*, 289–291. [[CrossRef](#)]
59. Hsieh, G.-W.; Li, F.M.; Beecher, P.; Nathan, A.; Wu, Y.; Ong, B.S.; Milne, W.I. High performance nanocomposite thin film transistors with bilayer carbon nanotube-polythiophene active channel by ink-jet printing. *J. Appl. Phys.* **2009**, *106*, 123706. [[CrossRef](#)]
60. Österholm, A.M.; Shen, D.E.; Gottfried, D.S.; Reynolds, J.R. Full Color Control and High-Resolution Patterning from Inkjet Printable Cyan/Magenta/Yellow Colored-to-Colorless Electrochromic Polymer Inks. *Adv. Mater. Technol.* **2016**, *1*, 1600063. [[CrossRef](#)]
61. Baklar, M.; Wöbkenberg, P.H.; Sparrowe, D.; Gonçalves, M.; McCulloch, I.; Heeney, M.; Anthopoulos, T.; Stingelin, N. Ink-jet printed p-type polymer electronics based on liquid-crystalline polymer semiconductors. *J. Mater. Chem.* **2010**, *20*, 1927–1931. [[CrossRef](#)]
62. Khim, D.; Lee, W.-H.; Baeg, K.-J.; Kim, D.-Y.; Kang, I.-N.; Noh, Y.-Y. Highly stable printed polymer field-effect transistors and inverters via polyselenophene conjugated polymers. *J. Mater. Chem.* **2012**, *22*, 12774–12783. [[CrossRef](#)]
63. Lenhart, N.; Crowley, K.; Killard, A.J.; Smyth, M.R.; Morrin, A. Inkjet printable polyaniline-gold dispersions. *Thin Solid Film.* **2011**, *519*, 4351–4356. [[CrossRef](#)]
64. Cao, G.; Xu, J.; Cai, S.; Chen, Y.; Zhou, D.; Zhang, H.; Jiang, C.; Zhang, G.; Tian, Y. Highly Conductive and Dispersible Polyaniline Microtubes Controlled by Methyl Orange. *ACS Appl. Polym. Mater.* **2022**, *5*, 593–601. [[CrossRef](#)]
65. Gomes, T.C.; Constantino, C.J.L.; Lopes, E.M.; Job, A.E.; Alves, N. Thermal inkjet printing of polyaniline on paper. *Thin Solid Film.* **2012**, *520*, 7200–7204. [[CrossRef](#)]
66. do Nascimento, G.M.; de Souza, M.A. Spectroscopy of Nanostructured Conducting Polymers. In *Nanostructured Conductive Polymers*; John Wiley & Sons, Ltd.: Hoboken, NJ, USA, 2010; pp. 341–373.
67. Ngamna, O.; Morrin, A.; Killard, A.J.; Moulton, S.E.; Smyth, M.R.; Wallace, G.G. Inkjet printable polyaniline nanoformulations. *Langmuir* **2007**, *23*, 8569–8574. [[CrossRef](#)] [[PubMed](#)]
68. Jang, J.; Ha, J.; Cho, J. Fabrication of Water-Dispersible Polyaniline-Poly(4-styrenesulfonate) Nanoparticles For Inkjet-Printed Chemical-Sensor Applications. *Adv. Mater.* **2007**, *19*, 1772–1775. [[CrossRef](#)]
69. Bilbao, E.; Kapadia, S.; Riechert, V.; Amalvy, J.; Molinari, F.N.; Escobar, M.M.; Baumann, R.R.; Monsalve, L.N. Functional aqueous-based polyaniline inkjet inks for fully printed high-performance pH-sensitive electrodes. *Sens. Actuators B Chem.* **2021**, *346*, 130558. [[CrossRef](#)]
70. Ihalainen, P.; Määttä, A.; Mattinen, U.; Stepień, M.; Bollström, R.; Toivakka, M.; Bobacka, J.; Peltonen, J. Electrodeposition of PEDOT-Cl film on a fully printed Ag/polyaniline electrode. *Thin Solid Film.* **2011**, *519*, 2172–2175. [[CrossRef](#)]
71. Pfeiffer, S.; Hörhold, H.H. Synthesis of soluble MEH-PPV and MEH-PPB by horner condensation polymerization. *Synth. Met.* **1999**, *101*, 109–110. [[CrossRef](#)]
72. Tekin, E.; Holder, E.; Kozodaev, D.; Schubert, U.S. Controlled Pattern Formation of Poly [2-methoxy-5-(2'-ethylhexyloxy)-1,4-phenylenevinylene] (MEH-PPV) by Ink-Jet Printing. *Adv. Funct. Mater.* **2007**, *17*, 277–284. [[CrossRef](#)]
73. Mauthner, G.; Landfester, K.; Köck, A.; Brückl, H.; Kast, M.; Stepper, C.; List, E.J.W. Inkjet printed surface cell light-emitting devices from a water-based polymer dispersion. *Org. Electron.* **2008**, *9*, 164–170. [[CrossRef](#)]
74. Chang, S.-C.; Bharathan, J.; Yang, Y.; Helgeson, R.; Wudl, F.; Ramey, M.B.; Reynolds, J.R. Dual-color polymer light-emitting pixels processed by hybrid inkjet printing. *Appl. Phys. Lett.* **1998**, *73*, 2561–2563. [[CrossRef](#)]
75. Schlisske, S.; Rosenauer, C.; Rödlmeier, T.; Giringer, K.; Michels, J.J.; Kremer, K.; Lemmer, U.; Morsbach, S.; Daoulas, K.C.; Hernandez-Sosa, G. Ink Formulation for Printed Organic Electronics: Investigating Effects of Aggregation on Structure and Rheology of Functional Inks Based on Conjugated Polymers in Mixed Solvents. *Adv. Mater. Technol.* **2020**, *6*, 2000335. [[CrossRef](#)]
76. Kawase, T.; Shimoda, T.; Newsome, C.; Siringhaus, H.; Friend, R.H. Inkjet printing of polymer thin film transistors. *Thin Solid Film.* **2003**, *438–439*, 279–287. [[CrossRef](#)]
77. Egbe, D.A.M.; Bader, C.; Klemm, E.; Ding, L.; Karasz, F.E.; Grummt, U.-W.; Birckner, E. Influence of the Conjugation Pattern on the Photophysical Properties of Alkoxy-Substituted PE/PV Hybrid Polymers. *Macromolecules* **2003**, *36*, 9303–9312. [[CrossRef](#)]

78. Tekin, E.; Wijlaars, H.; Holder, E.; Egbe, D.A.M.; Schubert, U.S. Film thickness dependency of the emission colors of PPE-PPVs in inkjet printed libraries. *J. Mater. Chem.* **2006**, *16*, 4294–4298. [[CrossRef](#)]
79. Szindler, M.M.; Szindler, M.; Dobrzański, L.A. The structure and conductivity of polyelectrolyte based on MEH-PPV and potassium iodide (KI) for dye-sensitized solar cells. *Open Phys.* **2017**, *15*, 1022–1027. [[CrossRef](#)]
80. Holliday, S.; Li, Y.; Luscombe, C.K. Recent advances in high performance donor-acceptor polymers for organic photovoltaics. *Prog. Polym. Sci.* **2017**, *70*, 34–51. [[CrossRef](#)]
81. Gross, Y.M.; Ludwigs, S. P(NDI2OD-T2) revisited—Aggregation control as key for high performance n-type applications. *Synth. Met.* **2019**, *253*, 73–87. [[CrossRef](#)]
82. Liang, Y.; Chen, Z.; Jing, Y.; Rong, Y.; Facchetti, A.; Yao, Y. Heavily n-Dopable  $\pi$ -Conjugated Redox Polymers with Ultrafast Energy Storage Capability. *J. Am. Chem. Soc.* **2015**, *137*, 4956–4959. [[CrossRef](#)] [[PubMed](#)]
83. Gross, Y.M.; Trefz, D.; Dingler, C.; Bauer, D.; Vijayakumar, V.; Untilova, V.; Biniek, L.; Brinkmann, M.; Ludwigs, S. From Isotropic to Anisotropic Conductivities in P(NDI2OD-T2) by (Electro-)Chemical Doping Strategies. *Chem. Mater.* **2019**, *31*, 3542–3555. [[CrossRef](#)]
84. Baeg, K.-J.; Khim, D.; Kim, J.; Yang, B.-D.; Kang, M.; Jung, S.-W.; You, I.-K.; Kim, D.-Y.; Noh, Y.-Y. High-Performance Top-Gated Organic Field-Effect Transistor Memory using Electrets for Monolithic Printed Flexible NAND Flash Memory. *Adv. Funct. Mater.* **2012**, *22*, 2915–2926. [[CrossRef](#)]
85. Lee, J.; Chung, J.W.; Kim, D.H.; Lee, B.L.; Park, J.I.; Lee, S.; Hausermann, R.; Batlogg, B.; Lee, S.S.; Choi, I.; et al. Thin Films of Highly Planar Semiconductor Polymers Exhibiting Band-like Transport at Room Temperature. *J. Am. Chem. Soc.* **2015**, *137*, 7990–7993. [[CrossRef](#)]
86. Lee, J.; Chung, J.W.; Jang, J.; Kim, D.H.; Park, J.-I.; Lee, E.; Lee, B.-L.; Kim, J.-Y.; Jung, J.Y.; Park, J.S.; et al. Influence of Alkyl Side Chain on the Crystallinity and Trap Density of States in Thiophene and Thiazole Semiconducting Copolymer Based Inkjet-Printed Field-Effect Transistors. *Chem. Mater.* **2013**, *25*, 1927–1934. [[CrossRef](#)]
87. Fang, Y.; Wu, X.; Lan, S.; Zhong, J.; Sun, D.; Chen, H.; Guo, T. Inkjet-Printed Vertical Organic Field-Effect Transistor Arrays and Their Image Sensors. *ACS Appl. Mater. Interfaces* **2018**, *10*, 30587–30595. [[CrossRef](#)] [[PubMed](#)]
88. Teichler, A.; Holzer, S.; Nowotny, J.; Kretschmer, F.; Bader, C.; Perelaer, J.; Hager, M.D.; Hoepfner, S.; Schubert, U.S. Combinatorial screening of inkjet printed ternary blends for organic photovoltaics: Absorption behavior and morphology. *ACS Comb. Sci.* **2013**, *15*, 410–418. [[CrossRef](#)]
89. Ni, Z.; Wang, H.; Zhao, Q.; Zhang, J.; Wei, Z.; Dong, H.; Hu, W. Ambipolar Conjugated Polymers with Ultrahigh Balanced Hole and Electron Mobility for Printed Organic Complementary Logic via a Two-Step C–H Activation Strategy. *Adv. Mater.* **2019**, *31*, e1806010. [[CrossRef](#)]
90. Park, W.-T.; Kang, S.-J.; Noh, Y.-Y. High-Performance Printed Organic Ambipolar Complementary Inverters with Polyazine Containing Diketopyrrolopyrrole. *Mol. Cryst. Liq. Cryst.* **2014**, *600*, 123–128. [[CrossRef](#)]
91. Xia, Y.; Friend, R.H. Controlled Phase Separation of Polyfluorene Blends via Inkjet Printing. *Macromolecules* **2005**, *38*, 6466–6471. [[CrossRef](#)]
92. Scuratti, F.; Salazar-Rios, J.M.; Luzio, A.; Kowalski, S.; Allard, S.; Jung, S.; Scherf, U.; Loi, M.A.; Caironi, M. Charge Transport in High-Mobility Field-Effect Transistors Based on Inkjet Printed Random Networks of Polymer Wrapped Single-Walled Carbon Nanotubes. *Adv. Funct. Mater.* **2020**, *31*, 2006895. [[CrossRef](#)]
93. Zheng, H.; Zheng, Y.; Wang, J.; Wang, J.; Zhang, G.; Zhang, S.; Liu, M.; Hu, J.; Li, Y.; Hu, Y.; et al. Polymer light-emitting displays with printed cathodes. *Surf. Coat. Technol.* **2019**, *358*, 228–234. [[CrossRef](#)]
94. Hermerschmidt, F.; Papagiorgis, P.; Savva, A.; Christodoulou, C.; Itskos, G.; Choulis, S.A. Inkjet printing processing conditions for bulk-heterojunction solar cells using two high-performing conjugated polymer donors. *Sol. Energy Mater. Sol. Cells* **2014**, *130*, 474–480. [[CrossRef](#)]
95. Shin, E.-Y.; Choi, E.-Y.; Noh, Y.-Y. Parylene based bilayer flexible gate dielectric layer for top-gated organic field-effect transistors. *Org. Electron.* **2017**, *46*, 14–21. [[CrossRef](#)]
96. Kaloni, T.P.; Schreckenbach, G.; Freund, M.S. Band gap modulation in polythiophene and polypyrrole-based systems. *Sci. Rep.* **2016**, *6*, 36554. [[CrossRef](#)]
97. Qi, G.; Huang, L.; Wang, H. Highly conductive free standing polypyrrole films prepared by freezing interfacial polymerization. *Chem. Commun.* **2012**, *48*, 8246–8248. [[CrossRef](#)] [[PubMed](#)]
98. Weng, B.; Shepherd, R.; Chen, J.; Wallace, G.G. Gemini surfactant doped polypyrrole nanodispersions: An inkjet printable formulation. *J. Mater. Chem.* **2011**, *21*, 1918–1924. [[CrossRef](#)]
99. Omastová, M.; Bober, P.; Morávková, Z.; Peřinka, N.; Kaplanová, M.; Srový, T.; Hromádková, J.; Trchová, M.; Stejskal, J. Towards conducting inks: Polypyrrole–silver colloids. *Electrochim. Acta* **2014**, *122*, 296–302. [[CrossRef](#)]
100. Xing, R.; Ye, T.; Ding, Y.; Ding, Z.; Ma, D.; Han, Y. Thickness Uniformity Adjustment of Inkjet Printed Light-emitting Polymer Films by Solvent Mixture. *Chin. J. Chem.* **2013**, *31*, 1449–1454. [[CrossRef](#)]
101. Xing, R.; Ye, T.; Ding, Y.; Ma, D.; Han, Y. Formation of low surface energy separators with undercut structures via a full-solution process and its application in inkjet printed matrix of polymer light-emitting diodes. *Org. Electron.* **2009**, *10*, 313–319. [[CrossRef](#)]
102. Teichler, A.; Shu, Z.; Wild, A.; Bader, C.; Nowotny, J.; Kirchner, G.; Harkema, S.; Perelaer, J.; Schubert, U.S. Inkjet printing of chemically tailored light-emitting polymers. *Eur. Polym. J.* **2013**, *49*, 2186–2195. [[CrossRef](#)]

103. Yu, X.; Xing, R.; Peng, Z.; Lin, Y.; Du, Z.; Ding, J.; Wang, L.; Han, Y. To inhibit coffee ring effect in inkjet printing of light-emitting polymer films by decreasing capillary force. *Chin. Chem. Lett.* **2019**, *30*, 135–138. [[CrossRef](#)]
104. Liu, L.; Pei, Y.; Ma, S.; Sun, X.; Singler, T.J. Inkjet Printing Controllable Polydopamine Nanoparticle Line Array for Transparent and Flexible Touch-Sensing Application. *Adv. Eng. Mater.* **2020**, *22*, 1901351. [[CrossRef](#)]
105. Mitra, K.Y.; Polomoshnov, M.; Martínez-Domingo, C.; Mitra, D.; Ramon, E.; Baumann, R.R. Fully Inkjet-Printed Thin-Film Transistor Array Manufactured on Paper Substrate for Cheap Electronic Applications. *Adv. Electron. Mater.* **2017**, *3*, 1700275. [[CrossRef](#)]
106. Le, T.H.; Kim, Y.; Yoon, H. Electrical and Electrochemical Properties of Conducting Polymers. *Polymers* **2017**, *9*, 150. [[CrossRef](#)] [[PubMed](#)]
107. Lu, H.; Li, X.; Lei, Q. Conjugated Conductive Polymer Materials and its Applications: A Mini-Review. *Front. Chem.* **2021**, *9*, 732132. [[CrossRef](#)] [[PubMed](#)]
108. Speakman, S.P.; Rozenberg, G.G.; Clay, K.J.; Milne, W.I.; Ille, A.; Gardner, I.A.; Bresler, E.; Steinke, J.H.G. High performance organic semiconducting thin films: Ink jet printed polythiophene [rr-P3HT]. *Org. Electron.* **2001**, *2*, 65–73. [[CrossRef](#)]
109. Liu, Y.; Cui, T. Polymer-Based Rectifying Diodes on a Glass Substrate Fabricated by Ink-Jet Printing. *Macromol. Rapid Commun.* **2005**, *26*, 289–292. [[CrossRef](#)]
110. Kwon, J.; Seol, Y.G.; Lee, N.-E.; Chung, I. Study on Ohmic contact improvement of organic Schottky diode utilizing self-assembled monolayer and PEDOT:PSS layers. *J. Vac. Sci. Technol. A Vac. Surf. Film.* **2010**, *28*, 879–885. [[CrossRef](#)]
111. Cadilha Marques, G.; Tahoori, M.; Aghassi-Hagmann, J.; Sukuramsyah, A.M.; Arnal Rus, A.; Bolat, S.; Aribia, A.; Feng, X.; Singaraju, S.A.; Ramon, E.; et al. Fabrication and Modeling of pn-Diodes Based on Inkjet Printed Oxide Semiconductors. *IEEE Electron Device Lett.* **2020**, *41*, 187–190. [[CrossRef](#)]
112. Mitra, K.Y.; Sternkiker, C.; Martínez-Domingo, C.; Sowade, E.; Ramon, E.; Carrabina, J.; Gomes, H.L.; Baumann, R.R. Inkjet printed metal insulator semiconductor (MIS) diodes for organic and flexible electronic application. *Flex. Print. Electron.* **2017**, *2*, 015003. [[CrossRef](#)]
113. Pöldsalu, I.; Rohtlaid, K.; Nguyen, T.M.G.; Plesse, C.; Vidal, F.; Khorram, M.S.; Peikolainen, A.-L.; Tamm, T.; Kiefer, R. Thin ink-jet printed trilayer actuators composed of PEDOT:PSS on interpenetrating polymer networks. *Sens. Actuators B Chem.* **2018**, *258*, 1072–1079. [[CrossRef](#)]
114. Pöldsalu, I.; Johanson, U.; Tamm, T.; Punning, A.; Greco, F.; Peikolainen, A.-L.; Kiefer, R.; Aabloo, A. Mechanical and electro-mechanical properties of EAP actuators with inkjet printed electrodes. *Synth. Met.* **2018**, *246*, 122–127. [[CrossRef](#)]
115. Pöldsalu, I.; Harjo, M.; Tamm, T.; Uibu, M.; Peikolainen, A.-L.; Kiefer, R. Inkjet-printed hybrid conducting polymer-activated carbon aerogel linear actuators driven in an organic electrolyte. *Sens. Actuators B Chem.* **2017**, *250*, 44–51. [[CrossRef](#)]
116. Simaite, A.; Mesnilgrente, F.; Tondu, B.; Souères, P.; Bergaud, C. Towards inkjet printable conducting polymer artificial muscles. *Sens. Actuators B Chem.* **2016**, *229*, 425–433. [[CrossRef](#)]
117. Lim, J.A.; Kim, J.-H.; Qiu, L.; Lee, W.H.; Lee, H.S.; Kwak, D.; Cho, K. Inkjet-Printed Single-Droplet Organic Transistors Based on Semiconductor Nanowires Embedded in Insulating Polymers. *Adv. Funct. Mater.* **2010**, *20*, 3292–3297. [[CrossRef](#)]
118. Passarella, B.; Scaccabarozzi, A.D.; Giorgio, M.; Perinot, A.; Marina Barbier, S.; Martin, J.; Caironi, M. Direct-writing of organic field-effect transistors on plastic achieving 22 MHz transition frequency. *Flex. Print. Electron.* **2020**, *5*, 034001. [[CrossRef](#)]
119. Hyun, W.J.; Bidoky, F.Z.; Walker, S.B.; Lewis, J.A.; Francis, L.F.; Frisbie, C.D. Printed, Self-Aligned Side-Gate Organic Transistors with a Sub-5  $\mu\text{m}$  Gate-Channel Distance on Imprinted Plastic Substrates. *Adv. Electron. Mater.* **2016**, *2*, 1600293. [[CrossRef](#)]
120. Kim, M.; Ha, H.-J.; Yun, H.-J.; You, I.-K.; Baeg, K.-J.; Kim, Y.-H.; Ju, B.-K. Flexible organic phototransistors based on a combination of printing methods. *Org. Electron.* **2014**, *15*, 2677–2684. [[CrossRef](#)]
121. Wang, H.; Cheng, C.; Zhang, L.; Liu, H.; Zhao, Y.; Guo, Y.; Hu, W.; Yu, G.; Liu, Y. Inkjet printing short-channel polymer transistors with high-performance and ultrahigh photoresponsivity. *Adv. Mater.* **2014**, *26*, 4683–4689. [[CrossRef](#)] [[PubMed](#)]
122. Plötner, M.; Wegener, T.; Richter, S.; Howitz, S.; Fischer, W.-J. Investigation of ink-jet printing of poly-3-octylthiophene for organic field-effect transistors from different solutions. *Synth. Met.* **2004**, *147*, 299–303. [[CrossRef](#)]
123. Kawase, T.; Moriya, S.; Newsome, C.J.; Shimoda, T. Inkjet Printing of Polymeric Field-Effect Transistors and Its Applications. *Jpn. J. Appl. Phys.* **2005**, *44*, 3649. [[CrossRef](#)]
124. Liu, Y.; Varahramyan, K.; Cui, T. Low-Voltage All-Polymer Field-Effect Transistor Fabricated Using an Inkjet Printing Technique. *Macromol. Rapid Commun.* **2005**, *26*, 1955–1959. [[CrossRef](#)]
125. Wang, J.Z.; Gu, J.; Zenhausern, F.; Sirringhaus, H. Low-cost fabrication of submicron all polymer field effect transistors. *Appl. Phys. Lett.* **2006**, *88*, 133502. [[CrossRef](#)]
126. Tobjörk, D.; Kaihovirta, N.J.; Mäkelä, T.; Pettersson, F.S.; Österbacka, R. All-printed low-voltage organic transistors. *Org. Electron.* **2008**, *9*, 931–935. [[CrossRef](#)]
127. Zhang, X.H.; Lee, S.M.; Domercq, B.; Kippelen, B. Transparent organic field-effect transistors with polymeric source and drain electrodes fabricated by inkjet printing. *Appl. Phys. Lett.* **2008**, *92*, 243307. [[CrossRef](#)]
128. Lin, C.-T.; Hsu, C.-H.; Lee, C.-H.; Wu, W.-J. Inkjet-Printed Organic Field-Effect Transistor by Using Composite Semiconductor Material of Carbon Nanoparticles and Poly(3-Hexylthiophene). *J. Nanotechnol.* **2011**, *2011*, 142890. [[CrossRef](#)]
129. Baeg, K.-J. Polymer Dielectrics and Orthogonal Solvent Effects for High-Performance Inkjet-Printed Top-Gated P-Channel Polymer Field-Effect Transistors. *ETRI J.* **2011**, *33*, 887–896. [[CrossRef](#)]

130. Grimaldi, I.A.; Del Mauro Ade, G.; Loffredo, F.; Morvillo, P.; Villani, F. Modelling of organic field effect transistors with inkjet printed poly(3,4-ethylenedioxythiophene): Poly(styrene sulfonate) electrodes: Study of the annealing effects. *J. Nanosci. Nanotechnol.* **2013**, *13*, 5175–5181. [[CrossRef](#)]
131. Schmidt, G.C.; Höft, D.; Bhuie, M.; Haase, K.; Bellmann, M.; Haidu, F.; Lehmann, D.; Zahn, D.R.T.; Hübner, A.C. Modified poly(3,4-ethylenedioxythiophene):poly(styrenesulfonate) source/drain electrodes for fully printed organic field-effect transistors consisting of a semiconductor blend. *Appl. Phys. Lett.* **2013**, *103*, 113302. [[CrossRef](#)]
132. Khim, D.; Xu, Y.; Baeg, K.J.; Kang, M.; Park, W.T.; Lee, S.H.; Kim, I.B.; Kim, J.; Kim, D.Y.; Liu, C.; et al. Large Enhancement of Carrier Transport in Solution-Processed Field-Effect Transistors by Fluorinated Dielectric Engineering. *Adv. Mater.* **2016**, *28*, 518–526. [[CrossRef](#)] [[PubMed](#)]
133. Bucella, S.G.; Luzio, A.; Gann, E.; Thomsen, L.; McNeill, C.R.; Pace, G.; Perinot, A.; Chen, Z.; Facchetti, A.; Caironi, M. Macroscopic and high-throughput printing of aligned nanostructured polymer semiconductors for MHz large-area electronics. *Nat. Commun.* **2015**, *6*, 8394. [[CrossRef](#)] [[PubMed](#)]
134. Kwak, D.; Choi, H.H.; Kang, B.; Kim, D.H.; Lee, W.H.; Cho, K. Tailoring Morphology and Structure of Inkjet-Printed Liquid-Crystalline Semiconductor/Insulating Polymer Blends for High-Stability Organic Transistors. *Adv. Funct. Mater.* **2016**, *26*, 3003–3011. [[CrossRef](#)]
135. Yang, H.; Zhang, G.; Zhu, J.; He, W.; Lan, S.; Liao, L.; Chen, H.; Guo, T. Improving Charge Mobility of Polymer Transistors by Judicious Choice of the Molecular Weight of Insulating Polymer Additive. *J. Phys. Chem. C* **2016**, *120*, 17282–17289. [[CrossRef](#)]
136. Higgins, S.G.; Muir, B.V.O.; Dell'Erba, G.; Perinot, A.; Caironi, M.; Campbell, A.J. Self-aligned organic field-effect transistors on plastic with picofarad overlap capacitances and megahertz operating frequencies. *Appl. Phys. Lett.* **2016**, *108*, 023302. [[CrossRef](#)]
137. Zhang, G.; Yang, H.; He, L.; Hu, L.; Lan, S.; Li, F.; Chen, H.; Guo, T. Importance of domain purity in semi-conducting polymer/insulating polymer blends transistors. *J. Polym. Sci. Part B Polym. Phys.* **2016**, *54*, 1760–1766. [[CrossRef](#)]
138. Perinot, A.; Kshirsagar, P.; Malvindi, M.A.; Pompa, P.P.; Fiammengo, R.; Caironi, M. Direct-written polymer field-effect transistors operating at 20 MHz. *Sci. Rep.* **2016**, *6*, 38941. [[CrossRef](#)] [[PubMed](#)]
139. Conti, S.; Lai, S.; Cosseddu, P.; Bonfiglio, A. An Inkjet-Printed, Ultralow Voltage, Flexible Organic Field Effect Transistor. *Adv. Mater. Technol.* **2017**, *2*, 1600212. [[CrossRef](#)]
140. Bucella, S.G.; Salazar-Rios, J.M.; Derenskyi, V.; Fritsch, M.; Scherf, U.; Loi, M.A.; Caironi, M. Inkjet Printed Single-Walled Carbon Nanotube Based Ambipolar and Unipolar Transistors for High-Performance Complementary Logic Circuits. *Adv. Electron. Mater.* **2016**, *2*, 1600094. [[CrossRef](#)]
141. Lai, S.; Cosseddu, P.; Zucca, A.; Loi, A.; Bonfiglio, A. Combining inkjet printing and chemical vapor deposition for fabricating low voltage, organic field-effect transistors on flexible substrates. *Thin Solid Film.* **2017**, *631*, 124–131. [[CrossRef](#)]
142. Bucella, S.G.; Perinot, A.; Caironi, M. All Polymer FETs Direct-Written on Flexible Substrates Achieving MHz Operation Regime. *IEEE Trans. Electron Devices* **2017**, *64*, 1960–1967. [[CrossRef](#)]
143. Lee, J.; Jang, J.; Chung, J.W.; Yoon, M.; Kim, D.H. Temperature and gate-bias-dependent charge transport in inkjet-printed polymer field-effect transistor. *J. Korean Phys. Soc.* **2021**, *79*, 1063–1068. [[CrossRef](#)]
144. Stucchi, E.; Maksimovic, K.; Bertolacci, L.; Viola, F.A.; Athanassiou, A.; Caironi, M. Biodegradable all-polymer field-effect transistors printed on Mater-Bi. *J. Inf. Disp.* **2021**, *22*, 247–256. [[CrossRef](#)]
145. Xia, Y.; Zhang, W.; Ha, M.; Cho, J.H.; Renn, M.J.; Kim, C.H.; Frisbie, C.D. Printed Sub-2 V Gel-Electrolyte-Gated Polymer Transistors and Circuits. *Adv. Funct. Mater.* **2010**, *20*, 587–594. [[CrossRef](#)]
146. Xue, F.; Su, Y.; Varahramyan, K. Modified PEDOT-PSS Conducting Polymer as S/D Electrodes for Device Performance Enhancement of P3HT TFTs. *IEEE Trans. Electron Devices* **2005**, *52*, 1982–1987. [[CrossRef](#)]
147. Lim, J.A.; Cho, J.H.; Park, Y.D.; Kim, D.H.; Hwang, M.; Cho, K. Solvent effect of inkjet printed source/drain electrodes on electrical properties of polymer thin-film transistors. *Appl. Phys. Lett.* **2006**, *88*, 082102. [[CrossRef](#)]
148. Li, S.P.; Newsome, C.J.; Kugler, T.; Ishida, M.; Inoue, S. Polymer thin film transistors with self-aligned gates fabricated using ink-jet printing. *Appl. Phys. Lett.* **2007**, *90*, 172103. [[CrossRef](#)]
149. Chou, W.-Y.; Lin, S.-T.; Cheng, H.-L.; Tang, F.-C.; Lin, Y.-J.; You, C.-F.; Wang, Y.-W. Excimer laser irradiation induced suppression of off-state leakage current in organic transistors. *Appl. Phys. Lett.* **2007**, *90*, 222103. [[CrossRef](#)]
150. Sholin, V.; Carter, S.A.; Street, R.A.; Arias, A.C. High work function materials for source/drain contacts in printed polymer thin film transistors. *Appl. Phys. Lett.* **2008**, *92*, 063307. [[CrossRef](#)]
151. Yan, H.; Chen, Z.; Zheng, Y.; Newman, C.; Quinn, J.R.; Dotz, F.; Kastler, M.; Facchetti, A. A high-mobility electron-transporting polymer for printed transistors. *Nature* **2009**, *457*, 679–686. [[CrossRef](#)] [[PubMed](#)]
152. Lee, M.-W.; Lee, M.-Y.; Choi, J.-C.; Park, J.-S.; Song, C.-K. Fine patterning of glycerol-doped PEDOT:PSS on hydrophobic PVP dielectric with ink jet for source and drain electrode of OTFTs. *Org. Electron.* **2010**, *11*, 854–859. [[CrossRef](#)]
153. Basiricò, L.; Cosseddu, P.; Fraboni, B.; Bonfiglio, A. Inkjet printing of transparent, flexible, organic transistors. *Thin Solid Film.* **2011**, *520*, 1291–1294. [[CrossRef](#)]
154. Kawase, T.; Sirringhaus, H.; Friend, R.H.; Shimoda, T. 6.1: Invited Paper: All-Polymer Thin Film Transistors Fabricated by High-Resolution Ink-jet Printing. *SID Symp. Dig. Tech. Pap.* **2001**, *32*, 40–43. [[CrossRef](#)]
155. Chen, M.; Peng, R.; Xiong, X.; Chen, S.; Zhang, G.; Lu, H.; Wang, X.; Qiu, L. Inkjet Printed Poly(3-hexylthiophene) Thin-Film Transistors: Effect of Self-Assembled Monolayer. *Mol. Cryst. Liq. Cryst.* **2014**, *593*, 201–213. [[CrossRef](#)]

156. Grau, G.; Kitsomboonloha, R.; Swisher, S.L.; Kang, H.; Subramanian, V. Printed Transistors on Paper: Towards Smart Consumer Product Packaging. *Adv. Funct. Mater.* **2014**, *24*, 5067–5074. [[CrossRef](#)]
157. Gomes, H.L.; Medeiros, M.C.R.; Villani, F.; Canudo, J.; Loffredo, F.; Miscioscia, R.; Martinez-Domingo, C.; Ramon, E.; Sowade, E.; Mitra, K.Y.; et al. All-inkjet printed organic transistors: Dielectric surface passivation techniques for improved operational stability and lifetime. *Microelectron. Reliab.* **2015**, *55*, 1192–1195. [[CrossRef](#)]
158. Lin, Y.; Liu, C.-F.; Song, Y.-J.; Yang, L.; Zeng, W.-J.; Lai, W.-Y.; Huang, W. Improved performances of inkjet-printed poly(3-hexylthiophene) organic thin-film transistors by inserting an ionic self-assembled monolayer. *RSC Adv.* **2016**, *6*, 40970–40974. [[CrossRef](#)]
159. Ha, J.; Yoo, H.; Seo, J.; Yoon, J.; Hong, Y. Photoresponse Analysis of All-Inkjet-Printed Single-Walled Carbon Nanotube Thin-Film Transistors for Flexible Light-Insensitive Transparent Circuit Applications. *ACS Appl. Mater. Interfaces* **2023**, *15*, 3192–3201. [[CrossRef](#)]
160. Takasu, I.; Sugi, K.; Nomura, Y.; Nakao, H.; Mori, K.; Amemiya, I.; Uchikoga, S. All-Solution-Processed Organic Thin Film Transistors Fabricated by Non-Piezoelectric Inkjet Printing. *ECS Trans.* **2006**, *3*, 307–312. [[CrossRef](#)]
161. Doggart, J.; Wu, Y.; Zhu, S. Inkjet printing narrow electrodes with <50  $\mu\text{m}$  line width and channel length for organic thin-film transistors. *Appl. Phys. Lett.* **2009**, *94*, 163503. [[CrossRef](#)]
162. Lin, C.-T.; Hsu, C.-H.; Chen, I.-R.; Lee, C.-H.; Wu, W.-J. Enhancement of carrier mobility in all-inkjet-printed organic thin-film transistors using a blend of poly(3-hexylthiophene) and carbon nanoparticles. *Thin Solid Film.* **2011**, *519*, 8008–8012. [[CrossRef](#)]
163. Wu, W.-J.; Lee, C.-H.; Hsu, C.-H.; Yang, S.-H.; Lin, C.-T. Adjustable threshold-voltage in all-inkjet-printed organic thin film transistor using double-layer dielectric structures. *Thin Solid Film.* **2013**, *548*, 576–580. [[CrossRef](#)]
164. Kim, S.H.; Kang, I.; Kim, Y.G.; Hwang, H.R.; Kim, Y.-H.; Kwon, S.-K.; Jang, J. High performance ink-jet printed diketopyrrolopyrrole-based copolymer thin-film transistors using a solution-processed aluminium oxide dielectric on a flexible substrate. *J. Mater. Chem. C* **2013**, *1*, 2408–2411. [[CrossRef](#)]
165. Zhang, G.; Zhang, P.; Chen, H.; Guo, T. Modification of polymer gate dielectrics for organic thin-film transistor from inkjet printing. *Appl. Phys. A* **2018**, *124*, 481. [[CrossRef](#)]
166. Lee, J.; Jang, J.T.; Jang, J.; Kim, J.; Chung, J.W.; Choi, S.-J.; Kim, D.M.; Kim, K.R.; Kim, D.H. Density-of-States-Based Physical Model for Ink-Jet Printed Thiophene Polymeric TFTs. *IEEE Trans. Electron Devices* **2020**, *67*, 283–288. [[CrossRef](#)]
167. Zhou, Y.; Fuentes-Hernandez, C.; Shim, J.; Meyer, J.; Giordano, A.J.; Li, H.; Winget, P.; Papadopoulos, T.; Cheun, H.; Kim, J.; et al. A universal method to produce low-work function electrodes for organic electronics. *Science* **2012**, *336*, 327–332. [[CrossRef](#)] [[PubMed](#)]
168. Sinno, H.; Nguyen, H.T.; Hägerström, A.; Fahlman, M.; Lindell, L.; Coulembier, O.; Dubois, P.; Crispin, X.; Engquist, I.; Berggren, M. Amphiphilic semiconducting copolymer as compatibility layer for printing polyelectrolyte-gated OFETs. *Org. Electron.* **2013**, *14*, 790–796. [[CrossRef](#)]
169. Singaraju, S.A.; Baby, T.T.; Neuper, F.; Kruk, R.; Haggmann, J.A.; Hahn, H.; Breitung, B. Development of Fully Printed Electrolyte-Gated Oxide Transistors Using Graphene Passive Structures. *ACS Appl. Electron. Mater.* **2019**, *1*, 1538–1544. [[CrossRef](#)]
170. Mannerbro, R.; Ranlöf, M.; Robinson, N.; Forchheimer, R. Inkjet printed electrochemical organic electronics. *Synth. Met.* **2008**, *158*, 556–560. [[CrossRef](#)]
171. Basiricò, L.; Cosseddu, P.; Scidà, A.; Fraboni, B.; Malliaras, G.G.; Bonfiglio, A. Electrical characteristics of ink-jet printed, all-polymer electrochemical transistors. *Org. Electron.* **2012**, *13*, 244–248. [[CrossRef](#)]
172. He, Y.; Jiang, S.; Chen, C.; Wan, C.; Shi, Y.; Wan, Q. Electrolyte-gated neuromorphic transistors for brain-like dynamic computing. *J. Appl. Phys.* **2021**, *130*, 190904. [[CrossRef](#)]
173. Liu, N.; Zhou, Y.; Ai, N.; Luo, C.; Peng, J.; Wang, J.; Pei, J.; Cao, Y. High-performance, all-solution-processed organic nanowire transistor arrays with inkjet-printing patterned electrodes. *Langmuir* **2011**, *27*, 14710–14715. [[CrossRef](#)]
174. Burns, S.E.; Cain, P.; Mills, J.; Wang, J.; Sirringhaus, H. Inkjet Printing of Polymer Thin-Film Transistor Circuits. *MRS Bull.* **2011**, *28*, 829–834. [[CrossRef](#)]
175. Molina-Lopez, F.; Gao, T.Z.; Kraft, U.; Zhu, C.; Ohlund, T.; Pfattner, R.; Feig, V.R.; Kim, Y.; Wang, S.; Yun, Y.; et al. Inkjet-printed stretchable and low voltage synaptic transistor array. *Nat. Commun.* **2019**, *10*, 2676. [[CrossRef](#)]
176. Ryu, G.-S.; Lee, M.W.; Song, C.K. Printed flexible OTFT backplane for electrophoretic displays. *J. Inf. Disp.* **2011**, *12*, 213–217. [[CrossRef](#)]
177. Daniel, J.; Arias, A.C.; Russo, B.; Krusor, B. 44.3: Flexible Electrophoretic Displays with Jet-Printed Backplanes. *SID Symp. Dig. Tech. Pap.* **2009**, *40*, 660–663. [[CrossRef](#)]
178. Daniel, J.; Arias, A.C.; Ready, S.; Krusor, B.; Street, R. P-21: Jet-Printed All-Additive Active-Matrix Pixel Circuits on Low-Temperature Flexible Substrates. *SID Symp. Dig. Tech. Pap.* **2007**, *38*, 249–251. [[CrossRef](#)]
179. Lee, J.; Kim, D.H.; Kim, J.Y.; Yoo, B.; Chung, J.W.; Park, J.I.; Lee, B.L.; Jung, J.Y.; Park, J.S.; Koo, B.; et al. Reliable and uniform thin-film transistor arrays based on inkjet-printed polymer semiconductors for full color reflective displays. *Adv. Mater.* **2013**, *25*, 5886–5892. [[CrossRef](#)]
180. Kawahara, J.; Andersson Ersman, P.; Nilsson, D.; Katoh, K.; Nakata, Y.; Sandberg, M.; Nilsson, M.; Gustafsson, G.; Berggren, M. Flexible active matrix addressed displays manufactured by printing and coating techniques. *J. Polym. Sci. Part B Polym. Phys.* **2013**, *51*, 265–271. [[CrossRef](#)]

181. Siringhaus, H.; Kawase, T.; Friend, R.H.; Shimoda, T.; Inbasekaran, M.; Wu, W.; Woo, E.P. High-resolution inkjet printing of all-polymer transistor circuits. *Science* **2000**, *290*, 2123–2126. [[CrossRef](#)]
182. Guo, Y.; Otley, M.T.; Li, M.; Zhang, X.; Sinha, S.K.; Treich, G.M.; Sotzing, G.A. PEDOT:PSS “Wires” Printed on Textile for Wearable Electronics. *ACS Appl. Mater Interfaces* **2016**, *8*, 26998–27005. [[CrossRef](#)]
183. Kraft, U.; Molina-Lopez, F.; Son, D.; Bao, Z.; Murmann, B. Ink Development and Printing of Conducting Polymers for Intrinsically Stretchable Interconnects and Circuits. *Adv. Electron. Mater.* **2019**, *6*, 1900681. [[CrossRef](#)]
184. Sivaramakrishnan, S.; Chia, P.J.; Yeo, Y.C.; Chua, L.L.; Ho, P.K. Controlled insulator-to-metal transformation in printable polymer composites with nanometal clusters. *Nat. Mater.* **2007**, *6*, 149–155. [[CrossRef](#)] [[PubMed](#)]
185. Mustonen, T.; Kordás, K.; Saukko, S.; Tóth, G.; Penttilä, J.S.; Helistö, P.; Seppä, H.; Jantunen, H. Inkjet printing of transparent and conductive patterns of single-walled carbon nanotubes and PEDOT-PSS composites. *Phys. Status Solidi B* **2007**, *244*, 4336–4340. [[CrossRef](#)]
186. Li, D.; Tao, Y.; Yao, S.; Tian, W.; Wang, G.; Li, B.; Wang, W.; Li, S.; Yang, J.; Yu, Q.; et al. Conductive Inks with 3D Conductive Networks of Polyaniline Crystals Nanofibers. *Mater. Highlights* **2021**, *2*, 41–45. [[CrossRef](#)]
187. Sternkiker, C.; Sowade, E.; Mitra, K.Y.; Zichner, R.; Baumann, R.R. Upscaling of the Inkjet Printing Process for the Manufacturing of Passive Electronic Devices. *IEEE Trans. Electron Devices* **2016**, *63*, 426–431. [[CrossRef](#)]
188. Correia, V.; Mitra, K.Y.; Castro, H.; Rocha, J.G.; Sowade, E.; Baumann, R.R.; Lanceros-Mendez, S. Design and fabrication of multilayer inkjet-printed passive components for printed electronics circuit development. *J. Manuf. Process.* **2018**, *31*, 364–371. [[CrossRef](#)]
189. Kang, B.J.; Lee, C.K.; Oh, J.H. All-inkjet-printed electrical components and circuit fabrication on a plastic substrate. *Microelectron. Eng.* **2012**, *97*, 251–254. [[CrossRef](#)]
190. Chen, B.; Cui, T.; Liu, Y.; Varahramyan, K. All-polymer RC filter circuits fabricated with inkjet printing technology. *Solid-State Electron.* **2003**, *47*, 841–847. [[CrossRef](#)]
191. Viola, F.A.; Brigante, B.; Colpani, P.; Dell’Erba, G.; Mattoli, V.; Natali, D.; Caironi, M. A 13.56 MHz Rectifier Based on Fully Inkjet Printed Organic Diodes. *Adv. Mater.* **2020**, *32*, e2002329. [[CrossRef](#)]
192. Perinot, A.; Caironi, M. Accessing MHz Operation at 2 V with Field-Effect Transistors Based on Printed Polymers on Plastic. *Adv. Sci.* **2019**, *6*, 1801566. [[CrossRef](#)]
193. Feng, X.; Scholz, A.; Tahoori, M.B.; Aghassi-Hagmann, J. An Inkjet-Printed Full-Wave Rectifier for Low-Voltage Operation Using Electrolyte-Gated Indium-Oxide Thin-Film Transistors. *IEEE Trans. Electron Devices* **2020**, *67*, 4918–4923. [[CrossRef](#)]
194. Baeg, K.-J.; Jung, S.-W.; Khim, D.; Kim, J.; Kim, D.-Y.; Koo, J.B.; Quinn, J.R.; Facchetti, A.; You, I.-K.; Noh, Y.-Y. Low-voltage, high speed inkjet-printed flexible complementary polymer electronic circuits. *Org. Electron.* **2013**, *14*, 1407–1418. [[CrossRef](#)]
195. Han, H.; Amegadze, P.S.K.; Park, J.; Baeg, K.-J.; Noh, Y.-Y. Effect of gate electrode conductivity on operation frequency of inkjet-printed complementary polymer ring oscillators. *Thin Solid Film.* **2013**, *546*, 141–146. [[CrossRef](#)]
196. Cadilha Marques, G.; von Seggern, F.; Dehm, S.; Breitung, B.; Hahn, H.; Dasgupta, S.; Tahoori, M.B.; Aghassi-Hagmann, J. Influence of Humidity on the Performance of Composite Polymer Electrolyte-Gated Field-Effect Transistors and Circuits. *IEEE Trans. Electron Devices* **2019**, *66*, 2202–2207. [[CrossRef](#)]
197. Cadilha Marques, G.; Garlapati, S.K.; Dehm, S.; Dasgupta, S.; Hahn, H.; Tahoori, M.; Aghassi-Hagmann, J. Digital power and performance analysis of inkjet printed ring oscillators based on electrolyte-gated oxide electronics. *Appl. Phys. Lett.* **2017**, *111*, 102103. [[CrossRef](#)]
198. Weller, D.; Cadilha Marques, G.; Aghassi-Hagmann, J.; Tahoori, M.B. An Inkjet-Printed Low-Voltage Latch Based on Inorganic Electrolyte-Gated Transistors. *IEEE Electron Device Lett.* **2018**, *39*, 831–834. [[CrossRef](#)]
199. Dell’Erba, G.; Perinot, A.; Grimoldi, A.; Natali, D.; Caironi, M. Fully-printed, all-polymer integrated twilight switch. *Semicond. Sci. Technol.* **2015**, *30*, 104005. [[CrossRef](#)]
200. Kwon, J.; Takeda, Y.; Fukuda, K.; Cho, K.; Tokito, S.; Jung, S. Three-Dimensional, Inkjet-Printed Organic Transistors and Integrated Circuits with 100% Yield, High Uniformity, and Long-Term Stability. *ACS Nano* **2016**, *10*, 10324–10330. [[CrossRef](#)] [[PubMed](#)]
201. Gardner, S.D.; Haider, M.R. An Inkjet-Printed Artificial Neuron for Physical Reservoir Computing. *IEEE J. Flex. Electron.* **2022**, *1*, 185–193. [[CrossRef](#)]
202. Rasheed, F.; Rommel, M.; Marques, G.C.; Wenzel, W.; Tahoori, M.B.; Aghassi-Hagmann, J. Channel Geometry Scaling Effect in Printed Inorganic Electrolyte-Gated Transistors. *IEEE Trans. Electron Devices* **2021**, *68*, 1866–1871. [[CrossRef](#)]
203. Erozan, A.T.; Weller, D.D.; Rasheed, F.; Bishnoi, R.; Aghassi-Hagmann, J.; Tahoori, M.B. A Novel Printed-Lookup-Table-Based Programmable Printed Digital Circuit. *IEEE Trans. Very Large Scale Integr. VLSI Syst.* **2020**, *28*, 1496–1504. [[CrossRef](#)]
204. Marques, G.C.; Birla, A.; Arnal, A.; Dehm, S.; Ramon, E.; Tahoori, M.B.; Aghassi-Hagmann, J. Printed Logic Gates Based on Enhancement- and Depletion-Mode Electrolyte-Gated Transistors. *IEEE Trans. Electron Devices* **2020**, *67*, 3146–3151. [[CrossRef](#)]
205. Higgins, S.G.; Muir, B.V.O.; Dell’Erba, G.; Perinot, A.; Caironi, M.; Campbell, A.J. Complementary Organic Logic Gates on Plastic Formed by Self-Aligned Transistors with Gravure and Inkjet Printed Dielectric and Semiconductors. *Adv. Electron. Mater.* **2016**, *2*, 1500272. [[CrossRef](#)]
206. Kwon, J.; Takeda, Y.; Fukuda, K.; Cho, K.; Tokito, S.; Jung, S. Vertically Stacked Complementary Organic Field-Effect Transistors and Logic Circuits Fabricated by Inkjet Printing. *Adv. Electron. Mater.* **2016**, *2*, 1600046. [[CrossRef](#)]

207. Mandal, S.; Dell'Erba, G.; Luzio, A.; Bucella, S.G.; Perinot, A.; Calloni, A.; Berti, G.; Bussetti, G.; Duò, L.; Facchetti, A.; et al. Fully-printed, all-polymer, bendable and highly transparent complementary logic circuits. *Org. Electron.* **2015**, *20*, 132–141. [[CrossRef](#)]
208. Baeg, K.-J.; Khim, D.; Kim, J.; Kim, D.-Y.; Sung, S.-W.; Yang, B.-D.; Noh, Y.-Y. Flexible Complementary Logic Gates Using Inkjet-Printed Polymer Field-Effect Transistors. *IEEE Electron Device Lett.* **2013**, *34*, 126–128. [[CrossRef](#)]
209. Baeg, K.-J.; Khim, D.; Kim, D.-Y.; Jung, S.-W.; Koo, J.B.; You, I.-K.; Yan, H.; Facchetti, A.; Noh, Y.-Y. High speeds complementary integrated circuits fabricated with all-printed polymeric semiconductors. *J. Polym. Sci. Part B Polym. Phys.* **2011**, *49*, 62–67. [[CrossRef](#)]
210. Tan, H.S.; Wang, B.C.; Kamath, S.; Chua, J.; Shojaei-Baghini, M.; Rao, V.R.; Mathews, N.; Mhaisalkar, S.G. Complementary Organic Circuits Using Evaporated F<sub>16</sub>CuPc and Inkjet Printing of PQT. *IEEE Electron Device Lett.* **2010**, *31*, 1311–1313. [[CrossRef](#)]
211. Chen, W.N.; Chu, D.P.; Li, S.P. Air stable complementary polymer circuits fabricated in ambient condition by inkjet printing. *Org. Electron.* **2012**, *13*, 98–103. [[CrossRef](#)]
212. Baeg, K.J.; Khim, D.; Kim, J.; Han, H.; Jung, S.W.; Kim, T.W.; Kang, M.; Facchetti, A.; Hong, S.K.; Kim, D.Y.; et al. Controlled charge transport by polymer blend dielectrics in top-gate organic field-effect transistors for low-voltage-operating complementary circuits. *ACS Appl. Mater. Interfaces* **2012**, *4*, 6176–6184. [[CrossRef](#)]
213. Chung, J.W.; Ko, Y.H.; Hong, Y.K.; Song, W.; Jung, C.; Tang, H.; Lee, J.; Lee, M.h.; Lee, B.-l.; Park, J.-i.; et al. Flexible nano-hybrid inverter based on inkjet-printed organic and 2D multilayer MoS<sub>2</sub> thin film transistor. *Org. Electron.* **2014**, *15*, 3038–3042. [[CrossRef](#)]
214. Ha, J.; Chung, S.; Pei, M.; Cho, K.; Yang, H.; Hong, Y. One-Step Interface Engineering for All-Inkjet-Printed, All-Organic Components in Transparent, Flexible Transistors and Inverters: Polymer Binding. *ACS Appl. Mater. Interfaces* **2017**, *9*, 8819–8829. [[CrossRef](#)] [[PubMed](#)]
215. Stucchi, E.; Dell'Erba, G.; Colpani, P.; Kim, Y.H.; Caironi, M. Low-Voltage, Printed, All-Polymer Integrated Circuits Employing a Low-Leakage and High-Yield Polymer Dielectric. *Adv. Electron. Mater.* **2018**, *4*, 1800340. [[CrossRef](#)]
216. Stucchi, E.; Scaccabarozzi, A.D.; Viola, F.A.; Caironi, M. Ultraflexible all-organic complementary transistors and inverters based on printed polymers. *J. Mater. Chem. C* **2020**, *8*, 15331–15338. [[CrossRef](#)]
217. Singaraju, S.A.; Marques, G.C.; Gruber, P.; Kruk, R.; Hahn, H.; Breitung, B.; Aghassi-Hagmann, J. Fully Printed Inverters using Metal-Oxide Semiconductor and Graphene Passives on Flexible Substrates. *Phys. Status Solidi RRL—Rapid Res. Lett.* **2020**, *14*, 2000252. [[CrossRef](#)]
218. Luczak, A.; Mitra, K.Y.; Baumann, R.R.; Zichner, R.; Luszczynska, B.; Jung, J. Fully inkjet-printed flexible organic voltage inverters as a basic component in digital NOT gates. *Sci. Rep.* **2022**, *12*, 10887. [[CrossRef](#)] [[PubMed](#)]
219. Pradhan, J.R.; Singh, M.; Dasgupta, S. Inkjet-Printed, Deep Subthreshold Operated Pseudo-CMOS Inverters with High Voltage Gain and Low Power Consumption. *Adv. Electron. Mater.* **2022**, *8*, 2200528. [[CrossRef](#)]
220. Kwon, J.; Kyung, S.; Yoon, S.; Kim, J.J.; Jung, S. Solution-Processed Vertically Stacked Complementary Organic Circuits with Inkjet-Printed Routing. *Adv. Sci.* **2016**, *3*, 1500439. [[CrossRef](#)]
221. Casula, G.; Lai, S.; Martino, L.; Santoro, F.; Bonfiglio, A.; Cosseddu, P. Printed, Low-Voltage, All-Organic Transistors and Complementary Circuits on Paper Substrate. *Adv. Electron. Mater.* **2020**, *6*, 1901027. [[CrossRef](#)]
222. Jung, S.; Sou, A.; Gili, E.; Siringhaus, H. Inkjet-printed resistors with a wide resistance range for printed read-only memory applications. *Org. Electron.* **2013**, *14*, 699–702. [[CrossRef](#)]
223. Ramon, E.; Sowade, E.; Martínez-Domingo, C.; Mitra, K.Y.; Alcalde, A.; Baumann, R.R.; Carrabina, J. Large-scale fabrication of all-inkjet-printed resistors and WORM memories on flexible polymer films with high yield and stability. *Flex. Print. Electron.* **2021**, *6*, 015003. [[CrossRef](#)]
224. Salaoru, I.; Maswoud, S.; Paul, S. Inkjet Printing of Functional Electronic Memory Cells: A Step Forward to Green Electronics. *Micromachines* **2019**, *10*, 417. [[CrossRef](#)]
225. Delfag, M.; Rachovitis, G.; González, Y.; Jehn, J.; Youssef, A.H.; Schindler, C.; Ruediger, A. Fully printed ZnO-based valency-change memories for flexible and transparent applications. *Flex. Print. Electron.* **2022**, *7*, 045001. [[CrossRef](#)]
226. Huber, B.; Schober, J.; Kreuzer, A.; Kaiser, M.; Ruediger, A.; Schindler, C. Inkjet-printed resistive memory cells for transparent electronics. *Microelectron. Eng.* **2018**, *194*, 85–88. [[CrossRef](#)]
227. Huber, B.; Popp, P.B.; Kaiser, M.; Ruediger, A.; Schindler, C. Fully inkjet printed flexible resistive memory. *Appl. Phys. Lett.* **2017**, *110*, 143503. [[CrossRef](#)]
228. Jung, S.-W. Nonvolatile Ferroelectric P(VDF-TrFE) Memory Transistors Based on Inkjet-Printed Organic Semiconductor. *ETRI J.* **2013**, *35*, 734–737. [[CrossRef](#)]
229. Bhansali, U.S.; Khan, M.A.; Alshareef, H.N. Organic ferroelectric memory devices with inkjet-printed polymer electrodes on flexible substrates. *Microelectron. Eng.* **2013**, *105*, 68–73. [[CrossRef](#)]
230. Kang, M.; Baeg, K.-J.; Khim, D.; Noh, Y.-Y.; Kim, D.-Y. Printed, Flexible, Organic Nano-Floating-Gate Memory: Effects of Metal Nanoparticles and Blocking Dielectrics on Memory Characteristics. *Adv. Funct. Mater.* **2013**, *23*, 3503–3512. [[CrossRef](#)]
231. Kim, C.; Song, J.M.; Lee, J.S.; Lee, M.J. All-solution-processed nonvolatile flexible nano-floating gate memory devices. *Nanotechnology* **2014**, *25*, 014016. [[CrossRef](#)] [[PubMed](#)]
232. Yang, B.-D. Printed Organic One-Time Programmable ROM Array Using Anti-fuse Capacitor. *ETRI J.* **2013**, *35*, 594–602. [[CrossRef](#)]
233. Jung, S.-W.; Na, B.S.; You, I.-K.; Koo, J.B.; Yang, B.-D.; Oh, J.-M. Inkjet-printed organic thin-film transistor and antifuse capacitor for flexible one-time programmable memory applications. *J. Korean Phys. Soc.* **2014**, *64*, 74–78. [[CrossRef](#)]

234. Jung, S.W.; Na, B.S.; Park, C.W.; Koo, J.B. Low-voltage-operated organic one-time programmable memory using printed organic thin-film transistors and antifuse capacitors. *J. Nanosci. Nanotechnol.* **2014**, *14*, 8167–8170. [[CrossRef](#)]
235. Shim, G.H.; Han, M.G.; Sharp-Norton, J.C.; Creager, S.E.; Foulger, S.H. Inkjet-printed electrochromic devices utilizing polyaniline-silica and poly(3,4-ethylenedioxythiophene)-silica colloidal composite particles. *J. Mater. Chem.* **2008**, *18*, 594–601. [[CrossRef](#)]
236. Huang, X.; Chen, J.; Xie, H.; Zhao, F.; Fan, S.; Zhang, Y. Inkjet printing of 2D polyaniline for fabricating flexible and patterned electrochromic devices. *Sci. China Mater.* **2022**, *65*, 2217–2226. [[CrossRef](#)]
237. Nguyen, T.-T.-N.; Chan, C.-Y.; He, J.-L. One-step inkjet printing of tungsten oxide-poly(3,4-ethylenedioxythiophene):polystyrene sulphonate hybrid film and its applications in electrochromic devices. *Thin Solid Film.* **2016**, *603*, 276–282. [[CrossRef](#)]
238. Pietsch, M.; Schlisske, S.; Held, M.; Strobel, N.; Wiecek, A.; Hernandez-Sosa, G. Biodegradable inkjet-printed electrochromic display for sustainable short-lifecycle electronics. *J. Mater. Chem. C* **2020**, *8*, 16716–16724. [[CrossRef](#)]
239. Coenen, M.J.J.; Slaats, T.M.W.L.; Eggenhuisen, T.M.; Groen, P. Inkjet printing the three organic functional layers of two-colored organic light emitting diodes. *Thin Solid Film.* **2015**, *583*, 194–200. [[CrossRef](#)]
240. Hu, Y.-X.; Lin, T.; Xia, X.; Mu, W.-Y.; Sun, Y.-L.; He, W.-Z.; Wei, C.-T.; Zhang, D.-Y.; Li, X.; Cui, Z. Novel phosphorescent iridium(III) emitters for both vacuum-deposition and inkjet-printing of OLEDs with exceptionally high efficiency. *J. Mater. Chem. C* **2019**, *7*, 4178–4184. [[CrossRef](#)]
241. Zhao, J.; Lo, L.W.; Wan, H.; Mao, P.; Yu, Z.; Wang, C. High-Speed Fabrication of All-Inkjet-Printed Organometallic Halide Perovskite Light-Emitting Diodes on Elastic Substrates. *Adv. Mater.* **2021**, *33*, e2102095. [[CrossRef](#)] [[PubMed](#)]
242. Hu, B.; Li, D.; Manandharm, P.; Fan, Q.; Kasilingam, D.; Calvert, P. CNT/conducting polymer composite conductors impart high flexibility to textile electroluminescent devices. *J. Mater. Chem.* **2012**, *22*, 1598–1605. [[CrossRef](#)]
243. Ohmori, M.; Ueno, S.; Kurachi, N.; Sawamura, M.; Hattori, M.; Inoue, T.; Miyabayashi, T.; Takao, Y.; Hibino, S.; Tsuchiya, I.; et al. Light-Emitting Seal Using Self-Aligned Organic Light-Emitting Structure. *Jpn. J. Appl. Phys.* **2008**, *47*, 472–475. [[CrossRef](#)]
244. Koizumi, H.; Ooshiro, K.; Soeda, K.; Homma, T. Effect of Drying Condition of Emitting Layer Formed by Ink-Jet Coating on Optical Property and Film Morphology of Polymer-Based Organic Light-Emitting Diodes. *ECS J. Solid State Sci. Technol.* **2019**, *8*, R36–R41. [[CrossRef](#)]
245. Villani, F.; Vacca, P.; Miscioscia, R.; Nenna, G.; Burrasca, G.; Fasolino, T.; Minarini, C.; Sala, D. OLED with Hole-Transporting Layer Fabricated by Ink-Jet Printing. *Macromol. Symp.* **2009**, *286*, 101–106. [[CrossRef](#)]
246. Villani, F.; Vacca, P.; Nenna, G.; Valentino, O.; Burrasca, G.; Fasolino, T.; Minarini, C.; della Sala, D. Inkjet Printed Polymer Layer on Flexible Substrate for OLED Applications. *J. Phys. Chem. C* **2009**, *113*, 13398–13402. [[CrossRef](#)]
247. Fisslthaler, E.; Sax, S.; Scherf, U.; Mauthner, G.; Moderegger, E.; Landfester, K.; List, E.J.W. Inkjet printed polymer light-emitting devices fabricated by thermal embedding of semiconducting polymer nanospheres in an inert matrix. *Appl. Phys. Lett.* **2008**, *92*, 183305. [[CrossRef](#)]
248. Kwon, J.-T.; Eom, S.-H.; Moon, B.-S.; Shin, J.-K.; Kim, K.-S.; Lee, S.-H.; Lee, Y.-S. Studies on Printing Inks Containing Poly[2-methoxy-5-(2-ethylhexyl-oxyl)-1,4-phenylenevinylene] as an Emissive Material for the Fabrication of Polymer Light-Emitting Diodes by Inkjet Printing. *Bull. Korean Chem. Soc.* **2012**, *33*, 464–468. [[CrossRef](#)]
249. Wang, M.; Yang, G.-Z.; Wang, M.; Liu, T. Effect of film thickness controlled by ink-jet printing method on the optical properties of an electroluminescent polymer. *Polym. Adv. Technol.* **2010**, *21*, 381–385. [[CrossRef](#)]
250. Wei, C.; Zhuang, J.; Zhang, D.; Guo, W.; Yang, D.; Xie, Z.; Tang, J.; Su, W.; Zeng, H.; Cui, Z. Pyridine-Based Electron-Transport Materials with High Solubility, Excellent Film-Forming Ability, and Wettability for Inkjet-Printed OLEDs. *ACS Appl. Mater. Interfaces* **2017**, *9*, 38716–38727. [[CrossRef](#)]
251. Liu, L.; Chen, D.; Xie, J.; Piao, J.; Liu, Y.; Wang, W.; Cao, K.; Chen, S. Universally applicable small-molecule co-host ink formulation for inkjet printing red, green, and blue phosphorescent organic light-emitting diodes. *Org. Electron.* **2021**, *96*, 106247. [[CrossRef](#)]
252. Gohda, T.; Kobayashi, Y.; Okano, K.; Inoue, S.; Okamoto, K.; Hashimoto, S.; Yamamoto, E.; Morita, H.; Mitsui, S.; Kodan, M. 58.3: A 3.6-In. 202-ppi Full-Color AMPLD Display Fabricated by Ink-Jet Method. *SID Symp. Dig. Tech. Pap.* **2006**, *37*, 1767–1770. [[CrossRef](#)]
253. Cao, X.; Ye, Y.; Liu, X.; Guo, T.; Tang, Q. 54.3: Realization of Uniform OLED Pixels based on Multi-nozzle by Inkjet printing. *SID Symp. Dig. Tech. Pap.* **2021**, *52*, 395–397. [[CrossRef](#)]
254. Shimoda, T.; Kanbe, S.; Kobayashi, H.; Seki, S.; Kiguchi, H.; Yudasaka, I.; Kimura, M.; Miyashita, S.; Friend, R.H.; Burroughes, J.H.; et al. 26.3: Multicolor Pixel Patterning of Light-Emitting Polymers by Ink-Jet Printing. *SID Symp. Dig. Tech. Pap.* **1999**, *30*, 376–379. [[CrossRef](#)]
255. Bharathan, J.; Yang, Y. Polymer electroluminescent devices processed by inkjet printing: I. Polymer light-emitting logo. *Appl. Phys. Lett.* **1998**, *72*, 2660–2662. [[CrossRef](#)]
256. Kobayashi, H.; Kanbe, S.; Seki, S.; Kiguchi, H.; Kimura, M.; Yudasaka, I.; Miyashita, S.; Shimoda, T.; Towns, C.R.; Burroughes, J.H.; et al. A novel RGB multicolor light-emitting polymer display. *Synth. Met.* **2000**, *111–112*, 125–128. [[CrossRef](#)]
257. Shimoda, T. 39.1: Invited Paper: Ink-jet Technology for Fabrication Processes of Flat Panel Displays. *SID Symp. Dig. Tech. Pap.* **2003**, *34*, 1178–1181. [[CrossRef](#)]
258. Wang, J.; Song, C.; Zhong, Z.; Hu, Z.; Han, S.; Xu, W.; Peng, J.; Ying, L.; Wang, J.; Cao, Y. In situ patterning of microgrooves via inkjet etching for a solution-processed OLED display. *J. Mater. Chem. C* **2017**, *5*, 5005–5009. [[CrossRef](#)]
259. Gereanu, A.-G.; Sartorio, C.; Bonasera, A.; Giuliano, G.; Cataldo, S.; Scopelliti, M.; Arrabito, G.; Pignataro, B. Pseudo-Planar Organic Heterojunctions by Sequential Printing of Quasi-Miscible Inks. *Coatings* **2021**, *11*, 586. [[CrossRef](#)]

260. Lee, S.H.; Lee, U.J.; Yu, J.H.; Yun, G.-Y.; Kang, K.-T.; Lee, J.K. Characterization of inkjet-printed P3TH:PCBM bulk heterojunction films for ITO-free polymer solar cells. *Macromol. Res.* **2013**, *22*, 219–222. [[CrossRef](#)]
261. Eom, S.H.; Park, H.; Mujawar, S.H.; Yoon, S.C.; Kim, S.-S.; Na, S.-I.; Kang, S.-J.; Khim, D.; Kim, D.-Y.; Lee, S.-H. High efficiency polymer solar cells via sequential inkjet-printing of PEDOT:PSS and P3HT:PCBM inks with additives. *Org. Electron.* **2010**, *11*, 1516–1522. [[CrossRef](#)]
262. Park, E.K.; Kim, J.H.; Lee, D.H.; Kim, K.S.; Kal, J.H.; Hahn, J.S.; Kim, Y.S. All Ink-Jet Printed P3HT:PCBM Organic Solar Cells on ITO-Coated Glass Substrate. *J. Nanosci. Nanotechnol.* **2015**, *15*, 8790–8796. [[CrossRef](#)] [[PubMed](#)]
263. Eggenhuisen, T.M.; Galagan, Y.; Coenen, E.W.C.; Voorthuijzen, W.P.; Slaats, M.W.L.; Kommeren, S.A.; Shanmugan, S.; Coenen, M.J.J.; Andriessen, R.; Groen, W.A. Digital fabrication of organic solar cells by Inkjet printing using non-halogenated solvents. *Sol. Energy Mater. Sol. Cells* **2015**, *134*, 364–372. [[CrossRef](#)]
264. Mitra, K.Y.; Alalawe, A.; Voigt, S.; Boeffel, C.; Baumann, R.R. Manufacturing of All Inkjet-Printed Organic Photovoltaic Cell Arrays and Evaluating their Suitability for Flexible Electronics. *Micromachines* **2018**, *9*, 642. [[CrossRef](#)] [[PubMed](#)]
265. Azzellino, G.; Grimaldi, A.; Binda, M.; Caironi, M.; Natali, D.; Sampietro, M. Fully inkjet-printed organic photodetectors with high quantum yield. *Adv. Mater.* **2013**, *25*, 6829–6833. [[CrossRef](#)] [[PubMed](#)]
266. Cesarini, M.; Brigante, B.; Caironi, M.; Natali, D. Reproducible, High Performance Fully Printed Photodiodes on Flexible Substrates through the Use of a Polyethylenimine Interlayer. *ACS Appl. Mater. Interfaces* **2018**, *10*, 32380–32386. [[CrossRef](#)] [[PubMed](#)]
267. Hoth, C.N.; Choulis, S.A.; Schilinsky, P.; Brabec, C.J. High Photovoltaic Performance of Inkjet Printed Polymer:Fullerene Blends. *Adv. Mater.* **2007**, *19*, 3973–3978. [[CrossRef](#)]
268. Aernouts, T.; Aleksandrov, T.; Girotto, C.; Genoe, J.; Poortmans, J. Polymer based organic solar cells using ink-jet printed active layers. *Appl. Phys. Lett.* **2008**, *92*, 033306. [[CrossRef](#)]
269. Hoth, C.N.; Schilinsky, P.; Choulis, S.A.; Brabec, C.J. Printing highly efficient organic solar cells. *Nano Lett.* **2008**, *8*, 2806–2813. [[CrossRef](#)]
270. Hoth, C.N.; Choulis, S.A.; Schilinsky, P.; Brabec, C.J. On the effect of poly(3-hexylthiophene) regioregularity on inkjet printed organic solar cells. *J. Mater. Chem.* **2009**, *19*, 5398–5404. [[CrossRef](#)]
271. Jung, J.; Kim, D.; Lim, J.; Lee, C.; Yoon, S.C. Highly Efficient Inkjet-Printed Organic Photovoltaic Cells. *Jpn. J. Appl. Phys.* **2010**, *49*, 05EB03. [[CrossRef](#)]
272. Lange, A.; Wegener, M.; Boeffel, C.; Fischer, B.; Wedel, A.; Neher, D. A new approach to the solvent system for inkjet-printed P3HT:PCBM solar cells and its use in devices with printed passive and active layers. *Sol. Energy Mater. Sol. Cells* **2010**, *94*, 1816–1821. [[CrossRef](#)]
273. Hoth, C.N.; Schilinsky, P.; Choulis, S.A.; Brabec, C.J. Photovoltaic Loss Analysis of Inkjet-Printed Polymer Solar Cells Using Pristine Solvent Formulations. *Macromol. Symp.* **2010**, *291–292*, 287–292. [[CrossRef](#)]
274. Lee, J.K.; Lee, U.J.; Kim, M.-K.; Lee, S.H.; Kang, K.-T. Direct writing of semiconducting polythiophene and fullerene derivatives composite from bulk heterojunction solar cell by inkjet printing. *Thin Solid Film.* **2011**, *519*, 5649–5653. [[CrossRef](#)]
275. Haldar, A.; Liao, K.-S.; Curran, S.A. Effect of printing parameters and annealing on organic photovoltaics performance. *J. Mater. Res.* **2012**, *27*, 2079–2087. [[CrossRef](#)]
276. Neophytou, M.; Cambarau, W.; Hermerschmidt, F.; Waldauf, C.; Christodoulou, C.; Pacios, R.; Choulis, S.A. Inkjet-printed polymer–fullerene blends for organic electronic applications. *Microelectron. Eng.* **2012**, *95*, 102–106. [[CrossRef](#)]
277. Lange, A.; Hollaender, A.; Wegener, M. Modified processing conditions for optimized organic solar cells with inkjet printed P3HT:PC61BM active layers. *Mater. Sci. Eng. B* **2013**, *178*, 299–305. [[CrossRef](#)]
278. Lim, G.-H.; Zhuo, J.-M.; Wong, L.-Y.; Chua, S.-J.; Chua, L.-L.; Ho, P.K.H. A transition solvent strategy to print polymer:fullerene films using halogen-free solvents for solar cell applications. *Org. Electron.* **2014**, *15*, 449–460. [[CrossRef](#)]
279. Haldar, A.; Liao, K.-S.; Curran, S.A. Fabrication of inkjet printed organic photovoltaics on flexible Ag electrode with additives. *Sol. Energy Mater. Sol. Cells* **2014**, *125*, 283–290. [[CrossRef](#)]
280. Bruno, A.; Villani, F.; Grimaldi, I.A.; Loffredo, F.; Morvillo, P.; Diana, R.; Haque, S.; Minarini, C. Morphological and spectroscopic characterizations of inkjet-printed poly(3-hexylthiophene-2,5-diyl): Phenyl-C61-butyric acid methyl ester blends for organic solar cell applications. *Thin Solid Film.* **2014**, *560*, 14–19. [[CrossRef](#)]
281. Eom, S.H.; Senthilarasu, S.; Uthirakumar, P.; Yoon, S.C.; Lim, J.; Lee, C.; Lim, H.S.; Lee, J.; Lee, S.-H. Polymer solar cells based on inkjet-printed PEDOT:PSS layer. *Org. Electron.* **2009**, *10*, 536–542. [[CrossRef](#)]
282. Steirer, K.X.; Berry, J.J.; Reese, M.O.; van Hest, M.F.A.M.; Miedaner, A.; Liberatore, M.W.; Collins, R.T.; Ginley, D.S. Ultrasonically sprayed and inkjet printed thin film electrodes for organic solar cells. *Thin Solid Film.* **2009**, *517*, 2781–2786. [[CrossRef](#)]
283. De Girolamo Del Mauro, A.; Diana, R.; Grimaldi, I.A.; Loffredo, F.; Morvillo, P.; Villani, F.; Minarini, C. Polymer solar cells with inkjet-printed doped-PEDOT: PSS anode. *Polym. Compos.* **2013**, *34*, 1493–1499. [[CrossRef](#)]
284. Murali, B.; Kim, D.-G.; Kang, J.-W.; Kim, J. Inkjet-printing of hybrid transparent conducting electrodes for organic solar cells. *Phys. Status Solidi A* **2014**, *211*, 1801–1806. [[CrossRef](#)]
285. Kommeren, S.; Coenen, M.J.J.; Eggenhuisen, T.M.; Slaats, T.W.L.; Gorter, H.; Groen, P. Combining solvents and surfactants for inkjet printing PEDOT:PSS on P3HT/PCBM in organic solar cells. *Org. Electron.* **2018**, *61*, 282–288. [[CrossRef](#)]
286. Yang, Y.; Nakamichi, T.; Yoshioka, H.; Omi, S.; Goto, R.; Watanabe, H.; Oki, Y. Intensity Sensitive Organic Photodiodes Patterned by Inkjet Method. *Mol. Cryst. Liq. Cryst.* **2011**, *538*, 136–142. [[CrossRef](#)]

287. Singh, A.; Gupta, S.K.; Garg, A. Inverted polymer bulk heterojunction solar cells with ink-jet printed electron transport and active layers. *Org. Electron.* **2016**, *35*, 118–127. [[CrossRef](#)]
288. Teichler, A.; Eckardt, R.; Hoepfner, S.; Friebe, C.; Perelaer, J.; Senes, A.; Morana, M.; Brabec, C.J.; Schubert, U.S. Combinatorial Screening of Polymer:Fullerene Blends for Organic Solar Cells by Inkjet Printing. *Adv. Energy Mater.* **2011**, *1*, 105–114. [[CrossRef](#)]
289. Fauzia, V.; Umar, A.A.; Salleh, M.M.; Yahaya, M. The Effect of Donor:Acceptor Ratio on the Generated Photocurrent of Inkjet Printed Blended Poly (3-Octylthiophene-2,5-Diyl) and (6,6)-Phenyl C<sub>71</sub> Butyric Acid Methyl Ester Bulk Heterojunction Organic Solar Cells. *Mater. Sci. Forum* **2010**, 663–665, 823–827. [[CrossRef](#)]
290. Fauzia, V.; Umar, A.A.; Salleh, M.M.; Yahaya, M. The effect of solvent on the morphology of an inkjet printed active layer of bulk heterojunction solar cells. *Adv. Nat. Sci. Nanosci. Nanotechnol.* **2011**, *2*, 015014. [[CrossRef](#)]
291. Fauzia, V.; Umar, A.A.; Salleh, M.M.; Yahaya, M. Study Phase Separation of Donor: Acceptor in Inkjet Printed Thin Films of Bulk Heterojunction Organic Solar Cells Using AFM Phase Imaging. *Adv. Mater. Res.* **2011**, *364*, 465–469. [[CrossRef](#)]
292. Morvillo, P.; Grimaldi, I.A.; Diana, R.; Loffredo, F.; Villani, F. Study of the microstructure of inkjet-printed P3HT:PCBM blend for photovoltaic applications. *J. Mater. Sci.* **2012**, *48*, 2920–2927. [[CrossRef](#)]
293. Lange, A.; Wegener, M.; Fischer, B.; Janietz, S.; Wedel, A. Solar Cells with Inkjet Printed Polymer Layers. *Energy Procedia* **2012**, *31*, 150–158. [[CrossRef](#)]
294. Nakamichi, T.; Yang, Y.; Ohta, T.; Yoshioka, H.; Yahiro, M.; Era, M.; Watanabe, H.; Cui, Y.; Oki, Y.; Qian, G. Stackable spectral-sensitive conductive films based on cyanine aggregates via an inkjet method. *Dye. Pigment.* **2013**, *98*, 333–338. [[CrossRef](#)]
295. Lange, A.; Schindler, W.; Wegener, M.; Fostiropoulos, K.; Janietz, S. Inkjet printed solar cell active layers prepared from chlorine-free solvent systems. *Sol. Energy Mater. Sol. Cells* **2013**, *109*, 104–110. [[CrossRef](#)]
296. Lange, A.; Schindler, W.; Wegener, M.; Fostiropoulos, K.; Janietz, S. Inkjet printed solar cell active layers based on a novel, amorphous polymer. *J. Nanosci. Nanotechnol.* **2013**, *13*, 5209–5214. [[CrossRef](#)]
297. Jung, S.; Sou, A.; Banger, K.; Ko, D.-H.; Chow, P.C.Y.; McNeill, C.R.; Siringhaus, H. All-Inkjet-Printed, All-Air-Processed Solar Cells. *Adv. Energy Mater.* **2014**, *4*, 1400432. [[CrossRef](#)]
298. Eggenhuisen, T.M.; Galagan, Y.; Biezemans, A.F.K.V.; Slaats, T.M.W.L.; Voorthuizen, W.P.; Kommeren, S.; Shanmugam, S.; Teunissen, J.P.; Hadipour, A.; Verhees, W.J.H.; et al. High efficiency, fully inkjet printed organic solar cells with freedom of design. *J. Mater. Chem. A* **2015**, *3*, 7255–7262. [[CrossRef](#)]
299. Lamont, C.A.; Eggenhuisen, T.M.; Coenen, M.J.J.; Slaats, T.W.L.; Andriessen, R.; Groen, P. Tuning the viscosity of halogen free bulk heterojunction inks for inkjet printed organic solar cells. *Org. Electron.* **2015**, *17*, 107–114. [[CrossRef](#)]
300. Sankaran, S.; Glaser, K.; Gärtner, S.; Rödlmeier, T.; Sudau, K.; Hernandez-Sosa, G.; Colsmann, A. Fabrication of polymer solar cells from organic nanoparticle dispersions by doctor blading or ink-jet printing. *Org. Electron.* **2016**, *28*, 118–122. [[CrossRef](#)]
301. Grimoldi, A.; Colella, L.; La Monaca, L.; Azzellino, G.; Caironi, M.; Bertarelli, C.; Natali, D.; Sampietro, M. Inkjet printed polymeric electron blocking and surface energy modifying layer for low dark current organic photodetectors. *Org. Electron.* **2016**, *36*, 29–34. [[CrossRef](#)]
302. Maisch, P.; Tam, K.C.; Schilinsky, P.; Egelhaaf, H.-J.; Brabec, C.J. Shy Organic Photovoltaics: Digitally Printed Organic Solar Modules With Hidden Interconnects. *Sol. RRL* **2018**, *2*, 1800005. [[CrossRef](#)]
303. Gribkova, O.L.; Saf'yanova, L.V.; Tameev, A.R.; Lypenko, D.A.; Tverskoi, V.A.; Nekrasov, A.A. A Water-Soluble Polyaniline Complex for Ink-Jet Printing of Optoelectronic Devices. *Tech. Phys. Lett.* **2018**, *44*, 239–242. [[CrossRef](#)]
304. Maisch, P.; Eisenhofer, L.M.; Tam, K.C.; Distler, A.; Voigt, M.M.; Brabec, C.J.; Egelhaaf, H.-J. A generic surfactant-free approach to overcome wetting limitations and its application to improve inkjet-printed P3HT:non-fullerene acceptor PV. *J. Mater. Chem. A* **2019**, *7*, 13215–13224. [[CrossRef](#)]
305. Corzo, D.; Almasabi, K.; Bihar, E.; Macphee, S.; Rosas-Villalva, D.; Gasparini, N.; Inal, S.; Baran, D. Digital Inkjet Printing of High-Efficiency Large-Area Nonfullerene Organic Solar Cells. *Adv. Mater. Technol.* **2019**, *4*, 1900040. [[CrossRef](#)]
306. Ganesan, S.; Gollu, S.R.; Alam Khan, J.; Kushwaha, A.; Gupta, D. Inkjet printing of zinc oxide and P3HT:ICBA in ambient conditions for inverted bulk heterojunction solar cells. *Opt. Mater.* **2019**, *94*, 430–435. [[CrossRef](#)]
307. Gribkova, O.L.; Kabanova, V.A.; Tameev, A.R.; Nekrasov, A.A. Ink-Jet Printing of Polyaniline Layers for Perovskite Solar Cells. *Tech. Phys. Lett.* **2019**, *45*, 858–861. [[CrossRef](#)]
308. Corzo, D.; Bihar, E.; Alexandre, E.B.; Rosas-Villalva, D.; Baran, D. Ink Engineering of Transport Layers for 9.5% Efficient All-Printed Semitransparent Nonfullerene Solar Cells. *Adv. Funct. Mater.* **2020**, *31*, 2005763. [[CrossRef](#)]
309. Bihar, E.; Corzo, D.; Hidalgo, T.C.; Rosas-Villalva, D.; Salama, K.N.; Inal, S.; Baran, D. Fully Inkjet-Printed, Ultrathin and Conformable Organic Photovoltaics as Power Source Based on Cross-Linked PEDOT:PSS Electrodes. *Adv. Mater. Technol.* **2020**, *5*, 2000226. [[CrossRef](#)]
310. Perkhun, P.; Köntges, W.; Pourcin, F.; Esteouille, D.; Barulina, E.; Yoshimoto, N.; Pierron, P.; Margeat, O.; Videlot-Ackermann, C.; Bharwal, A.K.; et al. High-Efficiency Digital Inkjet-Printed Non-Fullerene Polymer Blends Using Non-Halogenated Solvents. *Adv. Energy Sustain. Res.* **2021**, *2*, 2000086. [[CrossRef](#)]
311. Gao, B.; Meng, J. Flexible CH<sub>3</sub>NH<sub>3</sub>PbI<sub>3</sub> perovskite solar cells with high stability based on all inkjet printing. *Sol. Energy* **2021**, *230*, 598–604. [[CrossRef](#)]
312. Chen, X.; Huang, R.; Han, Y.; Zha, W.; Fang, J.; Lin, J.; Luo, Q.; Chen, Z.; Ma, C.Q. Balancing the Molecular Aggregation and Vertical Phase Separation in the Polymer: Nonfullerene Blend Films Enables 13.09% Efficiency of Organic Solar Cells with Inkjet-Printed Active Layer. *Adv. Energy Mater.* **2022**, *12*, 2200044. [[CrossRef](#)]

313. Chen, C.-T.; Yang, H.-H. Inkjet printing of composite hole transport layers and bulk heterojunction structure for organic solar cells. *Thin Solid Film.* **2022**, *751*, 139217. [[CrossRef](#)]
314. Kit-Anan, W.; Olarnwanich, A.; Sriprachuabwong, C.; Karuwan, C.; Tuantranont, A.; Wisitsoraat, A.; Srituravanich, W.; Pimpin, A. Disposable paper-based electrochemical sensor utilizing inkjet-printed Polyaniline modified screen-printed carbon electrode for Ascorbic acid detection. *J. Electroanal. Chem.* **2012**, *685*, 72–78. [[CrossRef](#)]
315. Setti, L.; Fraleoni-Morgera, A.; Mencarelli, I.; Filippini, A.; Ballarin, B.; Dibiase, M. An HRP-based amperometric biosensor fabricated by thermal inkjet printing. *Sens. Actuators B Chem.* **2007**, *126*, 252–257. [[CrossRef](#)]
316. Chennit, K.; Delavari, N.; Mekhmoukhen, S.; Boukraa, R.; Fillaud, L.; Zrig, S.; Battaglini, N.; Piro, B.; Noël, V.; Zozoulenko, I.; et al. Inkjet-Printed, Coplanar Electrolyte-Gated Organic Field-Effect Transistors on Flexible Substrates: Fabrication, Modeling, and Applications in Biodetection. *Adv. Mater. Technol.* **2022**, *8*, 2200300. [[CrossRef](#)]
317. Oh, W.K.; Kim, S.; Shin, K.H.; Jang, Y.; Choi, M.; Jang, J. Inkjet-printed polyaniline patterns for exocytosed molecule detection from live cells. *Talanta* **2013**, *105*, 333–339. [[CrossRef](#)] [[PubMed](#)]
318. Li, L.; Pan, L.; Ma, Z.; Yan, K.; Cheng, W.; Shi, Y.; Yu, G. All Inkjet-Printed Amperometric Multiplexed Biosensors Based on Nanostructured Conductive Hydrogel Electrodes. *Nano Lett.* **2018**, *18*, 3322–3327. [[CrossRef](#)]
319. Bardpho, C.; Rattanarat, P.; Siangproh, W.; Chailapakul, O. Ultra-high performance liquid chromatographic determination of antioxidants in teas using inkjet-printed graphene-polyaniline electrode. *Talanta* **2016**, *148*, 673–679. [[CrossRef](#)]
320. Karuwan, C.; Sriprachuabwong, C.; Wisitsoraat, A.; Phokharatkul, D.; Sritongkham, P.; Tuantranont, A. Inkjet-printed graphene-poly(3,4-ethylenedioxythiophene):poly(styrene-sulfonate) modified on screen printed carbon electrode for electrochemical sensing of salbutamol. *Sens. Actuators B Chem.* **2012**, *161*, 549–555. [[CrossRef](#)]
321. Tseng, C.-C.; Chou, Y.-H.; Hsieh, T.-W.; Wang, M.-W.; Shu, Y.-Y.; Ger, M.-D. Interdigitated electrode fabricated by integration of ink-jet printing with electroless plating and its application in gas sensor. *Colloids Surf. A Physicochem. Eng. Asp.* **2012**, *402*, 45–52. [[CrossRef](#)]
322. Andò, B.; Baglio, S.; Di Pasquale, G.; Pollicino, A.; D’agata, S.; Gugliuzzo, C.; Lombardo, C.; Re, G. An Inkjet Printed CO<sub>2</sub> Gas Sensor. *Procedia Eng.* **2015**, *120*, 628–631. [[CrossRef](#)]
323. Bihar, E.; Wustoni, S.; Pappa, A.M.; Salama, K.N.; Baran, D.; Inal, S. A fully inkjet-printed disposable glucose sensor on paper. *npj Flex. Electron.* **2018**, *2*, 30. [[CrossRef](#)]
324. Setti, L.; Fraleoni-Morgera, A.; Ballarin, B.; Filippini, A.; Frascaro, D.; Piana, C. An amperometric glucose biosensor prototype fabricated by thermal inkjet printing. *Biosens. Bioelectron.* **2005**, *20*, 2019–2026. [[CrossRef](#)] [[PubMed](#)]
325. Yun, Y.H.; Lee, B.K.; Choi, J.S.; Kim, S.; Yoo, B.; Kim, Y.S.; Park, K.; Cho, Y.W. A glucose sensor fabricated by piezoelectric inkjet printing of conducting polymers and bienzymes. *Anal. Sci.* **2011**, *27*, 375. [[CrossRef](#)] [[PubMed](#)]
326. Weng, B.; Morrin, A.; Shepherd, R.; Crowley, K.; Killard, A.J.; Innis, P.C.; Wallace, G.G. Wholly printed polypyrrole nanoparticle-based biosensors on flexible substrate. *J. Mater. Chem. B* **2014**, *2*, 793–799. [[CrossRef](#)] [[PubMed](#)]
327. Song, E.; da Costa, T.H.; Choi, J.-W. A chemiresistive glucose sensor fabricated by inkjet printing. *Microsyst. Technol.* **2016**, *23*, 3505–3511. [[CrossRef](#)]
328. Song, E.; Tortorich, R.P.; da Costa, T.H.; Choi, J.-W. Inkjet printing of conductive polymer nanowire network on flexible substrates and its application in chemical sensing. *Microelectron. Eng.* **2015**, *145*, 143–148. [[CrossRef](#)]
329. Khan, S.; Ali, S.; Khan, A.; Wang, B.; Bermak, A. Printing Sensors on Biocompatible Substrates for Selective Detection of Glucose. *IEEE Sens. J.* **2021**, *21*, 4167–4175. [[CrossRef](#)]
330. Sriprachuabwong, C.; Karuwan, C.; Wisitsorratt, A.; Phokharatkul, D.; Lomas, T.; Sritongkham, P.; Tuantranont, A. Inkjet-printed graphene-PEDOT:PSS modified screen printed carbon electrode for biochemical sensing. *J. Mater. Chem.* **2012**, *22*, 5478–5485. [[CrossRef](#)]
331. Crowley, K.; Morrin, A.; Shepherd, R.L.; in het Panhuis, M.; Wallace, G.G.; Smyth, M.R.; Killard, A.J. Fabrication of Polyaniline-Based Gas Sensors Using Piezoelectric Inkjet and Screen Printing for the Detection of Hydrogen Sulfide. *IEEE Sens. J.* **2010**, *10*, 1419–1426. [[CrossRef](#)]
332. Beduk, T.; Bihar, E.; Surya, S.G.; Castillo, A.N.; Inal, S.; Salama, K.N. A paper-based inkjet-printed PEDOT:PSS/ZnO sol-gel hydrazine sensor. *Sens. Actuators B Chem.* **2020**, *306*, 127539. [[CrossRef](#)]
333. Crowley, K.; Morrin, A.; Hernandez, A.; Omalley, E.; Whitten, P.; Wallace, G.; Smyth, M.; Killard, A. Fabrication of an ammonia gas sensor using inkjet-printed polyaniline nanoparticles. *Talanta* **2008**, *77*, 710–717. [[CrossRef](#)]
334. Crowley, K.; O’Malley, E.; Morrin, A.; Smyth, M.R.; Killard, A.J. An aqueous ammonia sensor based on an inkjet-printed polyaniline nanoparticle-modified electrode. *Analyst* **2008**, *133*, 391–399. [[CrossRef](#)]
335. Lee, C.H.; Chuang, W.Y.; Cowan, M.A.; Wu, W.J.; Lin, C.T. A low-power integrated humidity CMOS sensor by printing-on-chip technology. *Sensors* **2014**, *14*, 9247–9255. [[CrossRef](#)] [[PubMed](#)]
336. Hibbard, T.; Crowley, K.; Killard, A.J. Direct measurement of ammonia in simulated human breath using an inkjet-printed polyaniline nanoparticle sensor. *Anal. Chim. Acta* **2013**, *779*, 56–63. [[CrossRef](#)]
337. Hibbard, T.; Crowley, K.; Kelly, F.; Ward, F.; Holian, J.; Watson, A.; Killard, A.J. Point of care monitoring of hemodialysis patients with a breath ammonia measurement device based on printed polyaniline nanoparticle sensors. *Anal. Chem.* **2013**, *85*, 12158–12165. [[CrossRef](#)] [[PubMed](#)]

338. Peřinka, N.; Drřková, M.; Randjelović, D.V.; Bondavalli, P.; Hajná, M.; Bober, P.; Syrový, T.; Bonnassieaux, Y.; Stejskal, J. Application of Ink-Jet Printing and Spray Coating for the Fabrication of Polyaniline/Poly(N-Vinylpyrrolidone)-Based Ammonia Gas Sensor. *Key Eng. Mater.* **2015**, *644*, 61–64. [[CrossRef](#)]
339. Clark, N.B.; Maher, L.J. Non-contact, radio frequency detection of ammonia with a printed polyaniline sensor. *React. Funct. Polym.* **2009**, *69*, 594–600. [[CrossRef](#)]
340. Peřinka, N.; Drřková, M.; Randjelović, D.V.; Bondavalli, P.; Hajná, M.; Bober, P.; Syrový, T.; Bonnassieaux, Y.; Stejskal, J. Characterization of Polyaniline-Based Ammonia Gas Sensors Prepared by Means of Spray Coating and Ink-Jet Printing. *Sens. Lett.* **2014**, *12*, 1620–1627. [[CrossRef](#)]
341. Ma, Z.; Chen, P.; Cheng, W.; Yan, K.; Pan, L.; Shi, Y.; Yu, G. Highly Sensitive, Printable Nanostructured Conductive Polymer Wireless Sensor for Food Spoilage Detection. *Nano Lett.* **2018**, *18*, 4570–4575. [[CrossRef](#)]
342. Dipak, P.; Tiwari, D.C.; Samadhiya, A.; Kumar, N.; Biswajit, T.; Singh, P.A.; Tiwari, R.K. Synthesis of polyaniline (printable nanoink) gas sensor for the detection of ammonia gas. *J. Mater. Sci. Mater. Electron.* **2020**, *31*, 22512–22521. [[CrossRef](#)]
343. Wongchoosuk, C.; Jangtaewee, P.; Lokavee, P.; Udomrat, S.; Sudkeaw, P.; Kerdcharoen, T. Novel Flexible NH<sub>3</sub> Gas Sensor Prepared by Ink-Jet Printing Technique. *Adv. Mater. Res.* **2012**, *506*, 39–42. [[CrossRef](#)]
344. Seekaew, Y.; Lokavee, S.; Phokharatkul, D.; Wisitorsaat, A.; Kerdcharoen, T.; Wongchoosuk, C. Low-cost and flexible printed graphene–PEDOT:PSS gas sensor for ammonia detection. *Org. Electron.* **2014**, *15*, 2971–2981. [[CrossRef](#)]
345. Li, S.; Li, Y.; Chen, S.; Tang, W.; Huang, Y.; Peng, S.; Qi, J.; Guo, X. Improved Sensitivity of Inkjet-Printed PEDOT:PSS Ammonia Sensor With “Nonideal” Morphology. *IEEE Sens. Lett.* **2018**, *2*, 2000204. [[CrossRef](#)]
346. Lv, D.; Chen, W.; Shen, W.; Peng, M.; Zhang, X.; Wang, R.; Xu, L.; Xu, W.; Song, W.; Tan, R. Enhanced flexible room temperature ammonia sensor based on PEDOT: PSS thin film with FeCl<sub>3</sub> additives prepared by inkjet printing. *Sens. Actuators B Chem.* **2019**, *298*, 126890. [[CrossRef](#)]
347. Fujita, H.; Hao, M.; Takeoka, S.; Miyahara, Y.; Goda, T.; Fujie, T. Paper-Based Wearable Ammonia Gas Sensor Using Organic–Inorganic Composite PEDOT:PSS with Iron(III) Compounds. *Adv. Mater. Technol.* **2022**, *7*, 2101486. [[CrossRef](#)]
348. Brannelly, N.T.; Killard, A.J. A Printed and Microfabricated Sensor Device for the Sensitive Low Volume Measurement of Aqueous Ammonia. *Electroanalysis* **2017**, *29*, 162–171. [[CrossRef](#)]
349. Zea, M.; Texido, R.; Villa, R.; Borros, S.; Gabriel, G. Specially Designed Polyaniline/Polypyrrole Ink for a Fully Printed Highly Sensitive pH Microsensor. *ACS Appl. Mater. Interfaces* **2021**, *13*, 33524–33535. [[CrossRef](#)] [[PubMed](#)]
350. Demuru, S.; Kunnel, B.P.; Briand, D. Real-Time Multi-Ion Detection in the Sweat Concentration Range Enabled by Flexible, Printed, and Microfluidics-Integrated Organic Transistor Arrays. *Adv. Mater. Technol.* **2020**, *5*, 2000328. [[CrossRef](#)]
351. Demuru, S.; Kunnel, B.P.; Briand, D. Thin film organic electrochemical transistors based on hybrid PANI/PEDOT:PSS active layers for enhanced pH sensing. *Biosens. Bioelectron. X* **2021**, *7*, 100065. [[CrossRef](#)]
352. Mabrook, M.F.; Pearson, C.; Petty, M.C. Inkjet-Printed Polymer Films for the Detection of Organic Vapors. *IEEE Sens. J.* **2006**, *6*, 1435–1444. [[CrossRef](#)]
353. Yoon, B.; Park, I.S.; Shin, H.; Park, H.J.; Lee, C.W.; Kim, J.M. A litmus-type colorimetric and fluorometric volatile organic compound sensor based on inkjet-printed polydiacetylenes on paper substrates. *Macromol. Rapid Commun.* **2013**, *34*, 731–735. [[CrossRef](#)] [[PubMed](#)]
354. Mabrook, M.F.; Pearson, C.; Petty, M.C. Inkjet-printed polypyrrole thin films for vapour sensing. *Sens. Actuators B Chem.* **2006**, *115*, 547–551. [[CrossRef](#)]
355. Li, B.; Santhanam, S.; Schultz, L.; Jeffries-El, M.; Iovu, M.C.; Sauvé, G.; Cooper, J.; Zhang, R.; Revelli, J.C.; Kusne, A.G.; et al. Inkjet printed chemical sensor array based on polythiophene conductive polymers. *Sens. Actuators B Chem.* **2007**, *123*, 651–660. [[CrossRef](#)]
356. Alshammari, A.S.; Alenezi, M.R.; Lai, K.T.; Silva, S.R.P. Inkjet printing of polymer functionalized CNT gas sensor with enhanced sensing properties. *Mater. Lett.* **2017**, *189*, 299–302. [[CrossRef](#)]
357. Timsorn, K.; Wongchoosuk, C. Inkjet printing of room-temperature gas sensors for identification of formalin contamination in squids. *J. Mater. Sci. Mater. Electron.* **2019**, *30*, 4782–4791. [[CrossRef](#)]
358. Vigna, L.; Verna, A.; Marasso, S.L.; Sangermano, M.; D’Angelo, P.; Pirri, F.C.; Cocuzza, M. The effects of secondary doping on ink-jet printed PEDOT:PSS gas sensors for VOCs and NO<sub>2</sub> detection. *Sens. Actuators B Chem.* **2021**, *345*, 130381. [[CrossRef](#)]
359. Hallil, H.; Zhang, Q.; Coquet, P.; Pichonat, E.; Happy, H.; Dejous, C.; Bahoumina, P.; Pieper, K.; Lachaud, J.L.; Rebiere, D.; et al. Differential Passive Microwave Planar Resonator- Based Sensor for Chemical Particle Detection in Polluted Environments. *IEEE Sens. J.* **2019**, *19*, 1346–1353. [[CrossRef](#)]
360. Chang, J.B.; Liu, V.; Subramanian, V.; Sivula, K.; Luscombe, C.; Murphy, A.; Liu, J.; Fréchet, J.M.J. Printable polythiophene gas sensor array for low-cost electronic noses. *J. Appl. Phys.* **2006**, *100*, 014506. [[CrossRef](#)]
361. Bihar, E.; Deng, Y.; Miyake, T.; Saadaoui, M.; Malliaras, G.G.; Rolandi, M. A Disposable paper breathalyzer with an alcohol sensing organic electrochemical transistor. *Sci. Rep.* **2016**, *6*, 27582. [[CrossRef](#)]
362. Jung, M.; Kim, K.; Kim, B.; Cheong, H.; Shin, K.; Kwon, O.S.; Park, J.J.; Jeon, S. Paper-Based Bimodal Sensor for Electronic Skin Applications. *ACS Appl. Mater. Interfaces* **2017**, *9*, 26974–26982. [[CrossRef](#)] [[PubMed](#)]
363. Correia, V.; Oliveira, J.; Perinka, N.; Costa, P.; Sowade, E.; Mitra, K.Y.; Baumann, R.R.; Lanceros-Mendez, S. All-Printed Piezoresistive Sensor Matrix with Organic Thin-Film Transistors as a Switch for Crosstalk Reduction. *ACS Appl. Electron. Mater.* **2020**, *2*, 1470–1477. [[CrossRef](#)]

364. Yuan, Y.; Peng, B.; Chi, H.; Li, C.; Liu, R.; Liu, X. Layer-by-layer inkjet printing SPS:PEDOT NP/RGO composite film for flexible humidity sensors. *RSC Adv.* **2016**, *6*, 113298–113306. [[CrossRef](#)]
365. Lo, L.W.; Zhao, J.; Wan, H.; Wang, Y.; Chakrabartty, S.; Wang, C. An Inkjet-Printed PEDOT:PSS-Based Stretchable Conductor for Wearable Health Monitoring Device Applications. *ACS Appl. Mater. Interfaces* **2021**, *13*, 21693–21702. [[CrossRef](#)]
366. Kuzubasoglu, B.A.; Sayar, E.; Bahadir, S.K. Inkjet-Printed CNT/PEDOT:PSS Temperature Sensor on a Textile Substrate for Wearable Intelligent Systems. *IEEE Sens. J.* **2021**, *21*, 13090–13097. [[CrossRef](#)]
367. Taccola, S.; Poliziani, A.; Santonocito, D.; Mondini, A.; Denk, C.; Ide, A.N.; Oberparleiter, M.; Greco, F.; Mattoli, V. Toward the Use of Temporary Tattoo Electrodes for Impedancemetric Respiration Monitoring and Other Electrophysiological Recordings on Skin. *Sensors* **2021**, *21*, 1197. [[CrossRef](#)]
368. Lilliu, S.; Böberl, M.; Sramek, M.; Tedde, S.F.; Macdonald, J.E.; Hayden, O. Inkjet-printed organic photodiodes. *Thin Solid Film.* **2011**, *520*, 610–615. [[CrossRef](#)]
369. Pace, G.; Grimoldi, A.; Rengert, Z.; Bazan, G.C.; Natali, D.; Caironi, M. Inkjet printed organic detectors with flat responsivity up to the NIR and inherent UV optical filtering. *Synth. Met.* **2019**, *254*, 92–96. [[CrossRef](#)]
370. Ruiz-Preciado, L.A.; Baek, S.; Strobel, N.; Xia, K.; Seiberlich, M.; Park, S.-m.; Lemmer, U.; Jung, S.; Hernandez-Sosa, G. Monolithically printed all-organic flexible photosensor active matrix. *Npj Flex. Electron.* **2023**, *7*, 6. [[CrossRef](#)]
371. Pace, G.; Grimoldi, A.; Natali, D.; Sampietro, M.; Coughlin, J.E.; Bazan, G.C.; Caironi, M. All-organic and fully-printed semitransparent photodetectors based on narrow bandgap conjugated molecules. *Adv. Mater.* **2014**, *26*, 6773–6777. [[CrossRef](#)]
372. Kim, T.Y.; Ha, J.; Cho, K.; Pak, J.; Seo, J.; Park, J.; Kim, J.K.; Chung, S.; Hong, Y.; Lee, T. Transparent Large-Area MoS<sub>2</sub> Phototransistors with Inkjet-Printed Components on Flexible Platforms. *ACS Nano* **2017**, *11*, 10273–10280. [[CrossRef](#)] [[PubMed](#)]
373. Kulkarni, M.V.; Apte, S.K.; Naik, S.D.; Ambekar, J.D.; Kale, B.B. Processing and formulation of inkjet printable conducting polyaniline based ink for low cost, flexible humidity sensors using untreated polymeric substrate. *Smart Mater. Struct.* **2012**, *21*, 035023. [[CrossRef](#)]
374. Kulkarni, M.V.; Apte, S.K.; Naik, S.D.; Ambekar, J.D.; Kale, B.B. Ink-jet printed conducting polyaniline based flexible humidity sensor. *Sens. Actuators B Chem.* **2013**, *178*, 140–143. [[CrossRef](#)]
375. Zhang, R.; Peng, B.; Yuan, Y. Flexible printed humidity sensor based on poly(3,4-ethylenedioxythiophene)/reduced graphene oxide/Au nanoparticles with high performance. *Compos. Sci. Technol.* **2018**, *168*, 118–125. [[CrossRef](#)]
376. Yuan, Y.; Zhang, Y.; Liu, R.; Liu, J.; Li, Z.; Liu, X. Humidity sensor fabricated by inkjet-printing photosensitive conductive inks PEDOT:PVMA on a paper substrate. *RSC Adv.* **2016**, *6*, 47498–47508. [[CrossRef](#)]
377. Morais, R.M.; Klem, M.d.S.; Nogueira, G.L.; Gomes, T.C.; Alves, N. Low Cost Humidity Sensor Based on PANI/PEDOT:PSS Printed on Paper. *IEEE Sens. J.* **2018**, *18*, 2647–2651. [[CrossRef](#)]
378. Nilsson, D. An all-organic sensor–transistor based on a novel electrochemical transducer concept printed electrochemical sensors on paper. *Sens. Actuators B Chem.* **2002**, *86*, 193–197. [[CrossRef](#)]
379. Majumdar, S.; Majumdar, H.S.; Tobjörk, D.; Österbacka, R. Towards printed magnetic sensors based on organic diodes. *Phys. Status Solidi A* **2009**, *206*, 2198–2201. [[CrossRef](#)]
380. Closson, A.; Richards, H.; Xu, Z.; Jin, C.; Dong, L.; Zhang, J.X.J. Method for Inkjet-printing PEDOT:PSS polymer electrode arrays on piezoelectric PVDF-TrFE fibers. *IEEE Sens. J.* **2021**, *21*, 26277–26285. [[CrossRef](#)]
381. Cruz, S.; Dias, D.; Viana, J.C.; Rocha, L.A. Inkjet Printed Pressure Sensing Platform for Postural Imbalance Monitoring. *IEEE Trans. Instrum. Meas.* **2015**, *64*, 2813–2820. [[CrossRef](#)]
382. Griffith, M.J.; Cooling, N.A.; Elkington, D.C.; Wasson, M.; Zhou, X.; Belcher, W.J.; Dastoor, P.C. Controlling Nanostructure in Inkjet Printed Organic Transistors for Pressure Sensing Applications. *Nanomaterials* **2021**, *11*, 1185. [[CrossRef](#)] [[PubMed](#)]
383. Ryu, D.; Meyers, F.N.; Loh, K.J. Inkjet-printed, flexible, and photoactive thin film strain sensors. *J. Intell. Mater. Syst. Struct.* **2014**, *26*, 1699–1710. [[CrossRef](#)]
384. Borghetti, M.; Serpelloni, M.; Sardini, E.; Pandini, S. Mechanical behavior of strain sensors based on PEDOT:PSS and silver nanoparticles inks deposited on polymer substrate by inkjet printing. *Sens. Actuators A Phys.* **2016**, *243*, 71–80. [[CrossRef](#)]
385. Kye, J.W.; Han, D.C.; Shin, H.J.; Yeom, S.-h.; Lee, W. Fabrication of Inkjet Printed Strain Gauge Using PEDOT:PSS. *J. Sens. Sci. Technol.* **2017**, *26*, 56–59. [[CrossRef](#)]
386. Kang, T.-K. Inkjet Printing of Highly Sensitive, Transparent, Flexible Linear Piezoresistive Strain Sensors. *Coatings* **2021**, *11*, 51. [[CrossRef](#)]
387. Rivadeneyra, A.; Bobinger, M.; Albrecht, A.; Becherer, M.; Lugli, P.; Falco, A.; Salmeron, J.F. Cost-effective PEDOT:PSS Temperature Sensors Inkjetted on a Bendable Substrate by a Consumer Printer. *Polymers* **2019**, *11*, 824. [[CrossRef](#)] [[PubMed](#)]
388. Khalaf, A.M.; Issa, H.H.; Ramirez, J.L.; Mohamed, S.A. All Inkjet-Printed Temperature Sensors Based on PEDOT:PSS. *IEEE Access* **2022**, *10*, 61094–61100. [[CrossRef](#)]
389. Yoon, B.; Shin, H.; Kang, E.M.; Cho, D.W.; Shin, K.; Chung, H.; Lee, C.W.; Kim, J.M. Inkjet-compatible single-component polydiacetylene precursors for thermochromic paper sensors. *ACS Appl. Mater. Interfaces* **2013**, *5*, 4527–4535. [[CrossRef](#)]
390. Ma, S.; Ribeiro, F.; Powell, K.; Lutian, J.; Moller, C.; Large, T.; Holbery, J. Fabrication of Novel Transparent Touch Sensing Device via Drop-on-Demand Inkjet Printing Technique. *ACS Appl. Mater. Interfaces* **2015**, *7*, 21628–21633. [[CrossRef](#)]
391. Ling, H.; Chen, R.; Huang, Q.; Shen, F.; Wang, Y.; Wang, X. Transparent, flexible and recyclable nanopaper-based touch sensors fabricated via inkjet-printing. *Green Chem.* **2020**, *22*, 3208–3215. [[CrossRef](#)]

392. Poldsalu, I.; Rohthead, K.; Plesse, C.; Vidal, F.; Nguyen, N.T.; Peikolainen, A.L.; Tamm, T.; Kiefer, R. Printed PEDOT:PSS Trilayer: Mechanism Evaluation and Application in Energy Storage. *Materials* **2020**, *13*, 491. [[CrossRef](#)] [[PubMed](#)]
393. Fan, L.; Zhang, N.; Sun, K. Flexible patterned micro-electrochemical capacitors based on PEDOT. *Chem. Commun.* **2014**, *50*, 6789–6792. [[CrossRef](#)] [[PubMed](#)]
394. Li, B.; Liang, X.; Li, G.; Shao, F.; Xia, T.; Xu, S.; Hu, N.; Su, Y.; Yang, Z.; Zhang, Y. Inkjet-Printed Ultrathin MoS<sub>2</sub>-Based Electrodes for Flexible In-Plane Microsupercapacitors. *ACS Appl. Mater. Interfaces* **2020**, *12*, 39444–39454. [[CrossRef](#)] [[PubMed](#)]
395. Li, Z.; Ruiz, V.; Mishukova, V.; Wan, Q.; Liu, H.; Xue, H.; Gao, Y.; Cao, G.; Li, Y.; Zhuang, X.; et al. Inkjet Printed Disposable High-Rate On-Paper Microsupercapacitors. *Adv. Funct. Mater.* **2021**, *32*, 2108773. [[CrossRef](#)]
396. Diao, J.; Yuan, J.; Ding, A.; Zheng, J.; Lu, Z. Flexible Supercapacitor Based on Inkjet-Printed Graphene@Polyaniline Nanocomposites with Ultrahigh Capacitance. *Macromol. Mater. Eng.* **2018**, *303*, 1800092. [[CrossRef](#)]
397. Xu, Y.; Hennig, I.; Freyberg, D.; James Strudwick, A.; Georg Schwab, M.; Weitz, T.; Chih-Pei Cha, K. Inkjet-printed energy storage device using graphene/polyaniline inks. *J. Power Sources* **2014**, *248*, 483–488. [[CrossRef](#)]
398. Stempien, Z.; Khalid, M.; Kozanecki, M.; Filipczak, P.; Wrzesinska, A.; Korzeniewska, E.; Sasiadek, E. Inkjet Printing of Polypyrrole Electroconductive Layers Based on Direct Inks Freezing and Their Use in Textile Solid-State Supercapacitors. *Materials* **2021**, *14*, 3577. [[CrossRef](#)] [[PubMed](#)]
399. Lawes, S.; Sun, Q.; Lushington, A.; Xiao, B.; Liu, Y.; Sun, X. Inkjet-printed silicon as high performance anodes for Li-ion batteries. *Nano Energy* **2017**, *36*, 313–321. [[CrossRef](#)]
400. Wang, C.; Park, M.J.; Seo, D.H.; Shon, H.K. Inkjet printing of graphene oxide and dopamine on nanofiltration membranes for improved anti-fouling properties and chlorine resistance. *Sep. Purif. Technol.* **2021**, *254*, 117604. [[CrossRef](#)]
401. Li, R.; Li, J.; Rao, L.; Lin, H.; Shen, L.; Xu, Y.; Chen, J.; Liao, B.-Q. Inkjet printing of dopamine followed by UV light irradiation to modify mussel-inspired PVDF membrane for efficient oil-water separation. *J. Membr. Sci.* **2021**, *619*, 118790. [[CrossRef](#)]
402. Afsari, M.; Park, M.J.; Kaleekkal, N.J.; Motsa, M.M.; Shon, H.K.; Tijing, L. Janus Distillation Membrane via Mussel-Inspired Inkjet Printing Modification for Anti-Oil Fouling Membrane Distillation. *Membranes* **2023**, *13*, 191. [[CrossRef](#)] [[PubMed](#)]
403. Shrestha, M.; Lu, Z.; Lau, G.K. Transparent Tunable Acoustic Absorber Membrane Using Inkjet-Printed PEDOT:PSS Thin-Film Compliant Electrodes. *ACS Appl. Mater. Interfaces* **2018**, *10*, 39942–39951. [[CrossRef](#)] [[PubMed](#)]
404. Almasri, R.M.; AlChamaa, W.; Tehrani-Bagha, A.R.; Khraiche, M.L. Highly Flexible Single-Unit Resolution All Printed Neural Interface on a Bioresorbable Backbone. *ACS Appl. Bio. Mater.* **2020**, *3*, 7040–7051. [[CrossRef](#)] [[PubMed](#)]
405. Fortunato, G.M.; De Maria, C.; Eglin, D.; Serra, T.; Vozzi, G. An ink-jet printed electrical stimulation platform for muscle tissue regeneration. *Bioprinting* **2018**, *11*, e00035. [[CrossRef](#)]
406. Bihar, E.; Roberts, T.; Zhang, Y.; Ismailova, E.; Hervé, T.; Malliaras, G.G.; De Graaf, J.B.; Inal, S.; Saadaoui, M. Fully printed all-polymer tattoo/textile electronics for electromyography. *Flex. Print. Electron.* **2018**, *3*, 034004. [[CrossRef](#)]
407. Weng, B.; Liu, X.; Shepherd, R.; Wallace, G.G. Inkjet printed polypyrrole/collagen scaffold: A combination of spatial control and electrical stimulation of PC12 cells. *Synth. Met.* **2012**, *162*, 1375–1380. [[CrossRef](#)]
408. Weng, B.; Liu, X.; Higgins, M.J.; Shepherd, R.; Wallace, G. Fabrication and characterization of cyto-compatible polypyrrole films inkjet printed from nanoformulations cyto-compatible, inkjet-printed polypyrrole films. *Small* **2011**, *7*, 3434–3438. [[CrossRef](#)]
409. Rajzer, I.; Rom, M.; Menaszek, E.; Pasiarb, P. Conductive PANI patterns on electrospun PCL/gelatin scaffolds modified with bioactive particles for bone tissue engineering. *Mater. Lett.* **2015**, *138*, 60–63. [[CrossRef](#)]

**Disclaimer/Publisher's Note:** The statements, opinions and data contained in all publications are solely those of the individual author(s) and contributor(s) and not of MDPI and/or the editor(s). MDPI and/or the editor(s) disclaim responsibility for any injury to people or property resulting from any ideas, methods, instructions or products referred to in the content.